NUREG/CR-3320
WHC-EP-0204
Vol. 2

LWR Pressure Vessel Surveillance Dosimetry Improvement Program

PSF Startup Experiments

Edited by
W. N. McElroy, R. Gold, E. D. McGarry

Pacific Northwest Laboratory
Operated by
Battelle Memorial Institute

Prepared for
U.S. Nuclear Regulatory Commission

NUREG/CR-3320
WHC-EP-0204
Vol. 2
R5

LWR Pressure Vessel Surveillance Dosimetry Improvement Program

PSF Startup Experiments

Manuscript Completed: November 1988
Date Published: July 1992

Edited by
W. N. McElroy[1], R. Gold[2], E. D. McGarry[3]

Pacific Northwest Laboratory
Richland, WA 99352

Prepared for
Division of Engineering
Office of Nuclear Regulatory Research
U.S. Nuclear Regulatory Commission
Washington, DC 20555
NRC FIN B9988

[1]Consultants and Technology Services, Richland, WA 99352
[2]Metrology Control Corporation, Richland, WA 99352
[3]National Institute of Standards and Technology, Gaithersburg, MD 20899

ABSTRACT

The metallurgical irradiation experiment at the Oak Ridge Research Reactor Poolside Facility (ORR-PSF) is one of the series of benchmark experiments in the framework of the Light Water Reactor Pressure Vessel Surveillance Dosimetry Improvement Program (LWR-PV-SDIP). The goal of this program is to test, against well-established benchmarks, the methodologies and data bases that are used to predict the irradiation embrittlement and fracture toughness of pressure and support structure steels. The prediction methodology includes procedures for neutron physics calculations, dosimetry and spectrum adjustment methods, metallurgical tests, and damage correlations. The benchmark experiments serve to validate, improve, and standardize these procedures. The results of this program are implemented in a set of ASTM standards on pressure vessel surveillance procedures. These, in turn, may be used as guides for the nuclear industry and for the USNRC.

To serve as a benchmark, a very careful characterization of the ORR-PSF experiment is necessary, both in terms of neutron flux-fluence spectra and of metallurgical test results. Statistically determined uncertainties must be given in terms of variances and covariancies to make comparisons between predictions and experimental results meaningful. This report supports analysis of the PSF Blind Test and provides experimental conditions, as-built documentation, and PSF physics-dosimetry results for the Startup, SSC-1, and SSC-2 experiments.

CONTENTS

CONTENTS (Cont'd)

FIGURES

FIGURES (cont'd)

TABLES

TABLES (cont'd)

FOREWORD

The Light Water Reactor Pressure Vessel Surveillance Dosimetry Improvement Program (LWR-PV-SDIP) was established by NRC to improve, test, verify, and standardize the physics-dosimetry-metallurgy, damage correlation, and associated reactor analysis methods, procedures, and data used to predict the integrated effect of neutron exposure to LWR pressure vessels and their support structures. A vigorous research effort attacking the same measurement and analysis problems exists worldwide; and strong cooperative links between US NRC-supported activities at HEDL, ORNL, NBS, and MEA and those supported by CEN/SCK (Mol, Belgium), EPRI (Palo Alto, CA, USA), KFA (Julich, Germany), and several UK laboratories have been extended to other countries. These cooperative links are strengthened by the active membership of the scientific staff from many countries a[illegible] the ASTM E10 Committee on Nuclear Technology and Applications [illegible] subcommittees are responsible for preparation of LWR surve[illegible]

The primary objective of this multilaboratory program was to prepare an updated and improved set of physics-dosimetry-metallurgy, damage correlation, and associated reactor analysis ASTM standards for LWR pressure vessel and support structure irradiation surveillance programs. Supporting this objective were a series of analytical and experimental validation and calibration studies in "Standard, Reference and Controlled Environment Benchmark Fields," research reactor "Test Regions," and operating power reactor "Surveillance Positions".

These studies served to establish and certify the precision and accuracy of the measurement and predictive methods recommended in the ASTM standards and used for the assessment and control of present and end-of-life (EOL) conditions of pressure vessel and support structure steels. Consistent and accurate and data analysis techniques and methods, therefore were developed, tested, and verified along with guidelines for required neutron field calculations to correlate changes in material properties with characteristics of the neutron field. Application of established ASTM standards should permit the reporting of measured material property changes and neutron exposures to an accuracy and precision within 10% to 30%, depending on the measured metallurgical variable and neutron environment.

Assessment of the radiation-induced degradation of material properties in a power reactor requires accurate definition of the neutron field from the outer region of the reactor core to the outer boundries of the pressure vessel. The accuracy of measurements on neutron fluence rate and spectrum is associated with two distinct components of LWR irradiation surveillance procedures: 1) proper application of calculational estimates of the neutron exposure at in- and ex-vessel surveillance positions, various locations in the vessel wall and in ex-vessel support structures, and 2) understanding the relationship between material property changes in reactor vessels and their support structures, and in metallurgical test specimens irradiated in test reactors and at accelerated neutron flux positions in operating power reactors.

The first component requires verification and calibration experiments in a variety of neutron irradiation test facilities, including LWR-PV mockups, power reactor surveillance positions, and related benchmark neutron fields. The benchmarks serve as a permanent reference measurement for neutron flux and fluence detection techniques. The second component requires serious extrapolation of an observed neutron-induced mechanical property change from research reactor "Test Regions" and operating power reactor "Surveillance Positions" to locations inside the body of the pressure vessel wall and to ex-vessel support structures. The neutron flux at the vessel inner wall is up to one order of magnitude lower than at surveillance specimen positions and up to two orders of magnitude lower than at test reactor positions. At the vessel outer wall, the neutron flux is one order of magnitude or more lower than at the vessel inner wall. Further, the neutron spectra at, within, and leaving the vessel are substantially different.

To meet reactor pressure vessel radiation monitoring requirements, a variety of neutron flux and fluence detectors are employed, most of which are passive. Each detector must be validated for application to the higher flux and harder neutron spectrum of the research reactor "Test Region" and to the lower flux and degraded neutron spectrum at "Surveillance Positions." Required detectors must respond to neutrons of various energies so that multigroup spectra can be determined with accuracy sufficient for adequate damage response estimates. Detectors being used, developed, and tested for the program include radiometric (RM) sensors, helium accumulation fluence monitor (HAFM) sensors, solid state track recorder (SSTR) sensors, and damage monitor (DM) sensors.

The necessity for pressure vessel mockup facilities for physics-dosimetry investigations and for irradiation of metallurgical specimens was recognized early in the formation of the NRC program. Experimental studies associated with high- and low-flux versions of a pressurized water reactor (PWR) pressure vessel mockup are in progress in the US, Belgium, France, and United Kingdom. The US low-flux version is known as the ORNL Poolside Critical Assembly (PCA) and the high-flux version is known as the Oak Ridge Research Reactor (ORR) Poolside Facility (PSF), both located at Oak Ridge, Tennessee. As specialized benchmarks, these facilities provide well-characterized neutron environments where active and passive neutron dosimetry, various types of LWR-PV and support structure neutron field calculations, and temperature-controlled metallurgical specimen exposures are brought together.

The two key low-flux pressure vessel mockups in Europe are known as the Mol-Belgium-VENUS and Winfrith-United Kingdom-NESDIP facilities. The VENUS Facility is being used for PWR core source and azimuthal lead-factor studies, while NESDIP is being used for PWR cavity and azimuthal lead-factor studies. A third and important low-fluence pressure vessel mockup in Europe is identified with a French PV-simulator at the periphery of the Triton reactor. It served as the irradiation facility for the DOMPAC dosimetry experiment to study surveillance capsule perturbations and through-PV-wall radial fluence and damage profiles (gradients) for PWRs of the Fessenheim 1 type.

Results of measurement and calculational strategies outlined here will be made available for use by the nuclear industry as ASTM standards. Code of Federal Regulations 10CFR50 (Cf83) already requires adherence to several ASTM standards that establish a surveillance program for each power reactor and incorporate metallurgical specimens, physics-dosimetry flux-fluence monitors, and neutron field evaluation. Revised and new standards in preparation will be carefully updated, flexible, and, above all, consistent.

This is the second of six planned NUREG reports on the ORR-PSF Experiments and Blind Test. Summary information on each of these six documents follows:

- NUREG/CR-3320
  PSF Physics-Dosimetry-Metallurgy Experiments:

  Vol. 1 (Date Published: July 1986)
  PSF Experiments Summary and Blind Test Results - W. N. McElroy, Editor

  This document provides PSF experiment summary information and the results of the comparison of measured and predicted physics-dosimetry-metallurgy results for the PSF experiment. This document contains (in an appendix) each final report of participants.

  Vol. 2 (This Document)
  PSF Startup Experiments - W. N. McElroy and R. Gold, Editors

  Beyond scope of title, this document supports analysis of the PSF Blind Test and provides experimental conditions, as-built documentation, and PSF physics-dosimetry results for the Startup, SSC-1, and SSC-2 experiments.

  Vol. 3 (Date Published: October 1987)
  PSF Physics-Dosimetry Program - W. N. McElroy and R. Gold, Editors

  Beyond scope of title, this document supports analysis of the PSF Experiment and Blind Test and provides experimental conditions, as-built documentation, and final PSF physics-dosimetry results for SSC, SPVC, and SVBC.

  Vol. 4 (Date Published: November 1987)
  PSF Metallurgy Program - W. N. McElroy and R. Gold, Editors

  Beyond scope of title, this document supports analysis of the PSF Experiments and Blind Test and provides experimental conditions, as-built documentation, and final metallurgical data on measured property changes in different pressure vessel steels for SSC-1 and -2 positions, and the (SPVC) simulated PV locations at the 0-T (inner surface), 1/4-T, and 1/2-T positions of the 4/12 PWR PV wall mockup. The corresponding SSC-1, SSC-2, and SPVC locations' neutron exposures are $\sim 2 \times 10^{19}$, $\sim 4 \times 10^{19}$, $\sim 4 \times 10^{19}$, $\sim 2 \times 10^{19}$, and $\sim 1 \times 10^{19}$ n/cm^2, respectively, for a ~550°F irradiation temperature. It contains and/or references available damage analysis results for SVBC using the Vol. 5 metallurgical data base.

ACKNOWLEDGMENTS

The success of the LWR Pressure Vessel Surveillance Dosimetry Improvement Program (LWR-PV-SDIP) depended upon the efforts and the free exchange of ideas and views by representatives of a large number of research, service, regulatory, vendor, architect/engineer, and utility organizations. The information reported herein could not have been developed without the continuing support of the respective funding organizations and their management and technical staffs. Special acknowledgement is due to C. Z. Serpan of NRC for having identified the need for an international program such as the LWR-PV-SDIP and for making it possible by taking a strong overall support and management lead.

The encouragement, help, and contributions of T. U, Marston of EPRI; C. Z. Serpan of NRC; E. B. Norris of SwRi; J. R. Hawthorne of MEA; G. R. Odette of USCB; D. Pachur of KFA; and A. F. Thomas, T. J. Williams, and R. Squires of RR&A in helping to formulate plans and providing information and guidance for Parts I, II, and III of the PSF Experiments and Blind Test require special and separate acknowledgment.

The dedication and professional skills of the ORR-PSF operations team at ORNL contributed significantly to the success of the PSF experimental program. The authors are indebted to staff members of the ORNL Operating Division Technical Service Group for their contributions and for their support to individual experimenters.

Additional acknowledgment is due A. Taboda, the NRC Program Manager, and to R. L. Knecht, H. H. Yoshikawa, and D. L. Blackburn of the Westinghouse Hanford Company (Westinghouse Hanford) for their constructive comments and help in the program management and the preparation and review of the program documentation. Contributions to this document resulting from interactions with other LWR-PV-SDIP participants, who are not identified as authors in this report, are also acknowledged. Very special acknowledgment is given to D. C. Smith of the Westinghouse Hanford Irradiation Environment Group and to the Westinghouse Hanford Technical Publications, Word Processing, Graphics, and Duplication personnel who contributed to this document.

ACRONYMS

ANO-1	Arkansas Nuclear One Reactor
ASTM	American Society for Testing and Materials
BC	Battelle Columbus
BMI	Battelle Memorial Institute, Columbus, Ohio
BSR	Bulk Shielding Reactor
BWR	Boiling Water Reactor
B&W	Babcock & Wilcox
CE	Combustion Engineering; Consensus Evaluation
CEN/SCK	Centre d'Etude de l'Energie Nucleaire, Mol, Belgium
CT	Compact Tension
CVN	Charpy-V Test Result
DM	Damage Monitor
DOE	Department of Energy
DOMPAC	Triton Reactor Thermal Shield and Pressure Vessel Mockup, Fontenay-aux-Roses, France
EFPY	Effective Full-Power Years
EIR	Eidgendossisches Institut für Reaktorforschung, Switzerland
ENDF	Evaluated Nuclear Data File
E&FT	Embrittlement and Fracture Toughness
EOF	End-of-Life
EPRI	Electric Power Research Institute, Palo Alto, California
FSAR	Final Safety Analysis Report
FERRET	Least-Squares Adjustment Code
G.A.M.I.N.	French Graphite Damage Monitor
GE	General Electric Company
HAFM	Helium Accumulation Fluence Monitor
HBR-II	H.B. Robinson PWR
HEDL	Hanford Engineering Development Laboratory, Richland, WA
HSST	Heavy Section Steel Technology
IAEA	International Atomic Energy Agency, Vienna, Austria
IKE	Institut für Kernenergetik und Energiesysteme der Universität Stuttgart, Federal Republic of Germany
KFA	Kernforschungsanlage Jülich GmbH, Federal Republic of Germany
KIC	Fracture Toughness Test Result

ACRONYMS (Cont'd)

LWR	Light Water Reactor
MEA	Materials Engineering Associates Inc., Oxen Hill, Maryland
MOL	Mol, Belgium
NBS	National Bureau of Standards (See National Institute of Standards and Technology)
NDC	National Dosimetry Center (at PNL)
NDTT	Nil Ductility Transition Temperature
ΔNDTT	Nil Ductility Transition Temperature Shift
NESDIP	NESTOR Shielding and Dosimetry Improvement Program, UK
NIST	National Institute of Standards and Technology (formerly National Bureau of Standards), Gaithersburg, Maryland)
NRC	Nuclear Regulatory Commission
NRDC	National Reactor Dosimetry Center (at HEDL)
NRL	Naval Research Laboratory, Washington, DC
NUREG	Nuclear Regulatory Commission Report Designation
ORNL	Oak Ridge National Laboratory
ORR	Oak Ridge (Research) Reactor (at ORNL)
ORR-PSF	Oak Ridge (Research) Reactor - Poolside Facility
PCA	Poolside Critical Assembly (at ORNL)
PSF	Poolside Facility (at ORNL)
PTS	Pressurized Thermal Shock
PV	Pressure Vessel
PVS	Pressure Vessel Simulator
PWR	Pressurized Water Reactor
RM	Radiometric Monitor
RM-I	PSF SDMF-1 Test
RM-II	PSF SSC-1 Test
RM-III	PSF 18-Day Test
RPV	Reactor Pressure Vessel
RT_{NDT}	Reference Temperature, Nil-Ductility Transition
SAND II	Spectrum Analysis by Neutron Detectors, Version II (A Multiple-Foil Adjustment Code)
SCK/CEN	Same as CEN/SCK
SDIP	Surveillance Dosimetry Improvement Program

ACRONYMS (Cont'd)

SDM	Sapphire Damage Monitor
SDMF	Simulated Dosimetry Measurement Facility
SPVC	Simulated Pressure Vessel Capsule
SSC	Simulated Surveillance Capsule
SSTR	Solid State Track Recorder
SUNY-NSTF	State University of New York - Nuclear Science and Technology Facilities, Buffalo, NY
SVBC	Simulated Void Box Capsule
SwRI	Southwest Research Institute, San Antonio, Texas
UCSB	University of California of Santa Barbara
UK	United Kingdom
US	United States
USE	Upper Shelf Energy
VB	Void Box
VENUS	PV Mockup (at Mol, Belgium)
W	French Tungsten Damage Monitor
West	Westinghouse

S.0 SUMMARY

W.N. McElroy, R. Gold (HEDL)*, F.B.K. Kam (ORNL), A. Fabry (CEN/SCK), D. McGarry (NBS)**, M. Austin (RR&A), and W. Schneider (KFA)

S.1 INTRODUCTION

The first Simulated Dosimetry Measurement Facility (SDMF 1) "Startup" and two Simulated Surveillance Capsule (SSC-1 and SSC-2) "Metallurgical" experiments at the Oak Ridge Research Reactor Poolside Facility (ORR-PSF) are three of the series of benchmark experiments in the framework of the LWR Pressure Vessel Surveillance Dosimetry Improvement Program (LWR-PV-SDIP), Fig. S.1 (Mc87). The goal of this program is given in the Forward of this document.

An important aspect of the program is to test the methodologies and data bases presently being used to predict the irradiation embrittlement and fracture toughness (E&FT) of PV steels in commercial power reactors at the end of their service life and to determine safe operating limits for the steels. This includes testing of the procedures for neutron physics calculations, dosimetry and spectrum adjustment methods, and damage correlations. The benchmark experiments in the framework of the LWR-PV-SDIP serve to validate, improve, and standardize these procedures. The results of this program are implemented in a set of ASTM Standards (Fig. S.2) on PV surveillance procedures, which are in various stages of completion (Mc87). These, in turn, may be used as guides for the nuclear industry and for the regulatory procedures for the NRC.

The ORR-PSF experiments were specifically designed to simulate the surveillance capsule-PV configuration in power reactors and to test the validity of the procedures that determine the radiation damage in the PV from test results of surveillance capsules. Emphasis was on radiation E&FT of PV steels and on damage correlation to test current E&FT prediction methodologies. For this purpose a PSF metallurgical Blind Test was initiated (Mc83d,Mc84b,Mc85b). Only the information normally contained in surveillance reports was given to the participants. The goal was to predict from this limited information the metallurgical test results in the PV wall capsule. Of particular interest was what effects, if any, differences in fluence rate and fluence spectrum in the surveillance capsule and in the PV wall might have on the E&FT predictions (Mc85b,Mc86,Mc87d,Mc87f).

To serve as benchmarks, careful position dependent characterization in terms of neutron fluence spectra, fluence rates and metallurgical test results was necessary for each of the ORR-PSF experiments: SDMF 1, 2, 3 and 4; SSC-1; SSC-2; SPVC; and SVBC. In addition properly determined uncertainties were needed in terms of variances and covariances to make comparisons between predictions and experimental results meaningful. Detailed descriptions of the PSF SDMF 1, SSC-1, and SSC-2 Experiments and their results are reported in this NUREG/CR-3320 report.

---

* WN McElroy is President of Consultants and Technology Services and R Gold is President of Metrology Control Corporation, both in Richland, WA.
** Renamed the "National Institute of Standards and Technology".

FIGURE S.1. Benchmark Experiments in the Framework of the LWR Pressure Vessel Surveillance Dosimetry Improvement Program.

Revised: August 1987

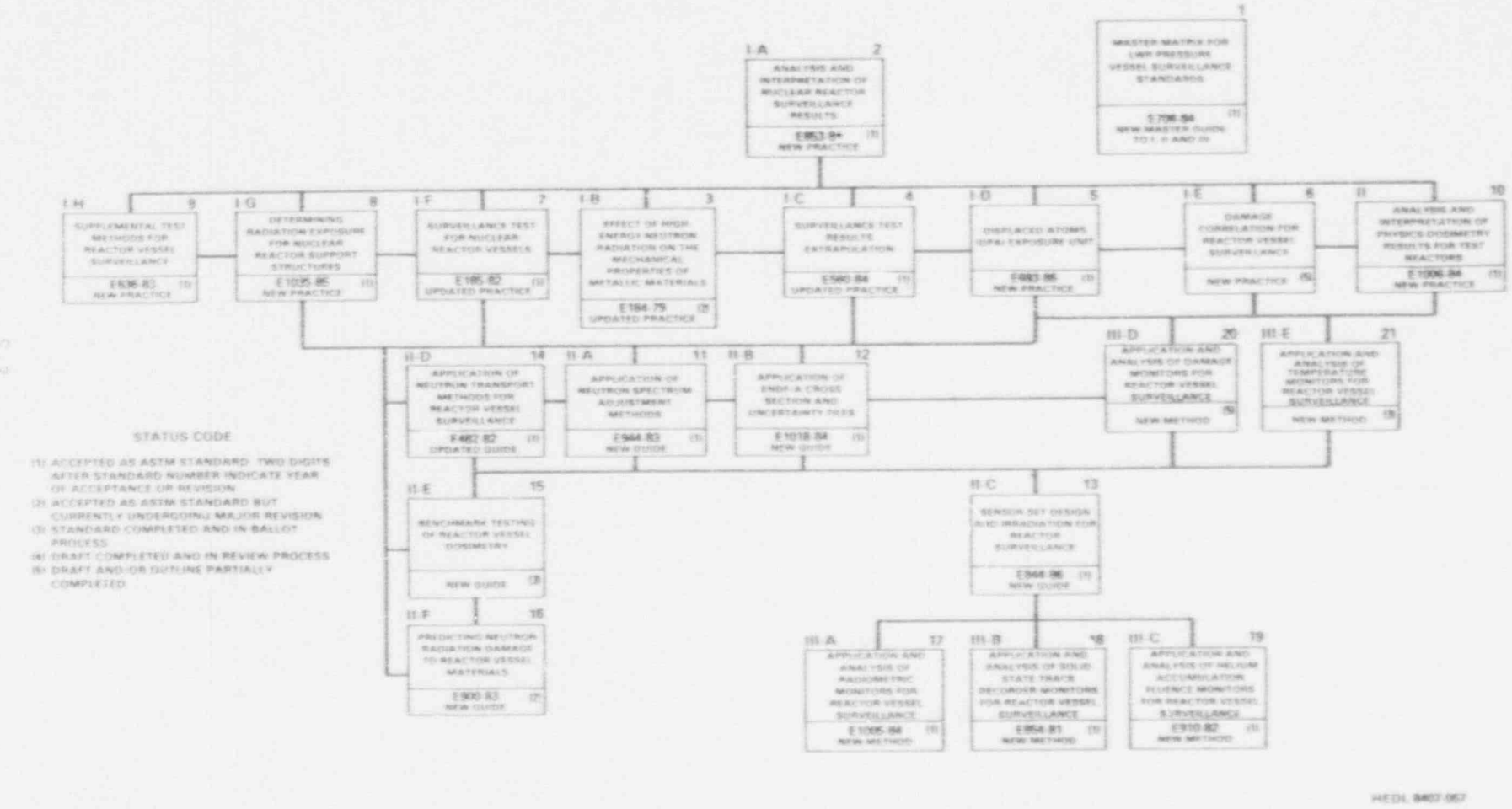

FIGURE S.2. ASTM Standards for Surveillance of LWR Nuclear Reactor Pressure Vessels and Their Support Structures.

S.2 NEUTRON PHYSICS CALCULATIONS

Differences among measurements and calculations for the PCA (Pool Critical Assembly; for low power studies) and PSF (Poolside Facility; for high power studies) have generally been in the 10% to 20% range. Somewhat larger differences between measurements and calculations have been noted for comparisons that include transport through several inches of iron and for particular dosimeters.

Results reported herein are related to the startup experiments at the PSF. The geometry and components used for this experiment are essentially equivalent to the PSF described in Section 1.1.

The results of calculations performed by ORNL and RR&A are discussed and/or referenced in Section 4.0. ORNL utilized a flux-synthesis technique based on three calculations (Ma82i,Ma84a). The source term was obtained from a three-dimensional diffusion theory calculation as reported in Section 1.2. Discrepancies between measurements and calculations relative to the startup experiments are within expected ranges based on previous evaluations (i.e., PCA, Refs. Mc81,Mc84i,Mc84f), known uncertainties associated with nuclear data, measurements, and applicable computational methodology.

Calculation of the PSF 4/12 irradiation facility was accomplished by RR&A using both the ANISN and MCBEND techniques. These RR&A ANISN (1-D) and MCBEND (3-D Monte Carlo) results provide a further basis for comparison and verification of the overall reliability of the ORNL and RR&A calculational results. The RR&A calculational results are used in Section 5.2 for a consistency analysis of the measured reaction rates in the UK dosimetry for the 18 day startup and the SSC1 and SSC2 experiments. They are also used in Section 6.1 in the derivation of recommended exposure parameter values for these experiments.

S.3 DOSIMETRY AND SPECTRUM-ADJUSTED RESULTS FOR THE PSF EXPERIMENTS

For the PSF Startup Experiments, Saclay (C.E.A) Graphite (G.A.M.I.M) and Tungsten (W) Damage Monitor (DM) exposure parameter values for four positions (SSC, OT, 1/4T, 1/2T) are presented in Section 2.2. A low power PSF startup experiment run was made for these French DM irradiations in order to avoid excessive heating on the G.A.M.I.M monitors. These experimentally derived graphite and tungsten damage/activation ratios are dimensionless quantities that are to be used with measured nickel fluences to derive damage fluences (E > 0.1 and 1.0 MeV) and dpa in iron.

As discussed in Section 3.0, the PSF startup experiments afforded an ideal opportunity for the intercomparison of the results of radiometric (RM) dosimetry measurements by a large number of program participants. While the agreement among the majority of the laboratories was, most often, satisfactory, with non-fissile dosimeter results generally falling within 5% and the fissionable dosimeter results falling within 10%, improvement is still required (See Table 3.6 on Identification of Problems) to routinely meet accuracy goals of the LWR-Pressure Vessel surveillance physics-dosimetry.

A 10% accuracy for the exposure parameter values for metallurgical specimens is quite sufficient for most metallurgical damage correlation studies. However, since the two year ORR-PSF physics-dosimetry-metallurgy experiment is intended to be a benchmark, higher accuracies and more thorough study of the uncertainties are required. Thus, for both the 2-year PSF and 18-day PSF startup experiments, comprehensive statistical analyses with the use of adjustment procedures were made by program participants to obtain complete three-dimensional fluence-spectrum maps (Figure S.3). These maps included not only the exposure parameter values of thermal fluence, fluence (E > 0.1 and 1.0 MeV), and dpa in iron, but also reaction rate values for all major broad energy and threshold reactions; see Ref. (Mc87c) for discussions of the results of the 2-year PSF Experiments.

The results of a consistency analysis and the RR&A exposure parameter values integrated over the appropriate exposure times for the ORR/PSF (4/12) 18-day Startup and SSC-1 and SSC-2 irradiations are presented in Sections 5.2 and 6.1. It is noted that the RR&A exposure values are given for the locations of the UK dosimetry capsules. Exposure parameter values for fluence (E > 0.1 and 1.0 MeV), dpa in iron, and dpa in sapphire are presented. The assigned uncertainties are in the 13% to 22% (one-sigma) range. The irradiation times are also given, which permits the derivation of fluence and dpa rates.

CEN/SCK derived average values of fluence rate [flux (E > 1 MeV)] at a nominal power of 30 MW from the different detector types irradiated in the 18-day startup test are presented in Ref. To82a. As stated by Tourwé et al. :

> *"Appreciable differences are observed in the flux (E > 1 MeV) data according to the interpretation based on the DOT spectra or on the ANISN spectra: The differences become more important when penetrating into the pressure vessel wall. The neutron flux > 1 MeV in the SSC position and the 1/4 T position could be determined with an accuracy better than 10%."*

For the 18-day startup test, HEDL analyzed the radiometric data supplied by six participants (Ke82) but did not derive any exposure parameter values.

The HEDL-ORNL recommended-consensus physics-dosimetry data and data bases for the metallurgical specimens for the SSC and SPVC experiments have been established and are discussed in Refs. Gu84d, St84, Mc86b, Mc87c, and Mc87d.

The KFA recommended physics-dosimetry data base for the metallurgical specimens for the SSC and SPVC experiments are presented in Ref. Sc86a.

In addition to these HEDL, ORNL and KFA results, other LWR-PV-SDIP participants have established their own evaluated data bases related to their use of data and/or analyses for Part I, II and III of the PSF Blind Test; see Ref. Mc86b.

Appendix B of Ref. Mc87c provides information on the HEDL analysis and derivation of exposure parameter values for the SVBC experiment; these results deserve more extensive study by LWR-PV-SDIP participants because they might provide more information on possible causes of some observed systematic biases between calculated and measured quantities (see Section 6.2 and Ref. Mc87c).

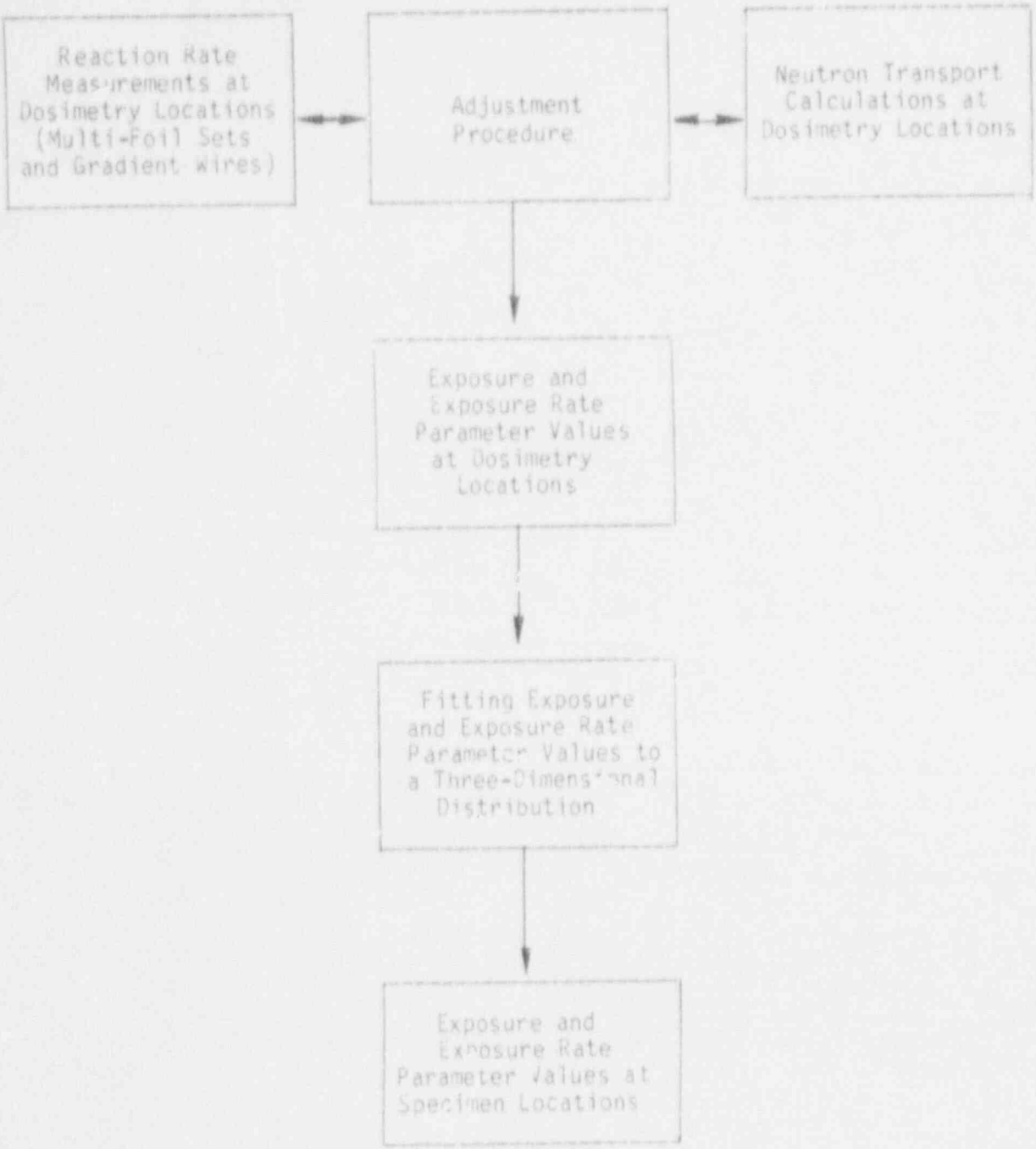

FIGURE S.3. Methodology for the Determination of Exposure and Exposure Rate Parameter Values and Uncertainties.

S.4 COMPARISON AND EVALUATION OF PHYSICS-DOSIMETRY RESULTS AND DATA

Physics-dosimetry analyses of the PCA and PCA Replica and the PSF experiments followed by the application of neutron flux-spectral adjustment procedures and sensitivity analyses have been perform at HEDL, ORNL, CEN/SCK, RR&A, AERE-Winfrith and other participating laboratories.

Under idealized environmental conditions (benchmark), modern computational techniques are currently capable of predicting absolute in-vessel neutron reaction rates per unit of reactor power to within 15% (one-sigma), but generally, not to within 5% (one-sigma). This is a great improvement compared with the situation prevailing a few years ago, before the PCA and PSF experiments were undertaken, where factors of two or more differences between FSAR predictions and surveillance capsule measurements were not uncommon. The achievable accuracy will be markedly less, however, in applications to actual nuclear power plants.

For the PCA, the results of the consistency analyses by HEDL, ORNL and RR&A indicate that the reactor physics calculations appear to be biased on the low side and differences outside the derived one-sigma uncertainties were observed in some cases. Comparisons of derived exposure parameter values in the PV block show differences between the three laboratories of up to 12%. No consistent bias between the results exists, when all the PCA configurations are considered.

For ORNL studies, and as previously stated, differences among measurements and calculations for the PCA and PSF have generally been in the 10% to 20% range. Somewhat larger differences between measurements and calculations have been noted for comparisons that include transport through several inches of iron and for particular dosimeters. Discrepancies between measurements and calculations relative to the PSF startup experiment are within expected ranges based on previous PCA evaluations, known uncertainties associated with nuclear data, measurements, and applicable computational methodology.

For RR&A studies, overall the results obtained by both the ANISN and MCBEND calculations achieved two of their main objectives: To provide (a) accurate neutron spectra for the analysis of dosimetry measurements made on the metallurgical PSF 4/12 irradiations and (b) scoping values of reaction rates and neutron fluxes throughout the experimental array. The underprediction by about 10% of reaction rates using the MCBEND technique was, however, something of a disappointment, given the success of the recent reanalysis of the PCA 12/13 "Blind Test" using the same technique. Nevertheless, these results were <u>not</u> inconsistent with the level of stochastic uncertainty achieved, which was necessarily limited by economic considerations. In that sense the MCBEND technique does provide more realistic and reliable estimates of reaction rates and fluxes than can be achieved by purely deterministic (i.e., ANISN and DOT) transport calculations whose uncertainty is entirely unquantified and where good agreement can often only be achieved after a judicious amount of 'a priori' benchmarking and 'ad hoc' synthesis.

To advance PV neutron transport methodology, more complete answers must be found for a number of existing inconsistencies between measured and calculated

reactor physics parameters for the PCA, PSF, VENUS, NESDIP and PWR and BWR cavity and surveillance capsule experiments. These inconsistencies are identified in Section 5.1.

ORNL reviewed the apparent C/E inconsistencies for the NESDIP2 and NESDIP3 benchmarks, and found that if the AERE-Winfrith measured spectrum is folded with the reaction cross sections used in obtaining the calculated activities, the resulting agreement with the measured activities is excellent; this lends great credibility to the measured spectrum, measured activities, and the dosimetry cross-sections.

To better understand the reasons for some of the inconsistencies between calculated and measured "through PV wall" quantities for the PCA and PSF benchmarks, HEDL has fit an exponential function [of the form $(\Phi t) = (\Phi t)_0 \exp(-br)$] to PCA, PSF, and Gundremmingen through wall dosimetry derived flux and/or fluence results. The least-squares derived exponential b-value for the PCA is about 6.3% higher than that observed for the PSF. Some differences between the PSF and PCA results should be anticipated because of differences that exist in these two PV mockups.

For Gundremmingen, a very preliminary b-value was obtained using fission spectrum derived values of fluxes that are based on EG&G-Idaho 54Fe(n,p)54Mn through wall activation measurements. Here again, an exponential representation is found to be an excellent fit to these data. It would be of considerable interest to repeat the Gundremmingen analysis using dosimetry adjusted flux (E > 1 MeV) values and to perform a similar analysis on measured 54Mn activation results from trepans that might be removed from the Shippingport PWR reactor vessel; presently, the only Shippingport steel specimens that are available are those that have been taken from trepans that were removed from the reactor shield tank.

A study of the consistency of the b-values for the PCA Replica, the other five PSF experiments and Gundremmingen should be accomplished. Such a study is needed to determine if there are any benchmark-to-benchmark undefined systematic differences that might be detected by differences in the b-values between the results of the PCA, PCA Replica, the seven PSF experiments and Gundremmingen.

1.0 DESCRIPTION OF THE EXPERIMENTAL FACILITY - SUMMARY

L. F. Miller

The Oak Ridge Research Reactor (ORR) is designed so that one face of the core is in close proximity to an open pool with an aluminum plate (window) separating the reactor core from the open pool. Several experimental facilities have been located in the pool next to the aluminum window for performing irradiation studies. The Poolside Facility (PSF), installed for the LWR Pressure Vessel Surveillance Dosimetry Program, was used in performing the PSF Startup Experiment in the Fall of 1979. Results from measurements and calculations are reported by Williams (Wi82) and Maerker (Ma84a). The specific configuration of the PSF for the PSF Startup Experiment is described by Williams (Wi82) and Section 1.1 of this report. Details of the PSF, as well as its location relative to the ORR core, are described in Section 1.1.

1.1 PHYSICAL DESCRIPTION OF THE PSF

L. F. Miller

The Pool Side Facility (PSF) is a versatile irradiation facility located in the pool adjacent to the ORR at ORNL and is designed specifically to accommodate functional objectives of the LWR Pressure Vessel Surveillance Dosimetry Improvement Program. One of these objectives is to generate a variety of radiation environments characteristic of commercial LWRs in which metallurgical test specimens can be irradiated. This is accomplished, in part, by allowing one to vary the distances between the following components:

1. the aluminum window adjacent to the reactor face and the thermal shield (TS), and

2. the TS and the pressure vessel simulator (PVS).

Other objectives obtained by the PSF include maintaining a specified temperature environment for the metallurgical test specimens and providing a stable structure that ensures accurate positioning of major components throughout the irradiation time period.

This report is limited to the description, measurement results, and analysis of SSC-1, SSC-2, and the PSF startup characterization experiment. Thus, this section, the physical description of the PSF, consists of a general description of the facility along with some details relative to SSC-1, SSC-2, and the PSF startup characterization experiment.

Figure 1.1.1 illustrates the major features of the ORR and the location of the PSF experiment. Note that the PSF is adjacent to an aluminum window which forms an integral boundary with the ORR pressure tank. The aluminum window is adjacent to the reactor lattice shown in Figure 1.1.2 and is nearly transparent to neutrons that leak from the ORR core. Exploded views of the PSF are given in Figures 1.1.3 and 1.1.4. The retraction mechanism shown in Figure 1.1.3 is used to move the entire support structure, along with the capsules, away from and toward the aluminum window. This capability allows the irradiation capsules to be retracted from or inserted into the ORR irradiation field as required by operational considerations. The notches in the support structure, shown in Figure 1.1.4, adjacent to the PVS allow for visual inspection of the distance between the PVS and TS. Exact positioning is accomplished by bolting the PVS supports to the carriage structure as illustrated by ORNL Drawing M11501-OR-10D. Dowel pins located in the rigid support structure determine the distance between the TS and aluminum window. These pins are engaged when the upper support structure, shown in Figure 1.1.3, is inserted toward the reactor with the retractor mechanism. Assembly, fabrication, and positioning details are provided by the ORNL drawing series M11501-OR, which is available from central files at ORNL.

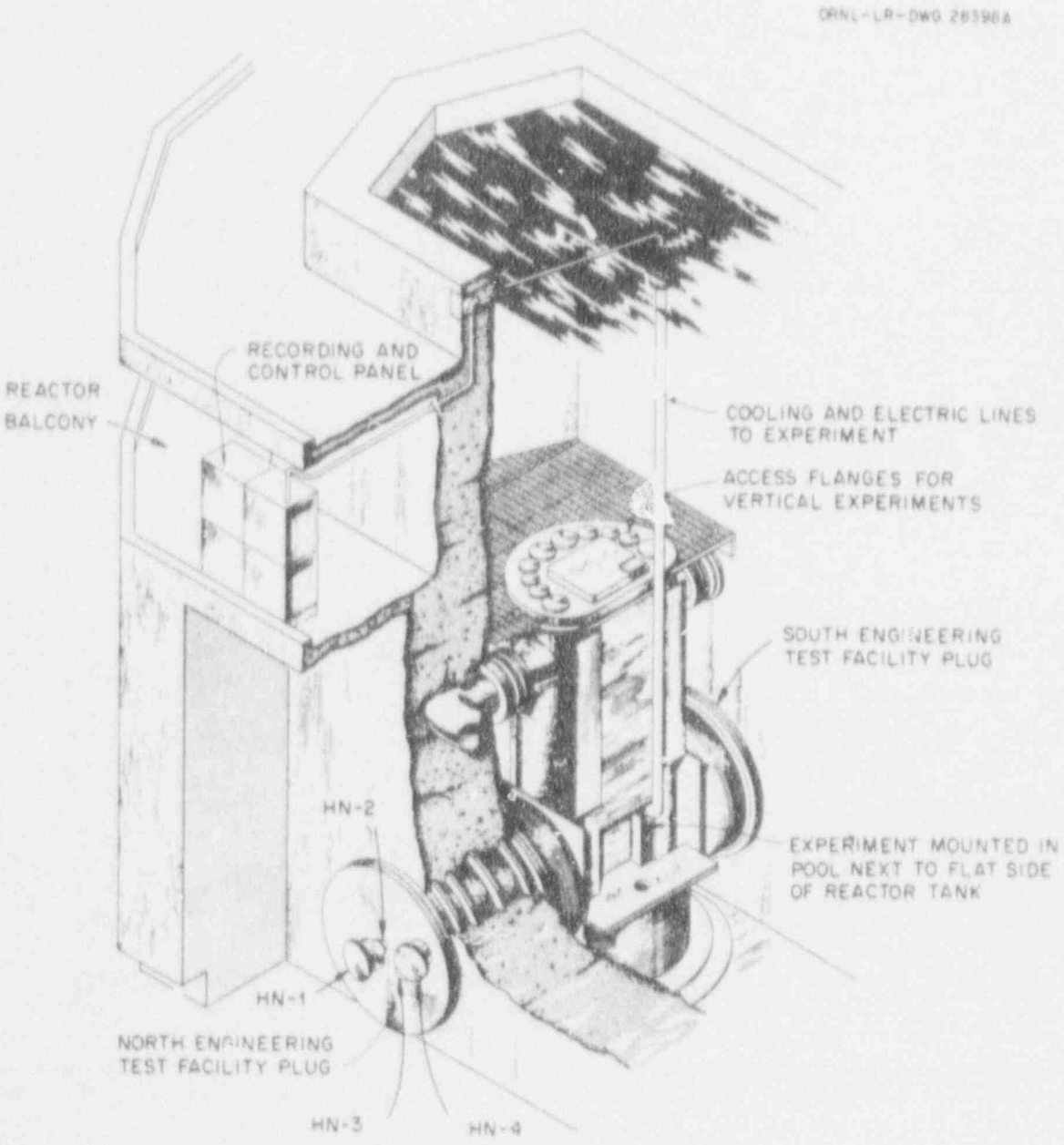

FIGURE 1.1.1. Illustration of Major Components of the Oak Ridge Research Reactor.

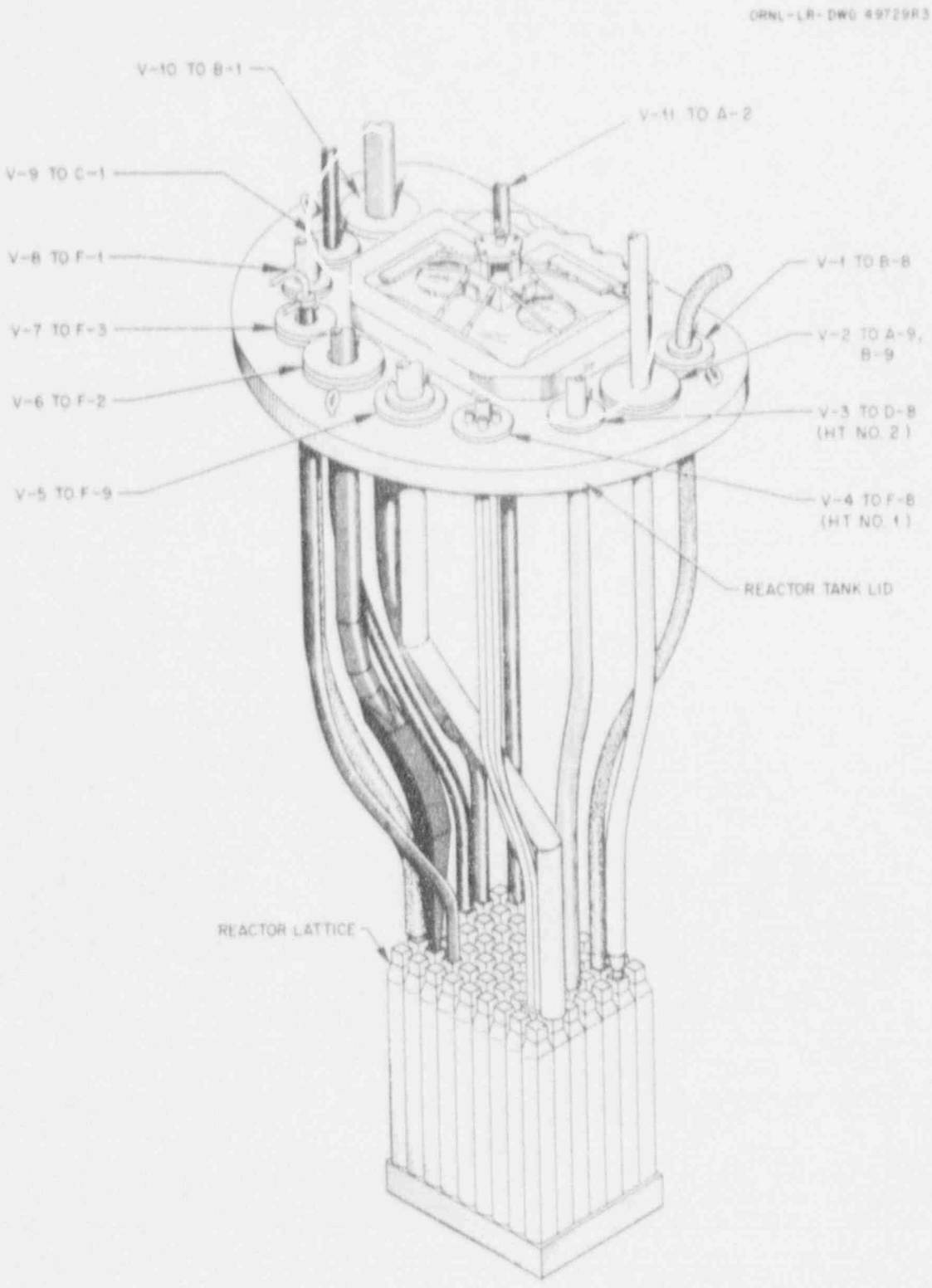

FIGURE 1.1.2. Illustration of the Oak Ridge Research Reactor Fuel Assembly Lattice and In-Core Access Tubes.

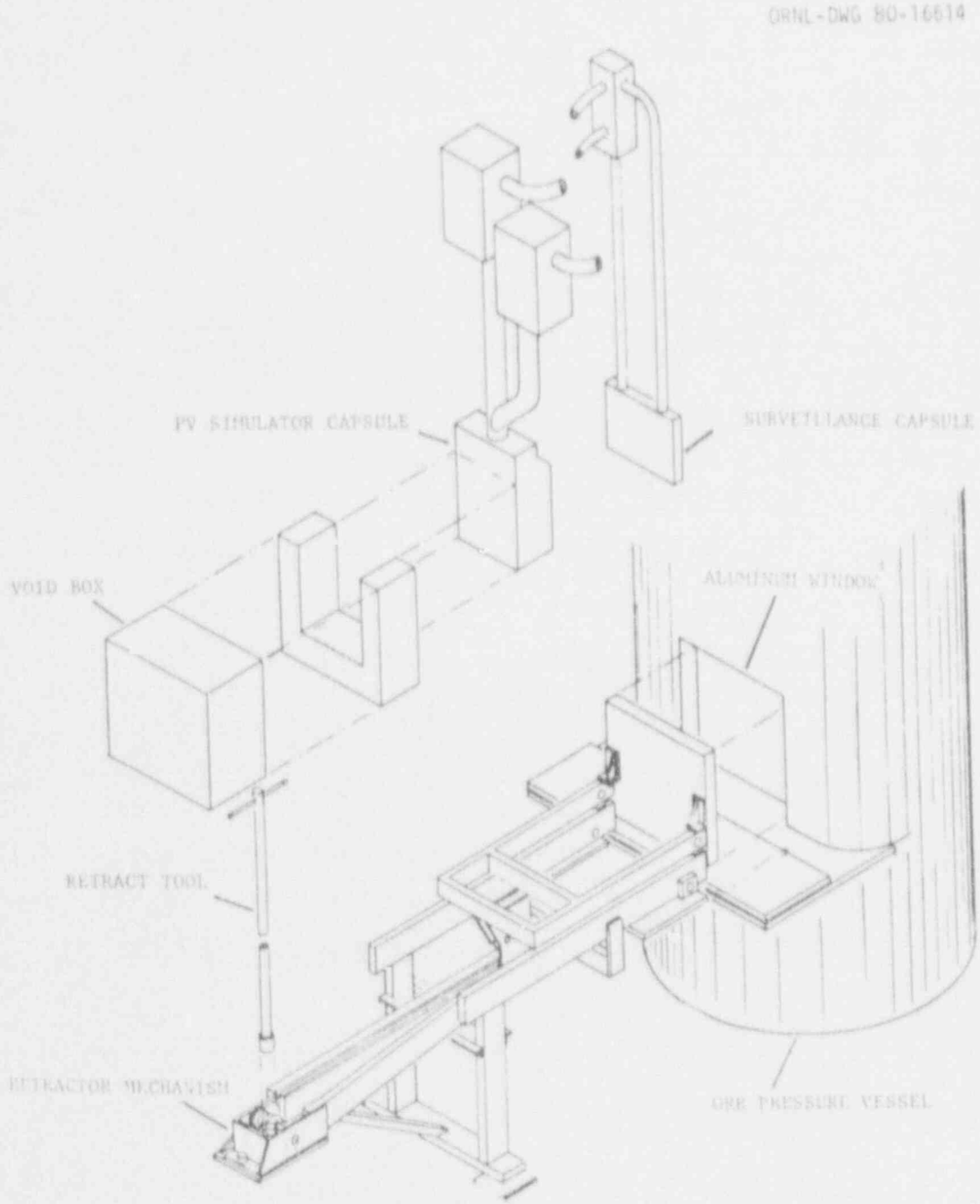

FIGURE 1.1.3. Illustration of the Pool Side Facility and the Oak Ridge Research Reactor Pressure Tank.

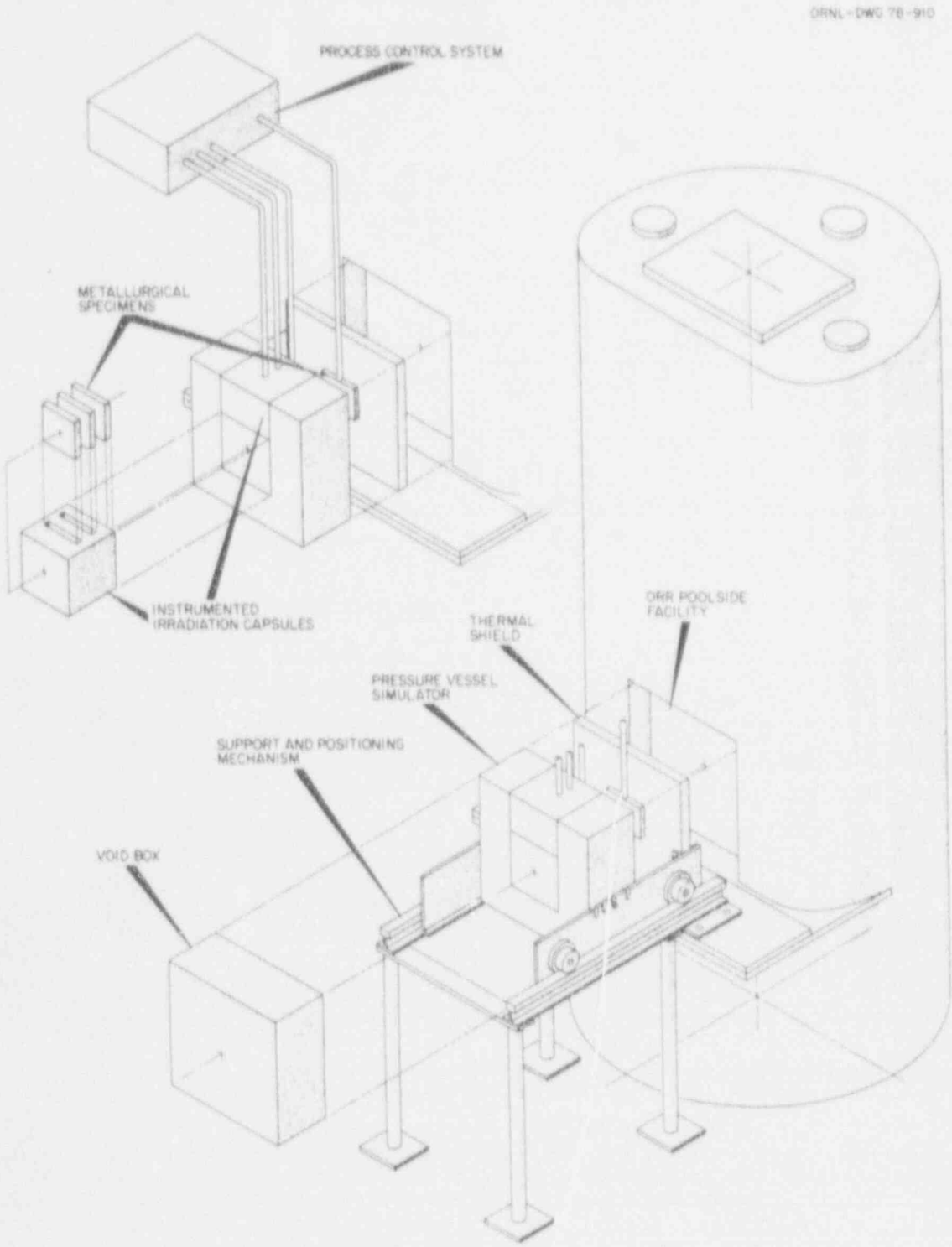

FIGURE 1.1.4. Illustration of the Pool Side Facility (PSF) Irradiation Capsules Relative to the ORR Pressure Tank and the PSF Support Structure.

For both SSC-1 and SSC-2, the front of the TS is displaced 4 cm from the outside of the aluminum window, and the front of the surveillance capsule is displaced 10.8 cm from the outside of the aluminum window. Elevation and plan views that locate the surveillance capsules relative to the aluminum window and other capsules installed in the PSF are provided by Figures 1.1.5 and 1.1.6. Detailed dimensions of surveillance capsule internals are given in Figure 1.1.7. Sectional views of SSC-1 and SSC-2 are illustrated in Figures 1.1.8 and 1.1.9. Specimen identifications are given by Figures 1.1.10 and 1.1.11.

A plan view of the Westinghouse Perturbation Experiment is shown in Figure 1.1.12 with essential dimensions listed. Note that there are two perturbed and two unperturbed vertical measurements and one horizontal traverse of measurements. Additional details relative to this experiment are provided by two papers (Ma82e,To82) in Proceedings of the Fourth ASTM-EURATOM Symposium on Reactor Dosimetry.

Details relative to the ORR-PSF Startup Experiment are given in Figures 1.1.13 and 1.1.14. These figures illustrate dimensional information necessary for analyses of data or calculations and provide the essential details for the determination of core composition. Results from calculations and measurements are discussed in Section 4.1.

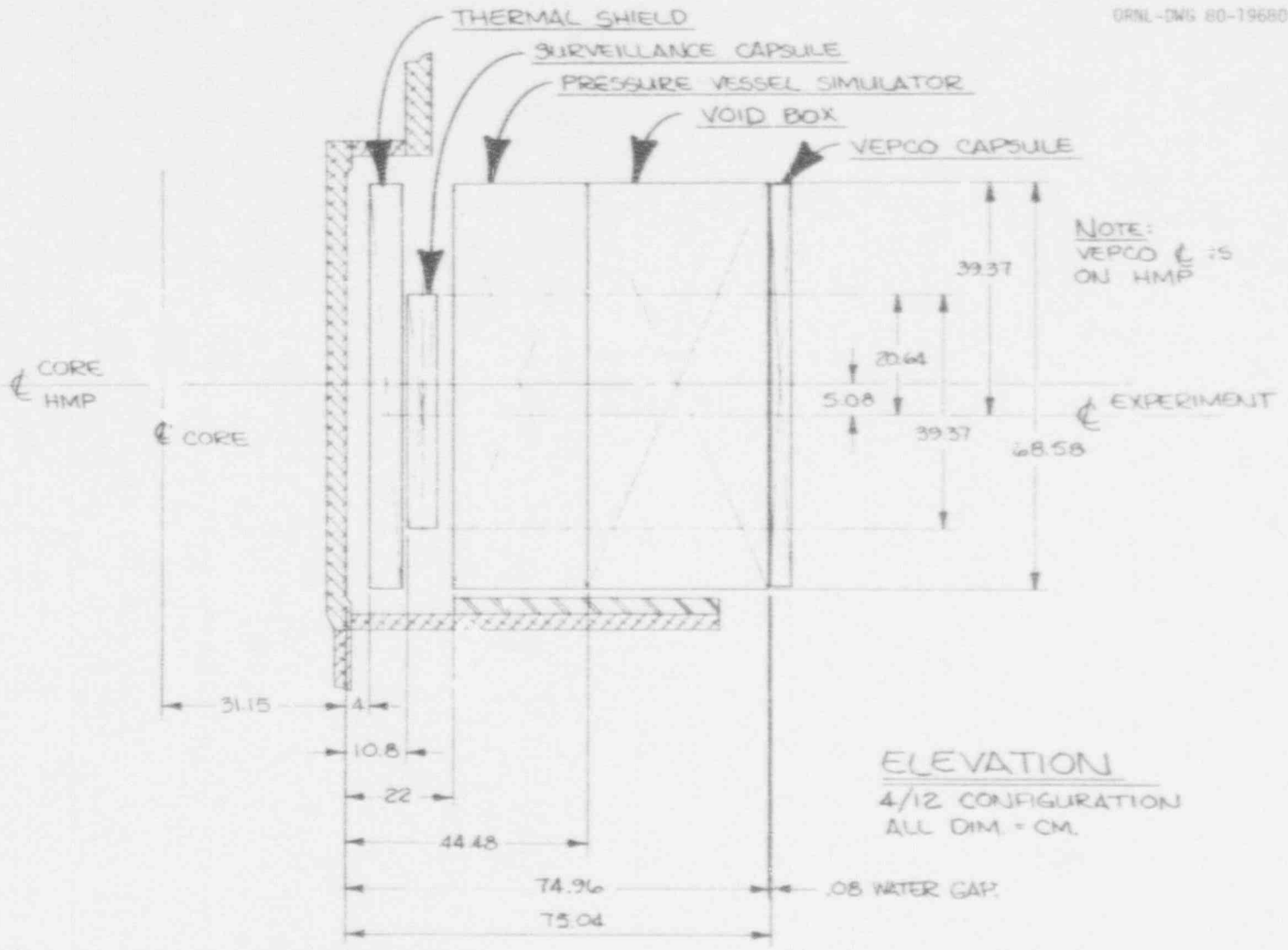

FIGURE 1.1.5. Elevation View Schematic of the Pool Side Facility Major Components with Dimensions Essential for Neutronics Calculations Listed.

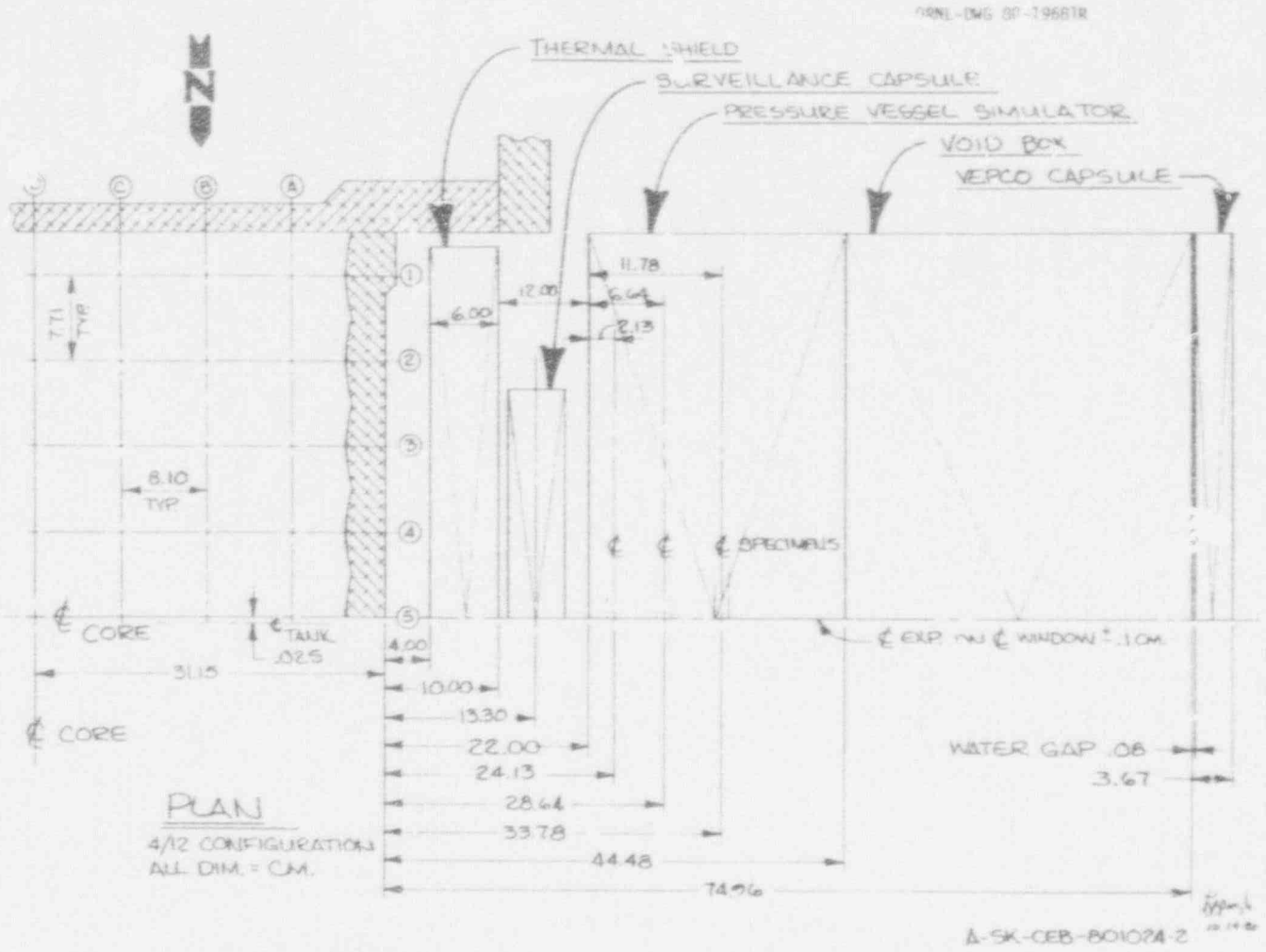

FIGURE 1.1.6. Plan View Schematic of the Pool Side Facility Major Components with Dimensions Essential for Neutronics Calculations Listed.

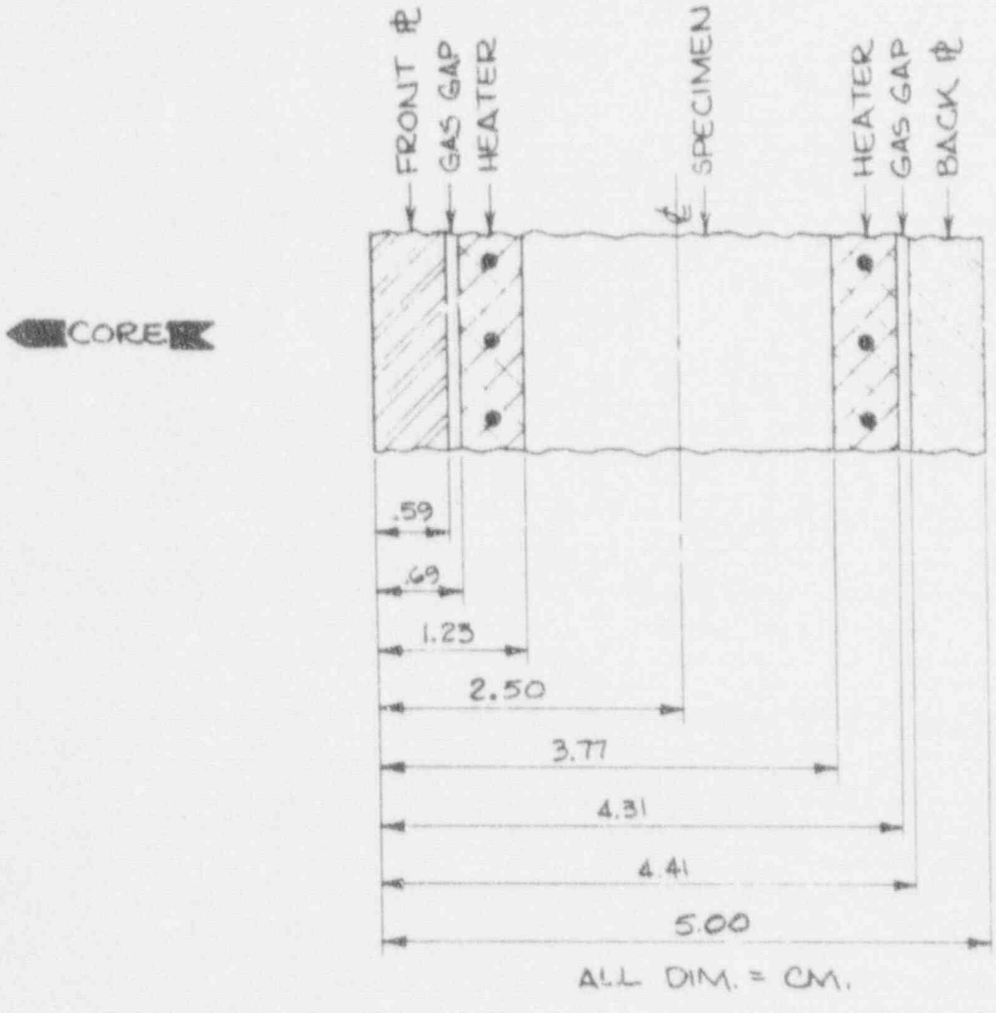

FIGURE 1.1.7. Side View Schematic of the Surveillance Capsule with Dimensions of Internal Components Listed.

ORNL-DWG 80-20402

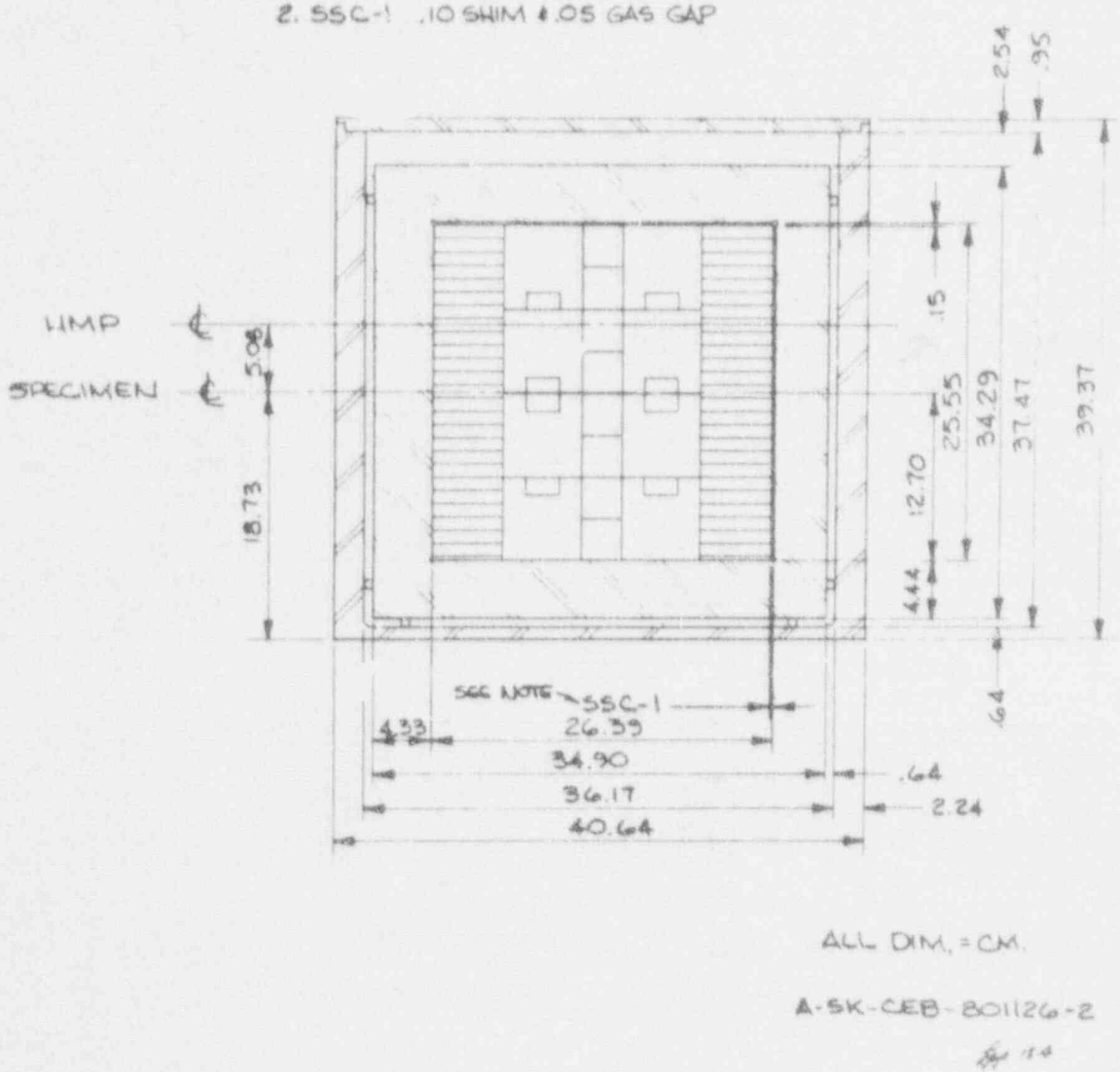

FIGURE 1.1.8. Front Sectional View Schematic of the First Simulated Surveillance Capsule (SSC-1) with Dimensions of Internal Components Listed.

ORNL-DWG 80-20403

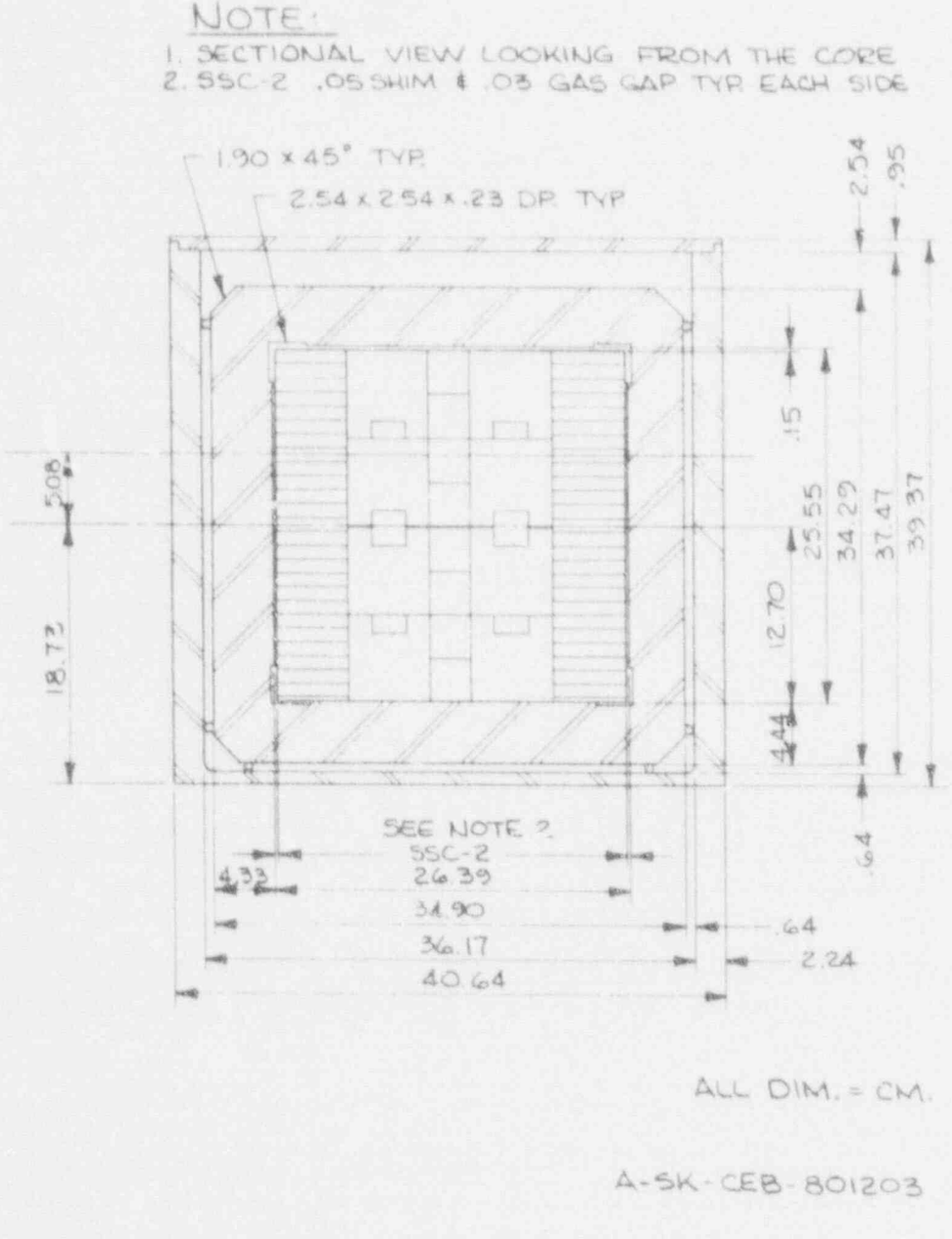

FIGURE 1.1.9. Front Sectional View Schematic of the Second Simulated Surveillance Capsule (SSC-2) with Dimensions of Internal Components Listed.

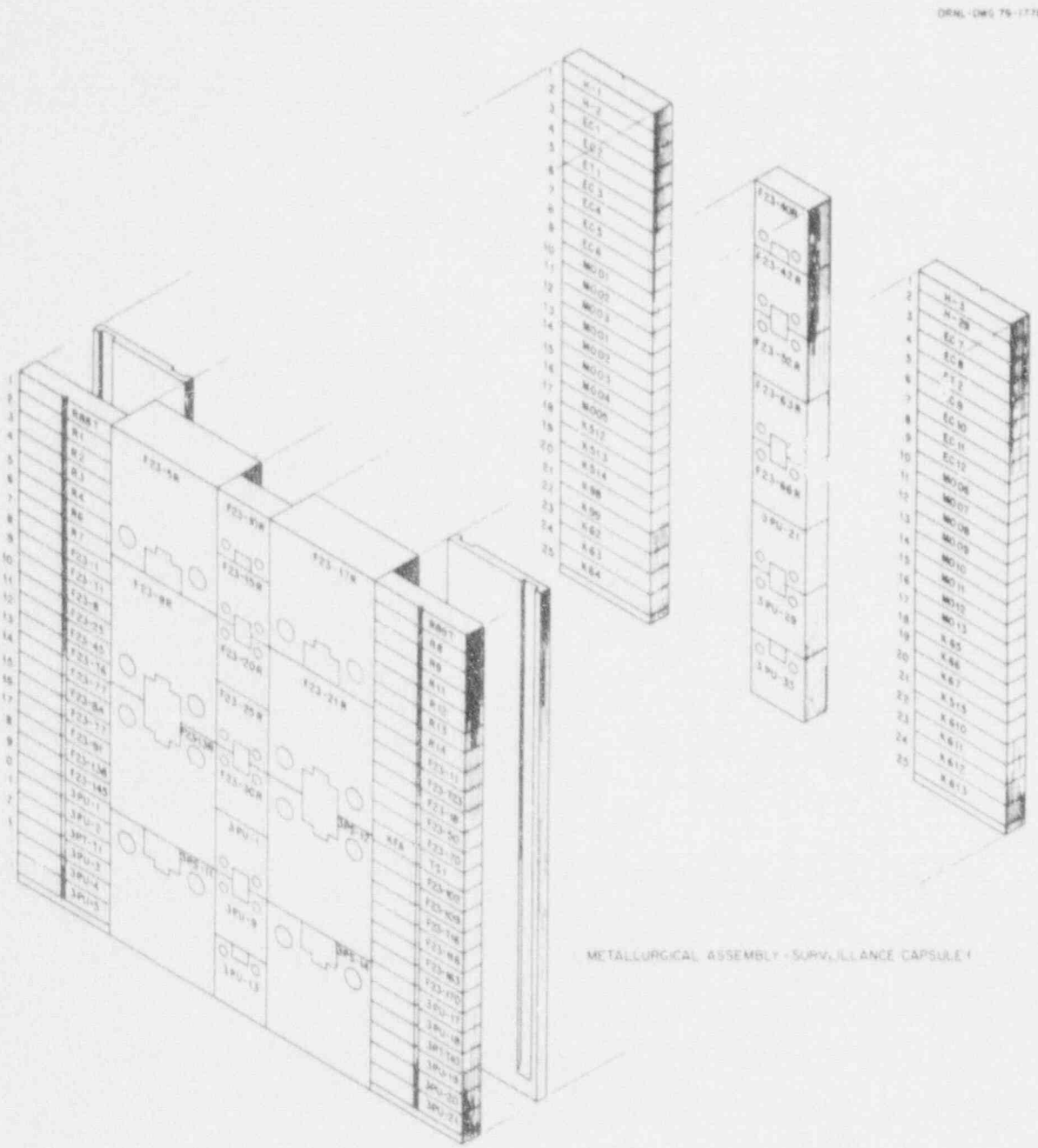

FIGURE 1.1.10. Specimen Identification for the First Simulated Surveillance Capsule (SSC-1).

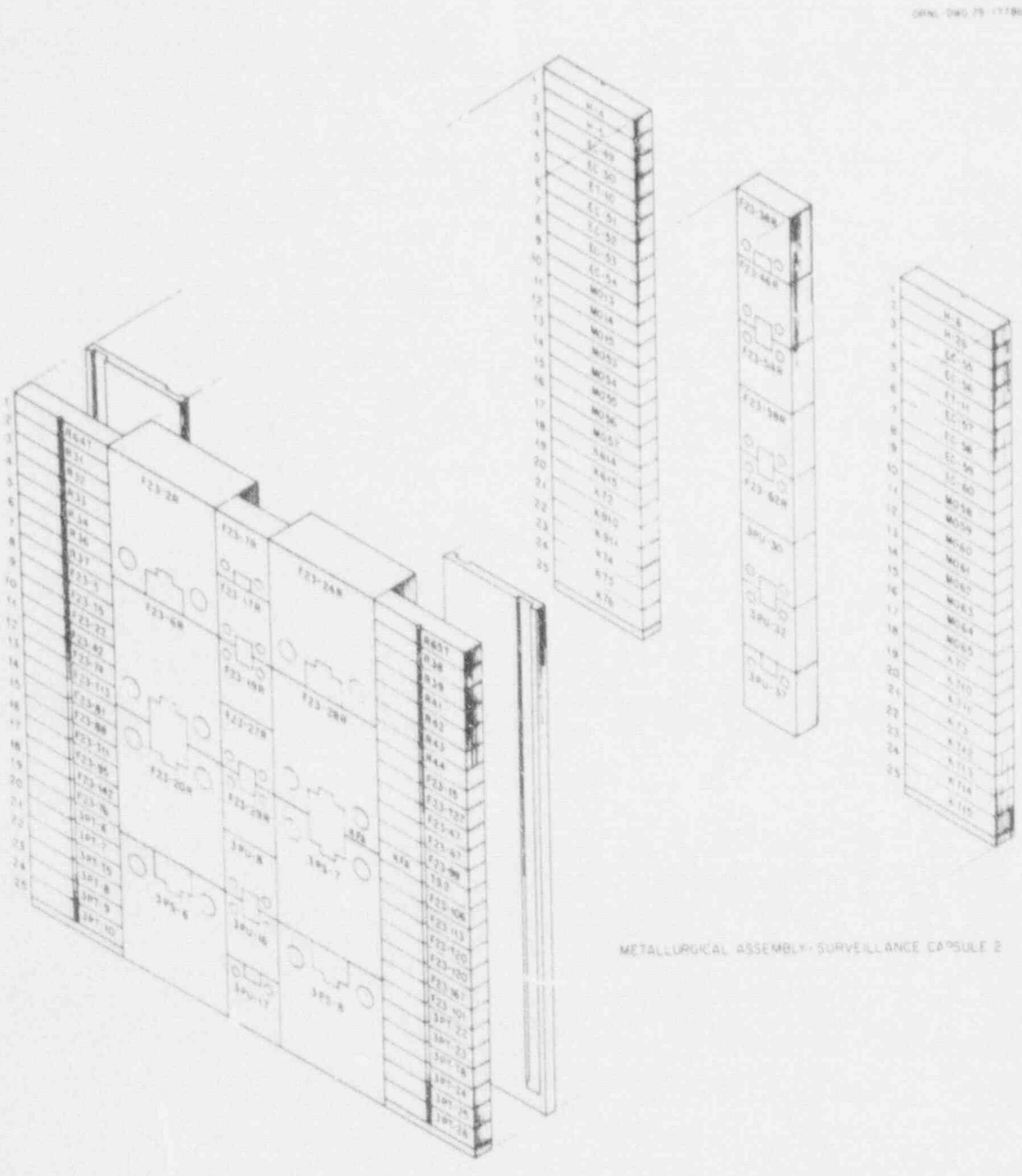

FIGURE 1.1.11. Specimen Identification for the Second Simulated Surveillance Capsule (SSC-2).

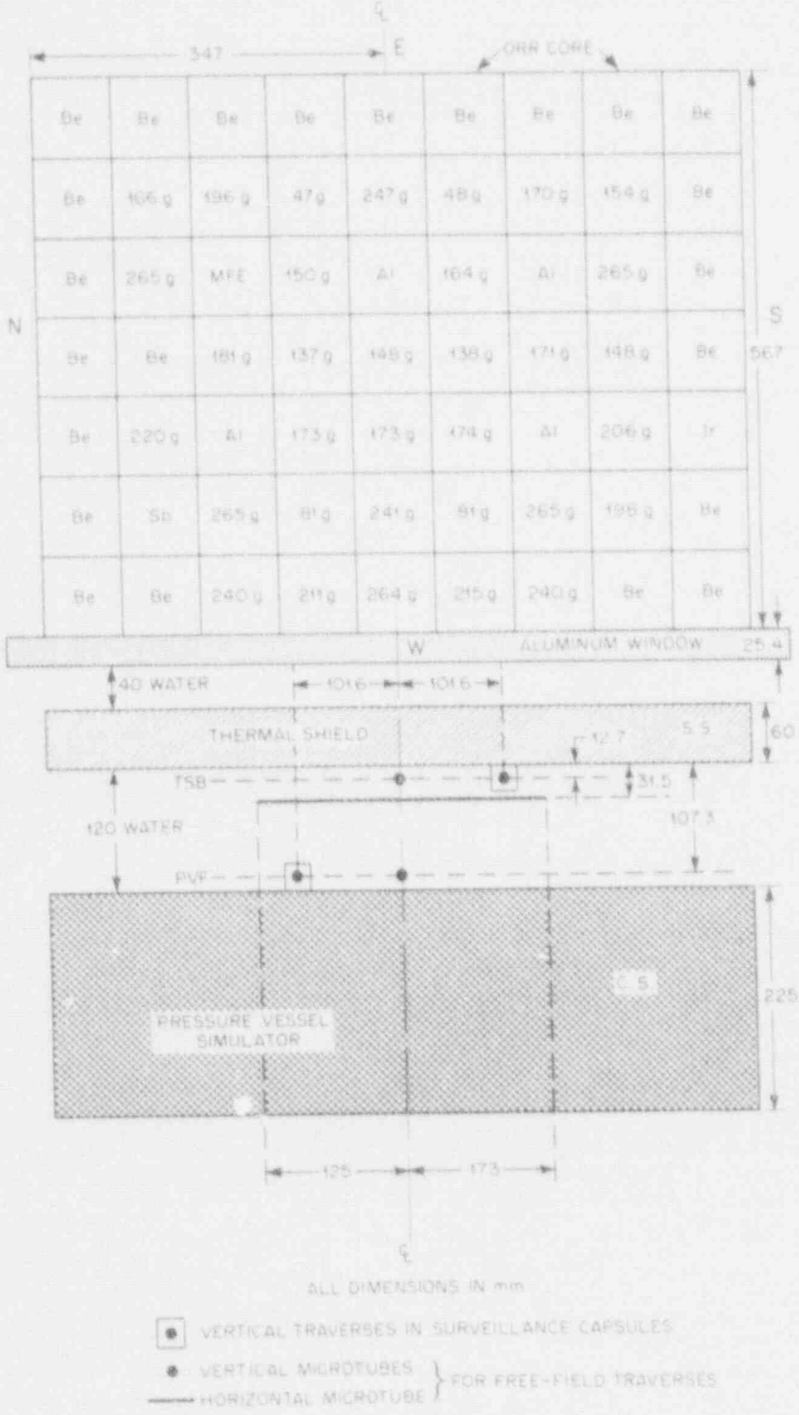

FIGURE 1.1.12. Horizontal Cut at Location of Maximum Axial Flux of ORR-PSF Westinghouse Perturbation Experiment.

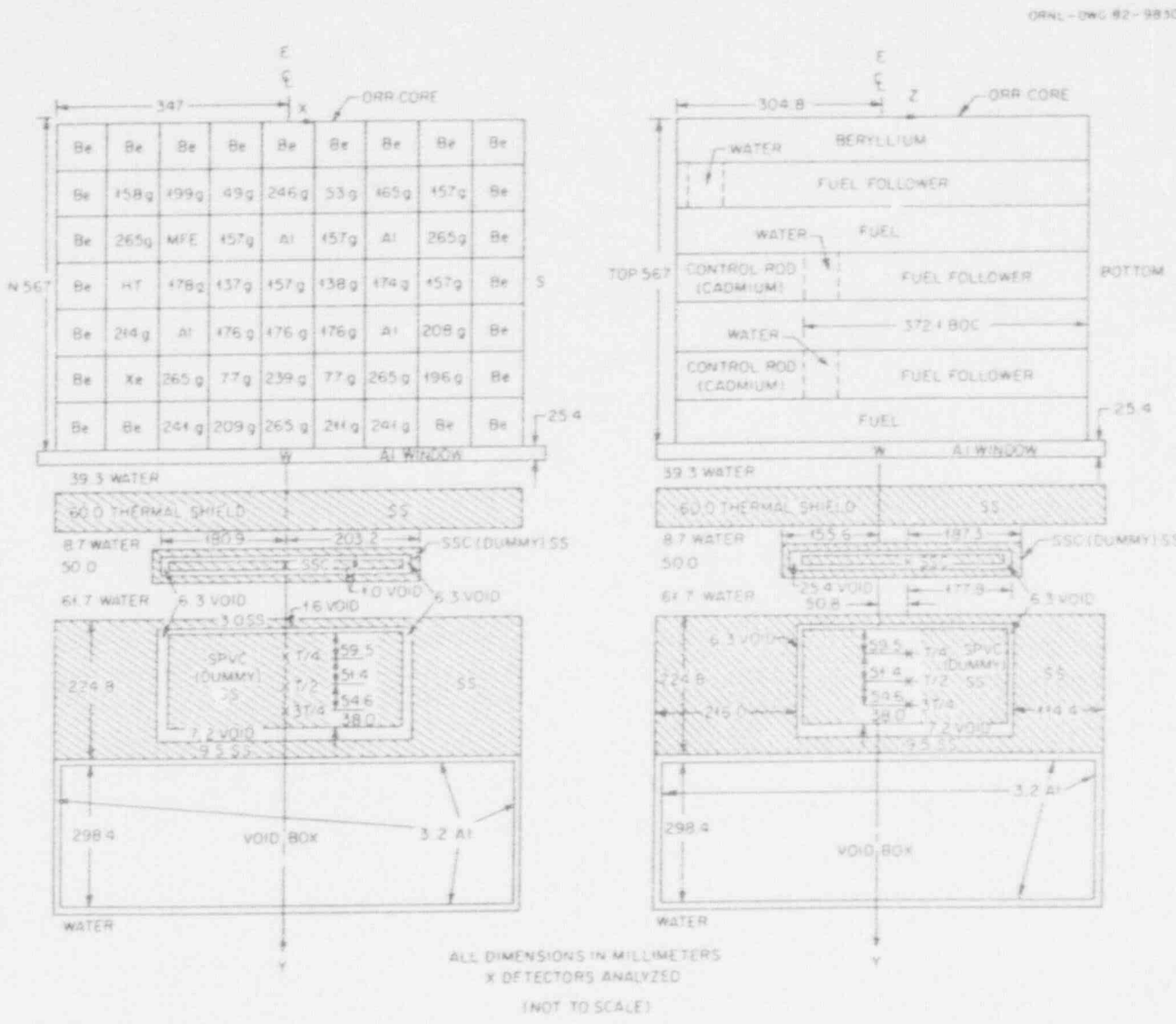

FIGURE 1.1.13. Horizontal (XY) Cut at location of Maximum Axial Flux of ORR-PSF Startup Experiment.

FIGURE 1.1.14. Vertical (YZ) Cut at Location of Radial Centerline of ORR-PSF Startup Experiment.

1.2 CALCULATED CORE POWER

L. F. Miller

The core power and neutron source distributions were calculated by Williams (Wi82) in order to perform transport calculations for the analysis of the PSF Startup Experiment. Results from the transport calculations were obtained by Williams (Wi82) and Maerker (Ma84a), but they did not document the fixed source for subsequent comparative calculations. Thus, the fixed neutron source used in these calculations is reported herein.

The core loading (151-A) at the beginning of the fuel cycle, during which the dosimeters were irradiated, is shown in Figure 1.2.1. Middle-of-cycle (MOC) burnup and control rod conditions were used to define input to the diffusion theory code VENTURE (Vo81), however, since the irradiations were performed during the last 18 days of the fuel cycle. These conditions were obtained by an auxiliary code, VIPORR, which generated applicable input for VENTURE.

PSF EXPERIMENT

Be	Be	Be	Be	Be	Be	Be	9
Be	Xe	214g	HT	265g	158g	Be	8
241g	265g	Al	178g	MFG	199g	Be	7
209g	77g	176g	137g	157g	49g	Be	6
265g	239g	176g	157g	Al	246g	Be	5
211g	77g	176g	138g	157g	53g	Be	4
241g	265g	Al	174g	Al	165g	Be	3
Be	196g	208g	157g	265g	157g	Be	2
Be	Be	Be	Be	Be	Be	Be	1
A	B	C	D	E	F	G	

COLUMN

ROW

FIGURE 1.2.1. Illustration of Core Loading and Locations by Row (Alphabetic) and Column (Numeric) Relative to the PSF Experiment and Core Orientation.

Results from the three-dimensional neutron source distribution are available on a mass-storage unit at ORNL and will be distributed for requests relevant to LWR dosimetry program objectives. However, it is not expected that the three-dimensional distribution will be used, since transport calculations typically require two-dimensional input. In particular, two-dimensional vertical and horizontal neutron source distributions are used as input for two two-dimensional transport calculations. Results from the horizontal and vertical transport calculations are used in a flux-synthesis technique (Ma84a) to obtain three-dimensional neutron-flux distributions external to the reactor core. Thus, the two-dimensional horizontal and vertical source distributions are reported herein.

The neutron source distributions listed in Tables 1.2.1 and 1.2.2 are obtained by integrating the three-dimensional distribution in the appropriate transverse directions. In particular, the horizontal distribution, given by Table 1.2.1 is defined by

$$S_H(x,z) = \int_0^H dy S(x,y,z) \quad .$$

The vertical distribution is given by

$$S_V(y,z) = \int_0^V dx S(x,y,z) \quad .$$

Note that the coordinate system used for the VENTURE calculations designates y as the vertical axis and z as the axis perpendicular to the experiment.

Each of the nine numbers listed in each fuel element location of Table 1.2.1 represents the absolute neutron source (in units of neutrons per square centimeter per second) for one-ninth of the fuel element (when multiplied by 10^{15}) with the ORR at 30 MW. The diffusion theory model for this calculation specifies a three-inch square pitch for the fuel elements. Thus, each number listed specifies the average source strength [$n/(cm^2 \cdot s)$] over a one-inch square area.

The nine numbers listed in each square for the vertical distribution, shown in Table 1.2.2, have the same units as those listed in Table 1.2.1 and represent the same area. The axial profile is broken into one-inch segments and the fuel elements remain on a three-inch square pitch.

Tables 1.2.1 and 1.2.2 (in conjunction with Figure 1.2.1 and with the physical description given in Section 1.1 of this report) should provide sufficient data and descriptive information for analyzing the PSF startup experiment and for performing relevant transport calculations.

TABLE 1.2.1

LISTING OF THE HORIZONTAL PLANE NEUTRON SOURCE DISTRIBUTION
FOR THE ORR PSF STARTUP EXPERIMENT

PSF EXPERIMENT

Col / Row	1			2			3			4			5			6			7			8			9		
	0	0	0	0	0	0	1.299	1.217	1.235	1.139	1.160	1.148	1.317	1.272	1.256	1.014	.9888	.9370	.9694	.9127	.9617	0	0	0	0	0	0
A	0	0	0	0	0	0	1.387	1.270	1.279	1.186	1.211	1.192	1.339	1.285	1.271	1.043	1.020	.9636	.9833	.9312	1.037	0	0	0	0	0	0
	0	0	0	0	0	0	1.511	1.407	1.402	1.332	1.375	1.351	1.510	1.447	1.428	1.172	1.150	1.079	1.081	1.025	1.178	0	0	0	0	0	0
	0	0	0	1.588	1.521	1.473	1.725	1.668	1.713	.5136	.5403	.5366	1.584	1.512	1.490	.4755	.4653	.4319	1.301	1.217	1.433	0	.1796	0	0	0	0
B	0	0	0	1.575	1.492	1.461	1.772	1.738	1.796	.5475	.5796	.5777	1.703	1.624	1.600	.5101	.4980	.4596	1.358	1.271	1.509	0	.3426	0	0	0	0
	0	0	0	1.613	1.514	1.485	1.844	1.821	1.867	.5621	.5972	.6011	1.817	1.745	1.707	.5311	.5130	.4699	1.402	1.335	1.507	0	1.852	0	0	0	0
	0	0	0	1.748	1.623	1.580	0	0	0	1.386	1.504	1.540	1.515	1.481	1.428	1.356	1.272	1.128	0	0	0	1.308	1.308	1.314	0	0	0
C	0	0	0	1.784	1.647	1.596	0	0	0	1.402	1.521	1.569	1.575	1.564	1.486	1.384	1.284	1.133	0	0	0	1.522	1.084	1.138	0	0	0
	0	0	0	1.843	1.706	1.647	0	0	0	1.373	1.457	1.504	1.564	1.552	1.477	1.332	1.232	1.103	0	0	0	1.180	1.171	1.227	0	0	0
	0	0	0	1.684	1.600	1.374	1.458	1.430	1.375	1.014	1.010	1.647	1.329	1.357	1.258	.9388	.8638	.8141	1.036	1.032	1.058	0	0	0	0	0	0
D	0	0	0	1.464	1.383	1.362	1.471	1.439	1.371	.9840	.9685	.9906	1.250	1.277	1.191	.8901	.8252	.7821	.9986	.9817	1.018	0	0	0	0	0	0
	0	0	0	1.368	1.279	1.260	1.341	1.327	1.295	.9717	.9770	.9837	1.152	1.162	1.115	.8835	.8287	.7625	.8119	.7572	.7949	0	0	0	0	0	0
	0	0	0	1.964	1.786	1.785	0	0	0	1.159	1.214	1.175	0	0	0	1.061	1.007	.8349	0	0	0	1.072	1.199	1.313	0	0	0
E	0	0	0	1.807	1.635	1.672	0	0	0	1.184	1.262	1.206	0	0	0	1.087	1.038	.8357	0	0	0	.8862	1.000	1.126	0	0	0
	0	0	0	1.766	1.619	1.669	0	0	0	1.212	1.303	1.235	0	0	0	1.108	1.077	.8825	0	0	0	.8987	.9910	1.098	0	0	0
	0	0	0	1.156	1.097	1.115	1.189	1.211	1.275	.4797	.5014	.4759	1.615	1.493	1.550	.3881	.3877	.3495	.9617	.8031	.7730	.6858	.6069	.7328	0	0	0
F	0	0	0	1.132	1.095	1.118	1.194	1.225	1.311	.4908	.5126	.4838	1.592	1.430	1.509	.3928	.4090	.3701	1.105	.9452	.8946	.7282	.7166	.7333	0	0	0
	0	0	0	1.122	1.115	1.151	1.241	1.281	1.366	.5062	.5240	.4982	1.711	1.556	1.620	.4063	.4126	.3866	1.210	1.057	.9930	.7807	.7503	.7432	0	0	0
	0	0	0	0	0	0	0	0	0	0	0	0	0	0	0	0	0	0	0	0	0	0	0	0	0	0	0
G	0	0	0	0	0	0	0	0	0	0	0	0	0	0	0	0	0	0	0	0	0	0	0	0	0	0	0
	0	0	0	0	0	0	0	0	0	0	0	0	0	0	0	0	0	0	0	0	0	0	0	0	0	0	0

Values listed must be multiplied by 10^{15} to obtain n/(cm^2·s). These values are obtained by integrating the three-dimensional volumetric source distribution over the axial (vertical) direction. Note that the "A" row faces the PSF experiment.

TABLE 1.2.2

LISTING OF THE VERTICAL PLANE NEUTRON SOURCE DISTRIBUTION
FOR THE ORR PSF STARTUP EXPERIMENT

TOP OF REACTOR CORE

G			F			E			D			C			B			A			Row / Depth (in.)
0	0	0	.4817	.4612	.4661	.3602	.3467	.3280	.3278	.3190	.3261	.3821	.3984	.3694	.3514	.3186	.3052	.2788	.2966	.3085	1
0	0	0	.5000	.4628	.4600	.3557	.3429	.3262	.32 [illegible] 7	.3299		.3917	.4058	.3824	.3570	.3269	.3151	.2876	.3018	.3226	2
0	0	0	.5633	.5195	.5085	.3937	.3783	.3652	.3575	.3612	.3685	.4423	.4591	.4348	.4008	.3741	.3621	.3336	.3488	.3703	3
0	0	0	.6433	.5954	.5783	.4454	.4268	.4121	.4012	.4139	.4[illegible]	.5084	.5293	.5016	.4565	.4323	.4197	.3903	.4081	.4289	4
0	0	0	.6178	.5758	.5509	.4551	.4360	.4.266	.3783	.3997	.4051	.5253	.5469	.5188	.4944	.4721	.4584	.4281	.4477	4.650	5
0	0	0	.6871	.6426	.6129	.5057	.4841	.4745	.4194	.4497	.4564	.5947	.6202	.5884	.5566	.5340	.5191	.4900	.5131	.5270	6
0	0	0	.7500	.7024	.6707	.5536	.5313	.5231	.4632	.4999	.5086	.6678	.6966	.6621	.6225	.5996	.5826	.5570	.5766	5.897	7
0	0	0	.8130	.7637	.7303	.6034	.5826	.5820	.5160	.5643	.5749	.7615	.7881	.7555	.7022	.6787	.6589	.6444	.6509	.6556	8
0	0	0	.8012	.7563	.7224	.6131	.6015	.6497	.5320	.6075	.6141	.8684	.8657	.8607	.8151	.8004	.7681	.8046	.7165	.6996	9
0	0	0	.8517	.8065	.7720	.6554	.6474	.7131	.5847	.6762	.6861	.9754	.9384	.9709	.9107	.8994	.8599	.9232	.7923	.7609	10
0	0	0	.8934	.8476	.8132	.6903	.6822	.7408	.9457	1.054	1.075	1.028	1.006	1.035	1.181	1.165	1.108	.9826	.8521	.8139	11
0	0	0	.9277	.8816	.8475	.7195	.7119	.7697	.9705	1.078	1.105	1.060	1.066	1.092	1.238	1.219	1.161	1.037	.9014	.8588	12
0	0	0	.[illegible]769	.9306	.8959	.[illegible]339	.7282	.7678	.9912	1.101	1.132	1.114	1.[illegible]76	1.128	1.285	1.265	1.705	1.078	.9379	.8896	13
0	0	0	.9959	.9500	.9155	.7500	.7455	.8069	1.018	1.133	1.166	1.149	1.135	1.164	1.326	1.305	1.242	1.113	.9866	.9143	14
0	0	0	1.004	.9594	.9254	.7580	.7545	.8173	1.030	1.148	1.182	1.168	1.155	1.186	1.312	1.292	1.229	1.136	.9824	.9270	15
0	0	0	.9976	.9527	.9[illegible]07	.7550	.7533	.8164	1.030	1.148	1.183	1.168	1.155	1.188	1.316	1.296	1.232	1.139	.9825	.9259	16
0	0	0	1.104	1.052	1.023	.7766	.7787	.8428	1.075	1.196	1.234	1.211	1.197	1.232	1.321	1.300	1.235	1.151	.9896	.9334	17
0	0	0	1.069	1.020	.9936	.7556	.7594	.8221	1.050	1.166	1.203	1.180	1.166	1.201	1.290	1.268	1.203	1.120	.9618	.9071	18
0	0	0	1.028	.9793	.9567	.7279	.7328	.7931	1.014	1.124	1.160	1.137	1.123	1.157	1.237	1.212	1.149	1.075	.9219	.8696	19
0	0	0	.9617	.9169	.9014	.6873	.6961	.7513	.9633	1.061	1.096	1.073	1.059	1.091	1.132	1.144	1.082	1.010	.8651	.8180	20
0	0	0	1.054	.9986	.9959	.6975	.7097	.7664	1.004	1.092	1.131	1.094	1.079	1.113	1.126	1.091	1.030	.9759	.8319	.7927	21
0	0	0	.9558	.9038	.9141	.6422	.6562	.7087	.9341	1.001	1.040	1.003	.9867	1.017	1.038	.5 [illegible]	.9356	.8828	.7523	.7221	22
0	0	0	.8782	.8354	.8574	.6028	.6173	.6648	.8849	.9333	.9723	.9343	.9205	.9611	.9827	.9280	.8699	.8044	.6879	.6622	23
0	0	0	.8761	.8654	.9050	.6349	.6531	.6889	.9086	.9460	.9866	.9635	.9598	.9637	1.009	.9456	.8856	.8320	.7210	.6702	24
0	0	0	0	0	0	0	0	0	.2762	.2518	.2745	0	0	0	.1600	.1462	.1429	0	0	0	25
0	0	0	0	0	0	0	0	0	.2601	.2312	2.554	0	0	0	.1491	.1340	.1329	0	0	0	26
0	0	0	0	0	0	0	0	0	.2241	.1987	.2200	0	0	0	.1570	.1399	.1397	0	0	0	27
0	0	0	0	0	0	0	0	0	.1901	.1710	.1883	0	0	0	.1661	.1477	.1478	0	0	0	28

BOTTOM OF REACTOR CORE

PSF EXPERIMENT

Values listed be multiplied by 10^{15} to obtain $n/(cm^2 \cdot s)$. The three-dimensional neutron volumetric source distribution is integrated over the horizontal transverse direction perpendicular to the axis of the experiment to obtain the values listed. Note that the "A" row faces the PSF experiment.

2.0 PSF STARTUP CHARACTERIZATION PROGRAM - SUMMARY

W. N. McElroy

An 18-day Simulated Dosimetry Measurement Facility (SDMF-1) "Startup Experiment" with dummy metallurgical capsules containing only dosimeters was performed prior to the two-year "PSF Metallurgical Experiments" to accurately determine the irradiation times needed to reach the target fluences.

As discussed in Section 3.0, the PSF startup experiments afforded an ideal opportunity for the intercomparison of the results of RM dosimetry measurements by a large number of program participants.

The startup experiments were also used to test the accuracy of ORNL and PR&A reactor physics calculations. Comparison of dosimetry results between the startup and the two-year PSF experiment showed significant differences, which were traced to differences in core loadings (Ma84b,To82a,Mc87c). A new set of transport calculations (described in Section 1.3 of Ref. Mc87c) was performed to account for 52 different core loadings for the two-year experiment.

Not including the SDMF-1 and other startup tests, six test irradiations have been performed in the ORR-PSF Benchmark Facility in support of the NRC LWR-PV Surveillance Dosimetry Improvement Program. These tests are identified in Appendix A of Ref. (Mc87c). Sections 2.1, 2.2 and 2.3 of this report provide information on Radiometric (RM), Graphite (G.A.M.I.N.), Tungsten (W), and Sapphire (SDM) Damage Monitor (DM) measurements performed by program participants.

As stated by A. Fabry (Fa82), the PSF "Startup Characterization Program" involved three steps:

> *"1. A simplified mock-up at the PCA (PCA 4/12 SSC), in which have been systematically applied the large array of passive and active, integral and spectrally-resolved techniques used in support of the PCA "Blind Test" (Mc81); this includes the Belgium silicon damage monitors and absolute core power based on experimental fission rate maps.*
>
> *2. A series of dedicated ORR irradiations at low and intermediate power in an "exact duplicate" of the PSF 4/12 SSC metallurgical configuration; the sensors exposed encompass (a) the radiometric 103Rh(n,n'), 115IN(n,n'), 58Ni(n,p) and 27Al(n,a) reactions extensively used at PCA (under 1 above and in Ref. Mc81) and BSR (HSST dosimetry mock-up, Ref. Ka82b), and (b) the French graphite and tungsten damage monitors (Al82b). Power normalization relative to the next step.*
>
> *3. An 18 day high power run (To82a) in the above 4/12 SSC duplicate; all high fluence U.S. and European neutron dosimeters have been exposed, including the UK sapphire damage monitors (Pe82); many laboratories participated; core power; and ORR heat balance."*

He further states:

"The primary objective was to:

-- Confirm the metallurgical irradiation configuration as defined by extensive mapping measurements at PCA ("trial and reject" of 8/7 SSC, 8/12 SSC, 9/12 SSC) and confirm the irradiation durations needed for the various capsules.

The complementary objectives were to:

-- Link PSF and HSST fluence dosimetry to PCA physics benchmarking metrology.

-- Provide an international neutron metrology and analysis opportunity, including the validation of UK, French, and Belgium damage monitors and of dosimetry cross section data for crucial but less well known long-half life radiometric monitors;

93Nb(n,n') versus 237Np(n,f) and 103 Rh(n,n')

63Cu(n,a) versus 27Al(n,a).

A number of papers (presented at the 4th ASTM-Euratom International Symposium on Reactor Dosimetry) deal with this experiment (De82,Al82b,Wi82,Ka82a,Pe82,To82a)."

2.1 LOW-POWER RADIOMETRIC MEASUREMENTS AND COMPARISON TO PCA DATA

E. D. McGarry (NBS)

Initial dosimetry to verify the fluence characteristics of the newly built PSF-SDMF were carried out at low power, about 1/100th of the nominal 30-Mw operating power of the Oak Ridge Research Reactor. Because of the closed instrumented construction of the PSF, as opposed to the open dosimetry-access pipes in the PCA, the fission chambers that were used so extensively in the PCA had to be replaced with radiometric dosimeters. The particular types of radiometric dosimeters [e.g., (n,n') reactions in rhodium and indium, the nickel (n,p) reaction, and the aluminum (n,a) reaction] had also been used in the PCA where they were calibrated against NBS fluence standards, see Section 2, Tables 2.2.6 and 2.2.7 of (Mc84i), and intercompared to fission chamber and SSTR measurements (Mc86c). Since the ORR-PSF was a 4/12 configuration (Mc84i) with a simulated surveillance capsule that had been designed and extensively studied at the PCA, these initial low-power measurements demonstrated that the spatial distribution of flux density and spectral indices (reaction rate ratios) were essentially the same for the PCA and PSF.

Subsequently, the PSF Start-up experiment with dosimetry in dummy surveillance capsules, in place of the instrumented capsules used for the metallurgical irradiations, was performed prior to the metallurgical irradiations to determine accurately the irradiation times needed to reach target fluences. It was at this point in the LWR-PV-SDI Program that longer half life radiometric dosimetry became the principal neutron-spectrum and fluence-monitoring technique for all subsequent PSF benchmark experiments. The PSF startup experiments were also used to benchmark radiometric dosimetry as described at the fourth ASTM-EURATOM Symposium on Reactor Dosimetry, where interlaboratory comparisons of radiometric results were initially described (Fe82,To82a).

Section 3.5 discusses the NBS counting and fluence standards provided to HEDL for benchmarking of radiometric sensors used in the PSF SDMF 1, 2, 3, and 4; SSC-1; SSC-2; SFVC; and SVBC experiments. More complete information on "Benchmark Field Referencing" in support of the LWR-PV-SDIP is provided in Section 2.2, Ref. Mc87c or Section 3.0, Ref. Mc88b.

2.2 GRAPHITE AND TUNGSTEN DAMAGE MONITORS MEASUREMENTS

A. Alberman, M. Benoist, and M. Thierry

2.2.1 Introduction to damage dosimetry technique

2.2.1.1 General background

Most damage parameters as : d.p.a., fluence (E > 0.1 Mev) cannot be derived directly by customary neutron fluence measurements. Fast neutron reaction thresholds are generally too high (1 Mev or more) for direct damage analysis, and computer codes (spectrum adjustment procedures) must be developed to infer fluence in the relatively un-measured energy range below 1 Mev. It is mandatory that damage measurements be made for code validation, and to determine their limitations when applied to "distorted" neutron environments. Distortion is a suitable word for pressure vessel spectra when, as shown later, most damage (up to 80 %) is caused by neutrons with energy below 1 Mev depending upon the location inside the pressure vessel.

2.2.1.2 Damage dosimetry

The preceding reasons led the Services des Piles de Saclay of Commissariat à l'Energie Atomique (C.E.A) , over the past 10 years, to develop damage dosimetry techniques using the OSIRIS reactor, its neutronic mockup ISIS, and surrounding facilities. The dosimetry strategy is to calibrate a material property change versus a fast neutron threshold reaction.

Damage monitor material selection resulted from the following statement: measurement of the subsequent property changes of test reactor dosimetry materials is most convenient if made at room temperature, by accurate means. But at room temperature, most point defects created by neutron bombardment are mobile (particularly self-interstitials) and can lead to recombination, non-linearity in measurement, etc. Since refractory metals can fulfill these requirements, graphite and tungsten were finally selected. The most convenient physical property measurement is electrical resistivity whose increased rate after irradiation is reported versus neutron fluence. Nickel was selected as the activation detector for two reasons: 1) the well known $^{58}Ni\ (n,p)^{58}Co$ cross section for fast reactor dosimetry and 2) a reaction rate suitable for the damage monitor range (10^{15}-10^{17} $n \cdot cm^{-2}$). The experimental damage/activation (DAR) ratio is then determined. Tungsten is representative of damage in structural metals.

2.2.1.3 Damage monitors

Graphite (G.A.M.I.N) and Tungsten (W) monitors shown in Figure 2.2.1 are designed for experimental device loadings (low-power runs or mock-ups). Their miniaturization allows measurements at numerous experimental points with resulting good accuracy. Their main characteristics are given in Table 2.2.1. More details on these techniques are given elsewhere (Ge75. A177, A179).

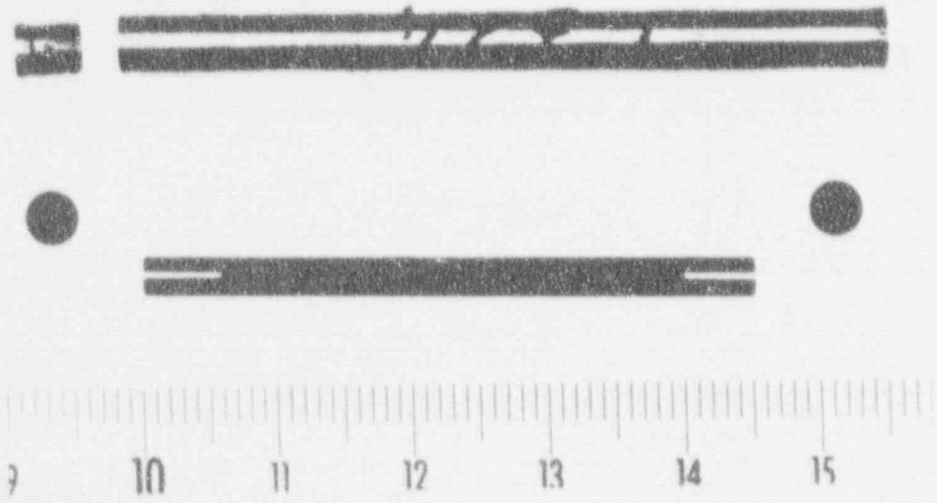

G.A.M.I.N. damage monitor

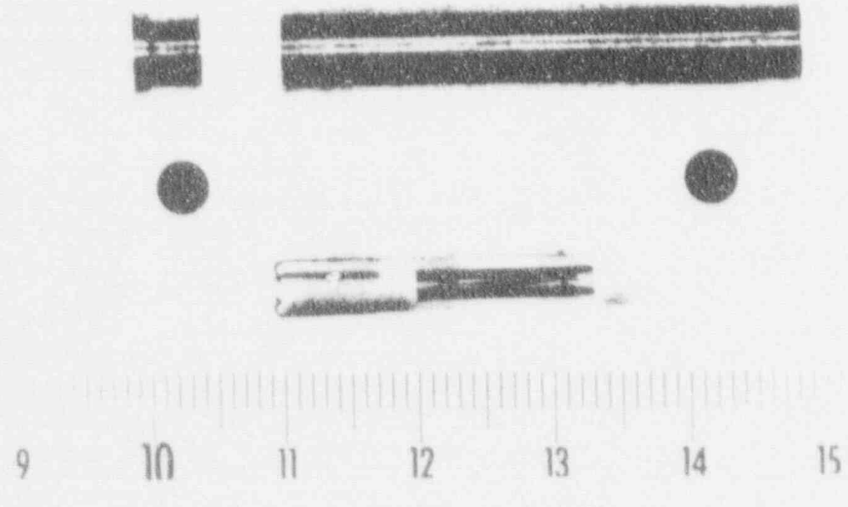

TUNGSTEN damage monitor

Fig. 2.2.1. Damage monitors

Special application to pressure vessel surveillance program (DOMPAC) was carried out (A183). In particular, french PV steels have been qualified by these techniques. It must be pointed out that resistivity measurements are performed in Saclay.

TABLE 2.2.1

DAMAGE MONITORS CHARACTERISTICS

	G.A.M.I.N.	TUNGSTEN
Sample/Al container . Length	45 / 55 mm	31 / 39 mm
. Outer diameter	2.85 / 5 mm	5 / 6.5 mm
Resistor type	4 contacts	4 contacts
Typical resistance value at 25°C	40 mΩ	1 Ω
Temperature range	30°C - 180°C	30°C - 300°C
Temperature dependance	yes	no
$\Delta R/R$ min, max	1 % to 15 %	0.4 % to 0,4 %
Damage fluence range ($n.cm^{-2}$)	$5.10^{15} < \phi_G < 10^{17}$	$7.10^{15} < \phi_W < 7.10^{16}$
Accuracy	$1\sigma < 3$ % (5 samples)	$1\sigma < 5$ % (6 samples)

2.2.2 Experimental results

2.2.2.1 Experimental conditions in the PSF

Three locations: surveillance, 1/4 and 3/4 thickness have been qualified by damage monitors in the PSF dosimetry capsule. A special plug was designed for the PSF and loaded at Saclay. This design positioned the W and G.A.M.I.N. monitors, surrounded by mild steel (see Figure 2.2) next to the core midplane. The plugs were equipped with thermocouples for G.A.M.I.N. temperature measurements and there was an elastomer gasket on top. Experimental conditions are given in Table 2.2.2. A low power run was requested to avoid excessive heating of the G.A.M.I.N. monitors.

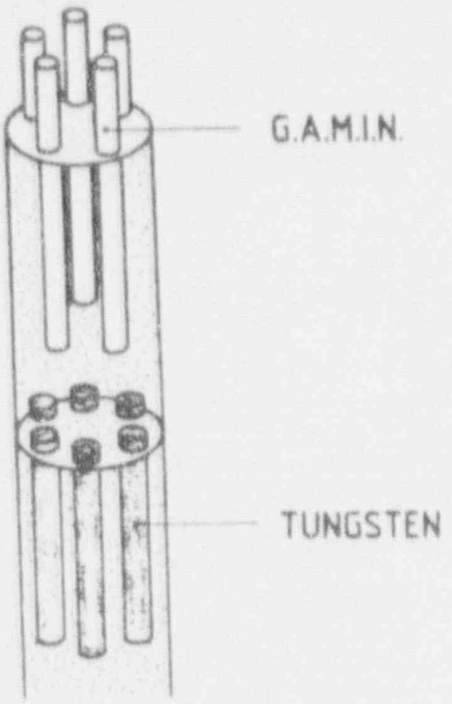

Fig. 2.2.2 Damage Monitors Loading

TABLE 2.2.2

EXPERIMENTAL CONDITIONS

Container	Position	Dosimetry runs start-up	Power	Temperature	Duration
A	SSC	26.10.1979 2h08	7.4 MW	75°C	2h00
B	1/4 T	26.10.1979 5h03	16.0 MW	66°C	12h35
C	3/4 T	26.10.1979 5h03	16.0 MW	52°C	23h00

2.2.2.2 G.A.M.I.N. results

Experimental graphite damage/activation ratio

$$r = 10^{-7} \frac{\Delta R/R^C}{A_{Ni}}$$

is given per each G.A.M.I.N. monitor in Table 2.2.3 :

$\Delta R/R^C$: graphite resistivity increase after linearization (ISIS standard procedure)

$A_{Ni} = \sigma_{Ni} \cdot \phi_{Ni}$ number of (n,p) reactions per target atom

ϕ_{Ni} : nickel equivalent fission fluence (average of 2 foils)

σ_{Ni} = 101 mbarn : average of ^{58}Ni (n,p) cross section over the fission spectrum

TABLE 2.2.3

G.A.M.I.N. RESULTS

Container	N° GAMIN	Position	$\Delta R/R^C$ (%)	$\phi_{Ni} \cdot 10^{-15}$ ($n.cm^{-2}$)	r	$\bar{r}$
	40	a	7.019	10.24	6.784	
	41	b	7.234	10.00	7.162	
A SSC	42	c	6.618	9.75	6.717	7.00
	43	d	6.077	8.39	7.171	
	44	e	6.479	8.95	7.164	
	45	a	9.181	10.20	8.912	
	46	b	9.249	10.34	8.852	
B 1/4 T	47	c	8.744	9.21	9.400	9.24
	31	d	8.355	8.59	9.630	
	32	e	8.674	9.11	9.427	
	33	a	5.663	2.27	24.70	
	34	b	6.109	2.50	24.19	
C 3/4 T	35	c	6.724	2.79	23.86	24.16
	36	d	6.350	2.66	24.45	
	37	e	5.828	2.36	24.45	

2.2.2.3 W results

The same way, experimental W damage/activation ratio

$$s = 10^{-5} \cdot \frac{\Delta R/R^r}{A_{Ni}}$$

is given in Table 2.2.4 :

$\Delta R/R^r$: W resistivity increase after discounting thermal damage ($\sim$ 5 %).

TABLE 2.2.4

TUNGSTEN RESULTS

Container		N°W	Position	$\Delta R/R^r$ (%)	$\phi_{Ni}.10^{-15}$ (n.cm^{-2})	s	$\bar{s}$
		141	f	0.102	11.99	8.445	
		142	g	0.097	11.21	8.595	
A	SSC	143	h	0.084	10.12	8.192	8.48
		155	i	0.089	9.90	8.860	
		156	j	0.091	10.85	8.331	
		157	k	0.186*	11.96	-	
		158	f	0.119	11.31	10.41	
		159	g	0.113	10.51	10.66	
B	1/4 T	160	h	0.212*	9.58	-	11.78
		161	i	0.122	9.52	12.66	
		162	j	0.151	10.46	14.30	
		145	k	0.124	11.27	10.88	
		146	f	0.095	2.92	32.16	
		148	g	0.073	2.79	25.83	
C	3/4 T	149	h	0.065	2.54	25.45	27.60
		150	i	(broken)	2.48	-	
		151	j	0.193*	2.61	-	
		154	k	0.079	2.81	26.97	

* aberrant value

2.2.2.4 Summary of results

Table 2.2.5 outlines the preceding results.

TABLE 2.2.5

SUMMARY OF DAMAGE MONITORS RESULTS

Container	Position	G.A.M.I.N.		TUNGSTEN	
		$\bar{r}$	$\Delta\bar{r}/\bar{r}$	$\bar{s}$	$\Delta\bar{s}/\bar{s}$
A	SSC	7.00	1.6 %	8.48	1.5 %
B	1/4 T	9.24	1.9 %	11.78	7 %
C	3/4 T	24.16	0.9 %	27.60	6.5 %

Without any additional analysis, it is clear that the surveillance and 1/4 T positions are fairly close with respect to neutron damaging effects (similar spectrum), while the 3/4 T position is about 3 times more "damage efficient". It must be pointed out that a very good consistency in these experimental results has been achieved, and also that nickel fluence must be discarded as a damage exposure parameter. The experimental damage/activation ratio, as shown in Figure 2.2.3, displays similar behavior throughout the SPVC and the vessel simulator, DOMPAC, operated by the Services des Piles de Saclay (A183).

2.2.3 Damage analysis. Exposure parameter deviation

2.2.3.1 Damage monitor analysis

Following EURATOM recommendations (Ge74) issued in 1974 by the EURATOM Working Group on Reactor Dosimetry, we refer to equivalent fission fluence as defined in 2.2.2.2. The damage/activation ratio for each type of damage monitor has been shown to be proportional to spectral indices (ratio of equivalent fission fluences) as follows:

G.A.M.I.N. : $\phi_G / \phi_{Ni} = 0.50\ r$

TUNGSTEN : $\phi_W / \phi_{Ni} = 0.\ s$

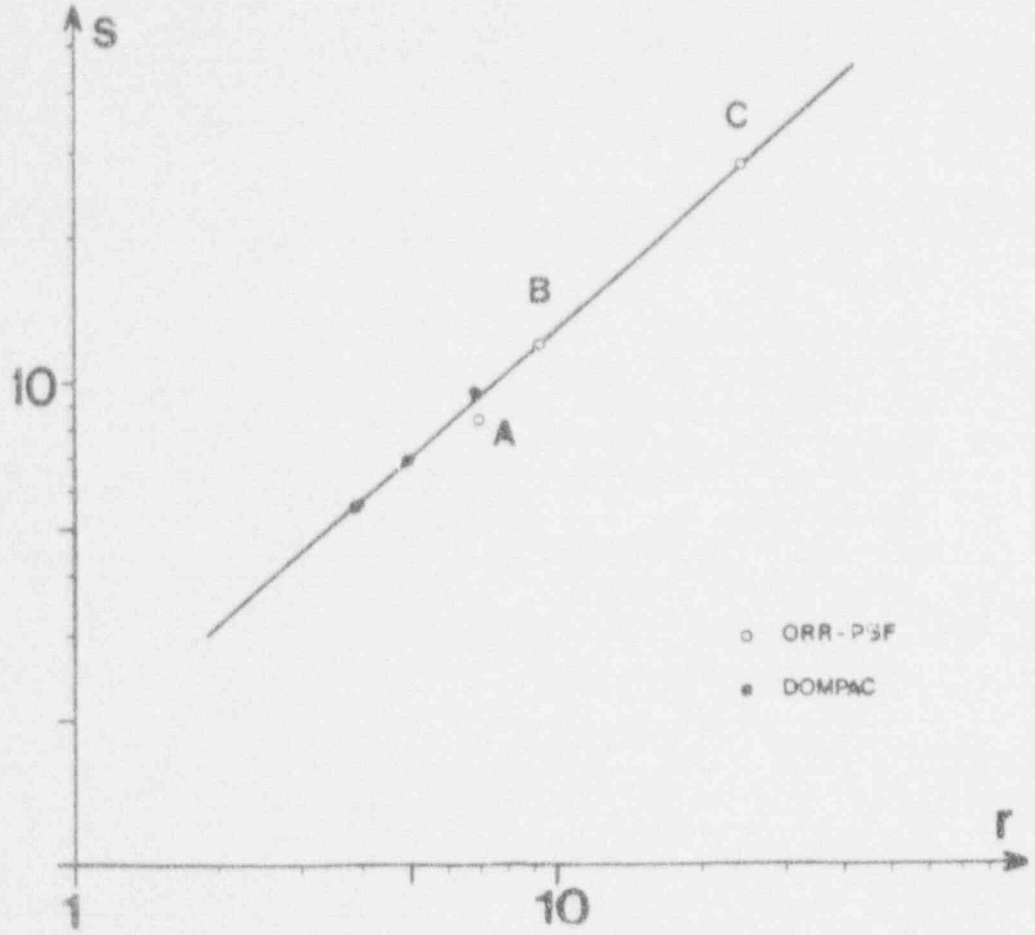

Fig. 2.2.3 Tungsten "s" / graphite "r" responses in PV simulators

The proportionality constant was found independant of spectra selection according to THOMPSON-WRIGHT model for graphite and "tailored" d.p.a. model (A182) for tungsten.
Effective thresholds found by intercomparisons are :

$$\phi_G \approx \phi\ (E > 0.075\ \text{MeV})$$
$$\phi_W \approx \phi\ (E > 0.3\ \text{MeV})$$

Damage analysis in tungsten is a very interesting topic, from the point of view that ϕ_W is fairly close to ϕ_{Fe} (steel damage fluence). It is possible to assess the W monitor response with respect to neutron energy after G.A.M.I.N. monitor response cross correlation.
Table 2.2.6 outlines the relative amount of damage produced in the three positions. It appears clear that over the pressure vessel thickness, the present damage analysis is certainly conservative, whereas usual fluence (E > 1 Mev) can be misleading.

TABLE 2.2.6

RELATIVE W MONITOR RESPONSE

		Measured damage percentage				DAR relative to SSC	
		10 keV	100 keV	1 MeV	10 MeV	W / Ni	W / ϕ > 1 MeV
A	SSC	6%	53%	41%		1	1
B	1/4 T	9%	56%	35%		1.18	1.19
C	3/4 T	8%	72%	20%		3.25	1.98

2.2.3.2 Exposure parameters in PV steels test positions

The simultaneous use of G.A.M.I.N. and W damage monitors provided accurate determination of neutron environments. Correlations have been derived in many reactor test positions (A182). Exposure parameters such as ϕ > 0.1 MeV, ϕ > 1 MeV, and d.p.a. ($=835.10^{-24}\ \phi_{Fe}$) are given in Table 2.2.7 with respect to nickel fluence in the four PV steels irradiation positions. Of course, these damage/activation ratio are dimensionless, actual damage fluence are to be obtained directly by means of nickel fluence adequate measurements.

TABLE 2.2.7

EXPERIMENTALLY DERIVED EXPOSURE PARAMETERS

Position	SSC	0 T	1/4 T	1/2T
$\frac{\phi > 0.1\ MeV}{\phi_{Ni}}$	3.43	2.79	4.59	7.88
$\frac{\phi > 1\ MeV}{\phi_{Ni}}$	0.95	0.88	1.08	1.35
$\frac{\phi_{Fe}\ (d.p.a.)}{\phi_{Ni}}$	2.01	1.73	2.42	3.50

2.3 HIGH-POWER 18-DAY DOSIMETRY RUN

W. N. McElroy (HEDL)

An 18-day Simulated Dosimetry Measurement Facility (SDMF-1) "Startup Experiment" with dummy metallurgical capsules containing only dosimeters was performed prior to the two-year "PSF Metallurgical Experiments" to accurately determine the irradiation times needed to reach the target fluences.

The startup experiments were also used to test the accuracy of ORNL and RR&A reactor physics calculations. The results of calculations performed by ORNL and RR&A are discussed and/or referenced in Section 4.0. ORNL utilized a flux-synthesis technique based on three calculations (Ma82i,Ma84a). The source term was obtained from a three-dimensional diffusion theory calculation as reported in Section 1.2. Ratios of calculated-to-experimental values [for the 46Ti(n,p) and 237Np(n,f) reaction rates] for the revised ORNL calculations range from 0.75 to 0.93. Discrepancies between measurements and calculations relative to the startup experiments are within expected ranges based on previous evaluations (i.e., PCA, Refs. Mc81,Mc84i,Mc84f), known uncertainties associated with nuclear data, measurements, and applicable computational methodology.

Details are provided elsewhere (Mc87c) of the calculational methods and data used and the results obtained by RR&A in the successful validation of the ANISN methodology and the subsequent calculation of the PSF 4/12 irradiation facility using both the ANISN and MCBEND techniques. These RR&A ANISN (1-D) and MCBEND (3-D Monte Carlo) results provide a further basis for comparison and verification of the overall reliability of the ORNL and RR&A calculational results. The RR&A calculational results are used in Section 5.2 for a consistency analysis of the measured reaction rates in the UK dosimetry for the 18 day startup and the SSC1 and SSC2 experiments. They are also used in Section 6.1 in the derivation of recommended exposure parameter values for these experiments.

Sections 2.3.1, 2.3.2 and 2.3.3 provide information (and/or references) on UK Radiometric (RM), CEN/SCK Radiometric (RM) and UK Sapphire Damage Monitor (SDM) measurements performed by program participants, respectively.

2.3. Results and Analysis of UK Activation Dosimetry in the ORR/PSF Characterisation Program

A. F. Thomas (Rolls-Royce & Associates Ltd., UK);
A. J. Fudge (AERE Harwell, UK)

2.3.1.1 Introduction

Rolls-Royce & Associates Ltd., in collaboration with AERE, Harwell have provided neutron dosimetry packs for inclusion in both the 18-day full power dosimetry/thermal characterisation irradiation run and the metallurgical capsule irradiations in the ORR/PSF 4/12 LWR Pressure Vessel Simulator. These have included a wide variety of neutron activation detector materials as well as sapphire direct damage monitors. The principal neutron activation rates of interest were as follows:

Dosimeter	Neutron Reaction
Nb	$^{93}Nb(n,n')^{93m}Nb$
Ni	$^{58}Ni(n,p)\ ^{58}Co$
Fe	$^{54}Fe(n,p)\ ^{54}Mn$
Ti	$^{46}Ti(n,p)\ ^{46}Sc$
Cu	$^{63}Cu(n,\alpha)\ ^{60}Co$
Co/Al	$^{59}Co(n,\gamma)\ ^{60}Co$
Fe	$^{58}Fe(n,\gamma)\ ^{59}Fe$

This report describes the experimental design and measurement and analysis results of the Rolls-Royce & Associates Ltd. neutron activation dosimetry carried out in the ORR/PSF (4/12) characterisation programme, in which both AERE Harwell and AEE Winfrith activation measurements are discussed. Results of the sapphire direct damage monitors exposed simultaneously in this irradiation are described in Sections 5.2 and 6.1; also, Section 2.6, Ref. Mc87c.

2.3.1.2 Experimental Dosimetry Capsules Preparation

Rolls-Royce & Associates Ltd. supplied ORNL with 6 dosimeter packs (see Fig. 2.3.1.1) contained in stainless steel capsules which were prepared by AERE Harwell in the following manner.

Discs of metal each 2.9mm in diameter are punched from pieces of foil 0.25mm thick obtained in a pure form from either Goodfellow Metals (UK) or Materials Research (UK). The materials used are nickel, iron, titanium, niobium and copper. Cobalt is also used as a cobalt/aluminium alloy (0.745% Co) in the form of a wire bent into rings. The foils and rings are weighed and placed in a 'standard' stainless steel capsule. In a 'standard' capsule a sapphire damage monitor (SDM) is wrapped in aluminium foil and also placed in the stainless steel capsule on top of the metal foils. The voids between the SDM and the capsule are packed with crumpled aluminium foil to ensure good

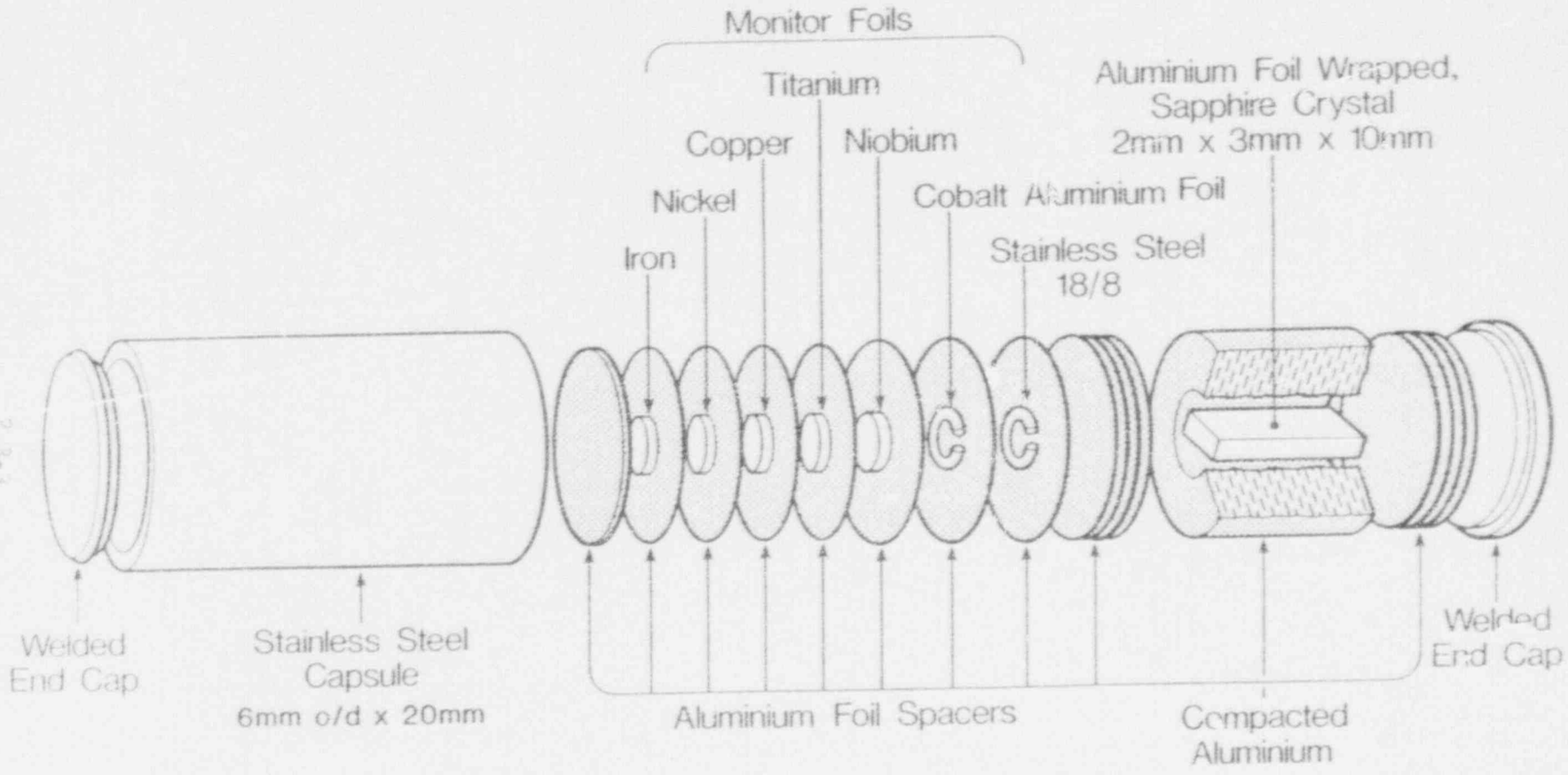

FIGURE 2.3.1.1. Sapphire Damage Monitor and Activation Monitors Irradiation Capsule.

thermal contact between the sapphire and the capsule. The end cap is then secured onto the capsule by electron beam or argon arc welding. The sealed capsule welds are then dressed to ensure that the diameter is no greater than 6mm (see Fig. 2.3.1.1).

The contents and weights of activation materials incorporated in these capsules are shown in Table 2.3.1.1.

Capsule Location and Irradiation

The capsules supplied by Rolls-Royce & Associates Ltd. were located within the ORR/PSF (4/12) LWR simulator by ORNL according to the specification given in Table 2.3.1.2 and as in Figure 2.3.1.2, and the irradiation of capsules began on 14th October 1979. The irradiation continued for 18 days and the reactor was shut down on 14th November 1979. The time and power histories of the irradiation are shown in Tables 2.3.1.3 and 2.3.1.4. After irradiation the dosimeter capsules were returned to AERE Harwell for activation analysis.

2.3.1.3 Activation Measurement Techniques

Following irradiation, the dosimetry capsules were dismantled and the activity on each of the dosimeters was measured first by AERE Harwell and, subsequently, also by AEE Winfrith. Each material was identified by a suitable means and all the various foils and wires (except niobium) were counted without chemical preparation on a Ge(Li) detector.

Table 2.3.1.1 - Contents of Rolls-Royce & Associates Ltd. Dosimeter Capsules Irradiated in the ORR/PSF 18-Day Dosimetry Characterisation Run

	Monitor Weight (mgs) Capsule Number					
Monitor Material	1	2	3	4	5	6
Fe	Not Used	18.03	16.76	19.32	17.09	18.78
Cu		22.72	21.80	21.82	20.51	20.87
Ni		20.35	20.72	20.36	21.80	21.72
Ti		10.91	11.07	10.11	10.51	10.24
Co/Al *		3.50	3.13	3.82	3.26	3.00
Nb		0.58	0.45	0.44	0.48	0.57
Location	-	½ T (offset)	SSC	½ T	½ T	½ T

* Co/Al wire contained 0.743% Co by weight

Table 2.3.1.2 - Details of Rolls-Royce & Associates Ltd. Dosimetry Capsule Locations in ORR/PSF (4/12) 18-Day Dosimetry Characterisation Run

Sample Number	Irradiation Location	Distance from Core Face (cm)	Axial Height Above Mid Plane (cm)	Lateral Offset (cm)
3	SSC	16.15	-0.35	0.0
4	PVS¼T	31.32	-12.2	0.0
2	¼T offset	31.32	-12.2	±10.16
5	¼T	36.52	-12.2	0.0
6	½T	41.92	-12.2	0.0

T is PV wall thickness e.g. ¼T = quarter thickness

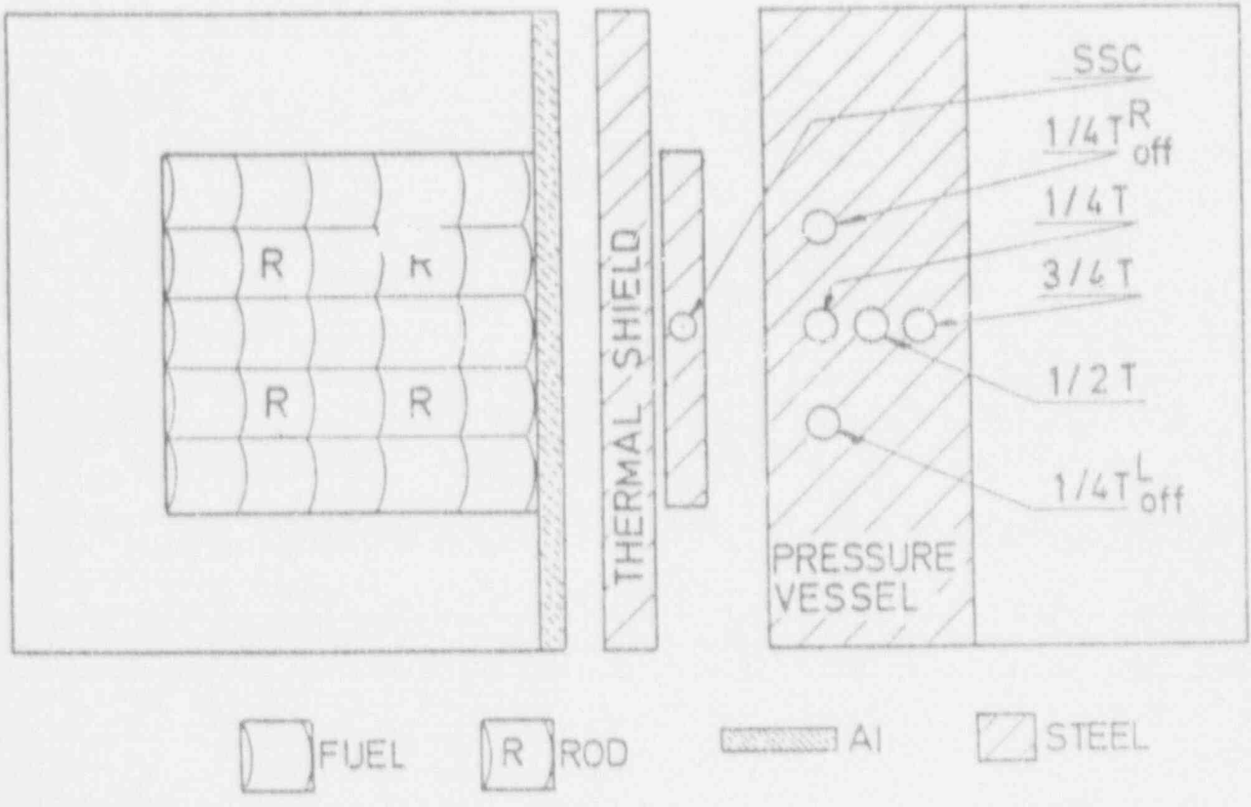

FIGURE 2.3.1.2. ORR/PSF (4/12) 18-Day Dosimetry Run Configuration.

Table 2.3.1.3 - Timing of Exposure for the ORR/PSF (4/12)
18-Day Dosimetry Characterisation Run

Location Channel * with Sample No. in Brackets	Effective Full Power (30 MW) Exposure (s)	Begin Exposure **	End Exposure **
SSC (3)	1.512×10^6	Oct 27; 2:26:00 pm	Nov 14; 8:54:50 am
PVF	1.494×10^6	Oct 27; 8:20:48 pm	idem
1/4 T (4)	1.512×10^6	Oct 27; 2:26:00 pm	Nov 14; 8:43:00 am
1/3 T_{off} (2)	1.338×10^6	Oct 29; 4:10:18 pm	Nov 14; 8:54:50 am
1/2 T (5)	1.491×10^6	Oct 27; 9:10:56 pm	idem
3/4 T (6)	1.489×10^6	Oct 27; 9:17:35 pm	idem

* SSC : Simulated Surveillance Capsule

PVF : Pressure Vessel Front

1/4 T : Vessel Quarter Thickness

1/4 T_{off} : Off-centred Vessel Quarter Thickness

1/2 T : Vessel Half Thickness

3/4 T : Vessel Three Quarter Thickness

** Local time, Oak Ridge, Tennessee (USA)

Table 2.3.1.4 - ORR Core Power History During the ORR/PSF (4/12) 18-Day Dosimetry Characterisation Run (ORR Cycle 151A)

Date	Integral * Power (MWh)	Hours Operated	Average Daily Power (MW)
10-27-79	600.00	24	25.00
10-28	722.24	25 **	28.89
10-29	702.78	24	29.28
10-30	714.68	24	29.78
10-31	717.04	24	29.88
11-1	684.45	23.65 ***	28.94
11-2	718.20	24	29.92
11-3	713.89	24	29.74
11-4	712.80	24	29.70
11-5	702.44	24	29.27
11-6	711.76	24	29.66
11-7	710.24	24	29.59
11-8	709.48	24	29.56
11-9	707.24	24	29.47
11-10	712.88	24	29.70
11-11	717.16	24	29.88
11-12	715.72	24	29.82
11-13	715.28	24	29.80
11-14	540.38	18.417 ****	29.34

* Core thermal balance measurement, ORR Weekly Report
** End of Daylight Saving time
*** Reactor was shut-down from 10:00 A.M. to 10:21 A.M.
**** Reactor was re-started 5.583 h after end of dosimetry run

The output from the Ge(Li) detector was fed from its preamplifier to a Canberra model 2021 spectroscopy amplifier. The amplifier output was in turn fed via a Canberra model 8621 analogue-to-digital convertor to a Canberra Series 80 multi-channel analyser. The gamma-ray spectra were then recorded on magnetic tape and the γ-peak areas were determined using the GAMANAL code (Gau 72). The activation dosimeters were counted for sufficiently long to give precisions of approx 1%.

The relative intensities of the activities induced at different locations were determined by positioning each sample in turn (with the exception of niobium) at a fixed distance from a γ-ray spectrometer and measuring the intensity of the γ-ray peaks of interest. The absolute activities were determined by taking one or two samples of each type into solution and preparing liquid sources for presentation to a spectrometer which had been calibrated using standard source solutions in nominally identical source holders.

The nuclear data used in the determination of absolute activities was taken from (Zi 79) and is summarised in Table 2.3.1.5. The values of absolute activity are given in Table 2.3.1.6 and are quoted in terms of disintegrations per second per milligram of dosimeter material.

Table 2.3.1.5 - Nuclear Data Used in Activation Analysis of Rolls-Royce & Associates Ltd. Dosimeters in the ORR/PSF (4/12) 18-Day Dosimetry Characterisation Run (Taken from (2))

Reaction	Isotopic Abundance	Product Half-Life (hrs)	Product γ-Ray Energy (KeV)	Abundance of Product γ-Ray
$^{54}Fe(n,p)^{54}Mn$	0.058	7.500×10^3	834.8	1.0
$^{58}Ni(n,p)^{58}Co$	0.683	1.700×10^3	810.8	0.995
$^{46}Ti(n,p)^{46}Sc$	0.081	2.012×10^3	889.3 1120.5	1.0 1.0
$^{63}Cu(n,\alpha)^{60}Co$	0.692	4.621×10^4	1137.2 1332.5	1.0 1.0
$^{93}Nb(n,n')^{93m}Nb$	1.000	1.438×10^5	16.6	0.116
$^{59}Co(n,\gamma)^{60}Co$	0.00745*	4.621×10^4	1137.2 1332.5	1.0 1.0
$^{58}Fe(n,\gamma)^{59}Fe$	0.003	1.069×10^3	1099.2 1291.6	0.56 0.438

* 0.745 w/o Cobalt in Aluminium Wire

Table 2.3.1.6 - Absolute Activities Measured on Rolls-Royce & Associates Ltd. Dosimeters Used in ORR/PSF (4/12) 18-Day Dosimetry Characterisation Run

Monitor Material	Nuclide Measured	Counting Laboratory	Activity Measured dps/mg of Dosimeter Material* Capsule 3 SSC	Capsule 4 ¼T	Capsule 2 ¼T (off-set)	Capsule 5 ½T	Capsule 6 ¾T
Iron	^{54}Mn	AERE	1.143E4	7.079E2	5.261E2	2.617E2	9.326E1
"	"	AEEW	1.171E4	6.920E2	4.960E2	2.630E2	9.020E1
"	"	AERE/AEEW	0.98	1.02	1.06	1.00	1.03
"	^{59}Fe	AERE	3.631E4	1.929E3	1.555E3	6.654E2	2.998E2
"	"	AEEW	3.753E4	-	-	-	-
"	"	AERE/AEEW	0.97	-	-	-	-
Copper	^{60}Co	AERE	1.549E2**	9.980E0	7.636E0	4.443E0	1.691E0**
"	"	AEEW	1.262E2	9.300E0	7.360E0	4.210E0	1.470E0
"	"	AERE/AEEW	1.22	1.07	1.04	1.05	1.15
Nickel	^{58}Co	AERE	6.347E5	3.847E4	2.877E4	1.501E4	5.440E3
"	"	AEEW	6.130E5	3.680E4	2.680E4	1.404E4	5.080E3
"	"	AERE/AEEW	1.04	1.05	1.07	1.07	1.07
Titanium	^{46}Sc	AERE	9.117E3	5.973E2	4.276E2	2.210E2	5.448E1**
"	"	AEEW	8.770E3	5.560E2	4.070E2	2.110E2	7.260E1
"	"	AERE/AEEW	1.04	1.07	1.05	1.05	0.75
Cobalt***	^{60}Co	AERE	9.725E4	3.640E3	Lost	2.527E3	1.209E3
"	"	AEEW	9.120E4	4.090E3	-	2.272E3	1.104E3
"	"	AERE/AEEW	1.07	0.89	-	1.11	1.10
Niobium	^{93m}Nb	AERE	-	-	-	-	-
"	"	AEEW	1.979E4	1.255E3	9.160E2	5.760E2	2.870E2
"	"	AERE/AEEW	-	-	-	-	-

* Activity quoted at end of irradiation (14/November/1979) except Co^{58} (28/November/1979).

** Probable counting errors.

*** 0.745 W/o Cobalt in aluminium wire.

Niobium Measurement

In the case of the niobium foils, the reaction of interest was $^{93}Nb(n,n')^{93m}Nb$. However, since ^{93m}Nb is a weak (16 keV) X-ray emitter only, it suffers from severe self-shielding in metallic form, and in addition fluorescence from contaminating tantalum atoms causes interference in measurement. Thus it was not possible to count ^{93m}Nb using the same methods employed for iron, nickel, titanium etc. Instead the method developed by CEN/SCK, Mol, Belgium was adopted (To 80) in which the niobium foils were dissolved and very thin ($\sim$0.1mgm/cm^2) sources prepared on filter paper for counting at a distance of 50mm from a high purity germanium X-ray spectrometer. However, the level of activity from the total of 0.5mgm of niobium in each deposit was low and the accurate determination of the absolute value of this activity required the use of an X-ray spectrometer with a high sensitivity to low energy ($\sim$16 KeV) X-rays. In order to do this the high purity germanium X-ray spectrometer was calibrated using absolutely calibrated radio-active sources, obtained from the Radiochemical Centre (TRC) at Amersham. The sources chosen were ^{241}Am, ^{109}Cd, ^{57}Co. These particular sources were chosen because they fulfilled the following criteria:-

(a) They have X-ray or gamma ray peaks in the region of interest i.e. around 17 KeV.

(b) These peaks have sufficiently well known modes of decay to give branching ratios accurate to about $\pm$ 2%.

(c) They have reasonably long half lives of at least 200 days.

The standard sources were made into thin deposits in the same way as for the niobium samples and presented to the spectrometer at the same position for counting. This position was co-axial with the aluminium can housing the germanium crystal, but 50 mm from the beryllium window. This distance from the detector was chosen in order to reduce the probability of sum-peaks occurring during calibration. This is a particular problem in this energy region because of the high value of the photo-electric cross-section which is the principal mechanism of photon detection at these energies.

This calibration method resulted in a detector calibration factor with an error of $\pm$ 3.2%.

Each deposit was measured twice and a weighted mean was taken of the niobium peak areas. In all cases the agreement between the two measurements was compatible with the errors. The K_α and K_β X-ray peaks were all resolved, and were analysed separately again using the GAMANAL code.

The disintegration rates were calculated using the expression below:

$$A = \frac{\left[\frac{K_\alpha}{E_\alpha} + \frac{K_\beta}{E_\beta}\right]}{B}$$

where K_α is the count-rate from the niobium K_α X-ray, E_α is the detector efficiency at this energy, and similarly for K_β. B is the branching ratio for the production of niobium K X-rays.

$E_\alpha = 9.40 \times 10^{-3} \pm 3\%$
$E_\beta = 9.85 \times 10^{-3} \pm 3\%$
$B = 0.116 \pm 3.4\%$

In order to establish the extent of any residual fluorescence effects, two deposits were produced from the SSC sample; one of 0.4523 mg, being of similar mass to the deposits from the other four samples, the other of 0.0412 mg, having a mass about ten times less. The measured specific activities of the two deposits differed by only 1.6%, with errors of 1.0% on the light deposit and 0.9% on the heavy. This test indicates that fluorescence effects, if they are present, are probably less than 1%.

Measurement Uncertainties

A summary of the estimated uncertainties in activity measurements made by both AERE, Harwell and AEE Winfrith is shown in Table 2.3.1.7. The random errors (typically $\sim \pm 1.5\%$) are due to counting statistics and uncertainties in the analysis of the gamma ray spectra using the GAMANAL code. The systematic errors are mainly due to uncertainties in the absolute calibration of the GeLi detector systems, although in the case of the ^{93m}Nb activity measurements made by AEE Winfrith an uncertainty of $\pm$ 3.4% was also assumed for the emission probability of the K X-rays.

Comparison of the AERE Harwell and AEE Winfrith measurements in the context of the above uncertainty estimates indicates general consistency between the two sets of measurements, the overall tendency for AERE Harwell measurements to be higher than AEE Winfrith being consistent with the likelihood of systematic calibration difference between the two laboratories. The exceptions to this general rule are the sometimes large and variable differences between the measurements of ^{60}Co (from ^{59}Co (n, γ) and ^{63}Cu(n,α) reactions) and the ^{46}Sc activity at the $\frac{1}{2}$T position.

Table 2.3.1.7 - Overall Uncertainties on Activity Measurements Made on Rolls-Royce & Associates Ltd. Dosimeters Used in the ORR/PSF (4/12) 18-Day Dosimetry Characterisation Run

Nuclide Measured	Counting Laboratory	Uncertainty (1σ)%	
		Random	Systematic
^{54}Mn	AERE	2.0	5.0
"	AEEW	1.6	2.0
^{59}Fe	AERE	2.0	5.0
"	AEEW	1.3	2.0
^{60}Co	AERE	2.0	5.0
"	AEEW	1.5	3.0
^{58}Co	AERE	2.0	5.0
"	AEEW	1.5	3.0
^{46}Sc	AERE	0	5.0
"	AEEW	1.0	3.0
^{93m}Nb	AERE	-	-
"	AEEW	1.0	4.5

Table 2.3.1.8 - Reaction Rates Measured on Rolls-Royce & Associates Ltd. Dosimeters Used in ORR/PSF (4/12) 18-Day Dosimetry Characterisation Run

Neutron Reaction	Reaction Rate at 30 MW (per Target Atom per Second)*				
	SSC	$\frac{1}{2}T$	$\frac{1}{2}T$ (offset)	$\frac{1}{4}T$	$\frac{1}{8}T$
$^{54}Fe(n,p)^{54}Mn$	4.88E-13	2.93E-14	2.42E-14	1.12E-14	3.91E-15
$^{58}Fe(n,\gamma)^{59}Fe$	4.81E-12	2.51E-13	2.25E-13	8.76E-14	3.95E-14
$^{63}Cu(n,\alpha)^{60}Co$	3.07E-15	2.34E-16	2.06E-16	1.06E-16	3.63E-17
$^{58}Ni(n,p)^{58}Co$	6.60E-13	3.91E-14	3.22E-14	1.50E-14	5.54E-15
$^{46}Ti(n,p)^{46}Sc$	6.61E-14	4.20E-15	3.41E-15	1.60E-15	5.37E-16
$^{59}Co(n,\gamma)^{60}Co$	1.97E-10	8.09E-12	-	5.09E-12	2.46E-12
$^{93}Nb(n,n')^{93m}Nb$	1.51E-12	9.58E-14	7.89E-14	4.46E-14	2.22E-14

* Mean of AERE and AEEW measurements except where measurement data was inconsistent (see Table 2.3.1.6).

2.3.1.4 Activation Analysis

The measured activities shown in Table 2.3.1.6 and the irradiation histories given in Tables 2.3.1.3 and 2.3.1.4 were processed by the Rolls-Royce & Associates Ltd. computer code ADA. This code treats the power history as a series of timesteps and calculates the radionuclide production and decay factor $f(\lambda,t)$ in

$$\text{Reaction Rate} = \phi\bar{\sigma} = \frac{A}{N.f(\lambda,t)}$$

where A = measured activity
N = target atom number density
$\bar{\sigma}$ = effective reaction cross-section
ϕ = neutron flux density
λ = decay constant of radionuclide

such that the reaction rate, $\phi\bar{\sigma}$, can be calculated. This code allows for burn up of target and product nuclides as well as branching reactions such as $Ni^{58}(n,p)Co^{58}$ which have metastable products such as Co^{58m}. These reaction rates are tabulated in Table 2.3.1.8.

For the purposes of this table, the activities used in calculating the reaction rates were the mean values of the AERE Harwell and AEE Winfrith measurements except for $^{46}Ti(n,p)^{46}Sc$ at the $\frac{1}{4}T$ position and $^{63}Cu(n,\alpha)^{60}Co$ at the SSC and $\frac{1}{4}T$ positions for which AEE Winfrith measurements were used, as these appeared more consistent with the rest of the reaction rate measurements.

In an attempt to establish the validity of the RR&A dosimetry results, the fast neutron reaction rates measured on the RR&A dosimetry packs were compared with the fast neutron reaction rates measured on the CEN/SCK (Mol, Belgium) Interlaboratory Dosimetry Packs which had been irradiated simultaneously. These reaction rates were measured by CEN/SCK and also by PTB (Braunschweig, W.Germany) and ECN (Petten, Holland) and a high degree of consistency was established (To 82a). Since these dosimetry packs were irradiated at different axial heights, for the purposes of comparison both the RR&A and CEN/SCK Interlaboratory reaction rate measurements were converted to equivalent core mid-plane values by applying axial correction factors derived from (Fa 80a) and reproduced here in Fig. 2.3.1.3 and in the form of Table 2.3.1.9.

Figure 2.3.1.3 - Absolute Vertical Fission Flux Distributions at ¼T Thickness of ORR/PSF Pressure Vessel Simulator Showing Location of UK and CEN/SCK Dosimetry in PSF (4/12) 18 Day Characterisation Run

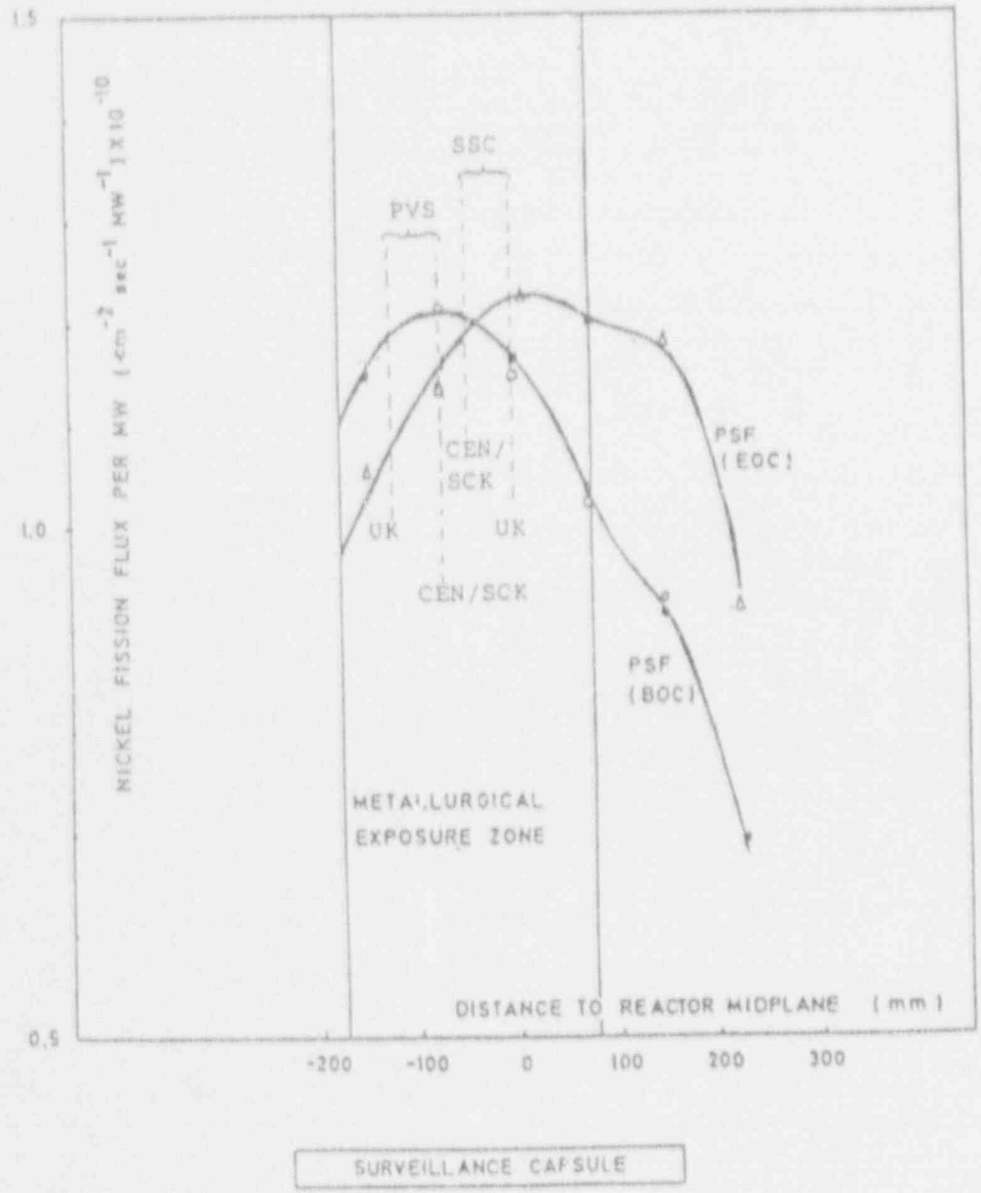

Table 2.3.1.9 - Correction Factors to Adjust ORR/PSF (4/12) Reaction Rate Measurements to Equivalent Core Mid-Plane Values

Location	Correction Factor to Core Mid-Plane	
	RRA	CEN/SCK
SSC	1.0	0.98
$\frac{1}{4}$T	1.06	1.02
$\frac{1}{4}$T (offset)	1.06	1.02
$\frac{1}{2}$T	1.06	1.02
$\frac{3}{4}$T	1.06	1.02

A summary of these comparisons is shown in Table 2.3.1.10. The uncertainties in the CEN/SCK Interlaboratory measurements have been quoted as being similar to those of AERE Harwell and AEE Winfrith (To 82a).

There appears to be a tendency for the RR&A dosimeter reaction rates to be on average about 5% higher than the CEN/SCK Interlaboratory dosimeters, although the $^{63}Cu(n,\alpha)^{60}Co$ at the $\frac{1}{4}$T and $\frac{3}{4}$T are up to 25-30% higher, whilst the $^{93}Nb(n,n')^{93m}Nb$ are up to 8% lower than CEN/SCK data. The possibility that the RR&A copper dosimeter foils were contaminated with cobalt has been investigated, but cobalt levels were found to be ~0.1 ppm, so that this is probably not the cause of the discrepancy.

2.3.1.5 Conclusions

1. Activation dosimetry measurements have been successfully made by Rolls-Royce & Associates Ltd., using standard AERE Harwell dosimetry packs and counting methods on the ORR/PSF (4/12) 18-day dosimetry characterisation run.

2. Intercomparison of activity measurements between AERE Harwell and AEE Winfrith on the Rolls-Royce & Associates Ltd. dosimeters revealed the existence of several discrepancies well outside the anticipated errors in counting methods.

3. Intercomparison of reaction rate measurements made on CEN/SCK (Belgium) and Rolls-Royce & Associates Ltd. (UK) dosimetry of the ORR/PSF (4/12) 18-day run indicates a bias of about +5% in favour of the UK measurements when both sets of results are corrected to reactor mid-plane values. However, there are several important exceptions to this trend, notably the $^{63}Cu(n,\alpha)Co^{60}$ and $^{93}Nb(n,n')^{93m}Nb$ reaction rates at the $\frac{1}{4}$T and $\frac{3}{4}$T PVS positions, where the discrepancies are well outside the uncertainties in correcting data to reactor mid-plane values.

Table 2.3.1.10 - Comparison of Reaction Rates Measured on Rolls-Royce and Associates Ltd. Dosimeters and those Measured on CEN/SCK Interlaboratory Dosimeters in ORR/PSF (4/12) 18-Day Dosimetry Characterisation Run (All Data Adjusted to Reactor Mid-Plane Equivalent Values)

Neutron Reaction	Dosimetry Pack	Reaction Rates at 30 MW (per Target Atom per Second)			
		SSC	$\frac{1}{4}$T	$\frac{1}{2}$T	$\frac{3}{4}$T
$^{54}Fe(n,p)^{54}Mn$	RRA	4.880E-13	3.106E-14	1.187E-14	4.145E-15
"	INTERLAB	4.635E-13	2.925E-14	1.110E-14	3.965E-15
"	RRA/INTERLAB	1.05	1.06	1.07	1.05
$^{63}Cu(n,\alpha)Co^{60}$	RRA	3.070E-15	2.480E-16	1.124E-17	3.848E-17
"	INTERLAB	2.920E-15	2.239E-16	8.539E-17	3.068E-17
"	RRA/INTERLAB	1.05	1.10	1.31	1.25
$^{58}Ni(n,p)^{58}Co$	RRA	6.599E-13	4.145E-14	1.590E-14	5.872E-15
"	INTERLAB	6.580E-13	4.061E-14	1.583E-14	5.806E-15
"	RRA/INTERLAB	1.00	1.02	1.00	1.01
$^{46}Ti(n,p)^{46}Sc$	RRA	6.610E-14	4.452E-15	1.696E-15	5.692E-16
"	INTERLAB	6.212E-14	4.274E-15	1.598E-15	5.595E-16
"	RRA/INTERLAB	1.06	1.04	1.06	1.02
$^{93}Nb(n,n')^{93m}Nb$	RRA	1.510E-12	1.015E-13	4.728E-14	2.353E-14
"	INTERLAB	1.575E-12	1.016E-13	5.141E-14	2.584E-14
"	RRA/INTERLAB	0.96	1.00	0.92	0.91

2.3.1.6 UK Measurements of ORNL Copper Foils Irradiated in the PSF Startup Characterization Program

2.3.1.6.1 Introduction

Within the framework of the ORR/PSF (4/12) characterisation run, ORNL supplied the UK with some copper foils which had been irradiated in the simulated surveillance capsule (SSC), and $\frac{1}{4}$T, $\frac{1}{2}$T and $\frac{3}{4}$T locations in the pressure vessel simulator (PVS) and were part of an interlaboratory comparison exercise. The activation measurement of these foils was carried out by AERE Harwell in the same manner as that reported for the UK dosimeters in Section 2.3.i and the analysis performed by Rolls-Royce & Associates Ltd., UK.

2.3.1.6.2 Results

The activity of interest was Co^{60} from the threshold reaction $^{63}Cu(n,\alpha)^{60}Co$. The results of the activation measurements are shown in Table 2.3.1.11.

Table 2.3.1.11 - Results of UK Activation Measurements on ORNL Copper Foils Irradiated in ORR/PSF (4/12) 18-Day Dosimetry Characterisation Run

Foil No.	Irradiation Location	Activity (dps/mg) Co^{60} at End of Irradiation	$^{63}Cu(n,\alpha)^{60}Co$ Reaction Rate reactions/atom.s	Predicted Neutron Flux (E > 1 MeV) $n/cm^2/s$
1	SSC	1.169E2 (0.99)*	2.840E-15	6.174E12
3	$\frac{1}{4}$T	8.667E0 (1.01)*	2.106E-16	4.129E11
2	$\frac{1}{2}$T	3.215E0 (1.02)*	7.922E-17	1.932E11
4	$\frac{3}{4}$T	1.162E0 (1.02)*	2.865E-17	8.682E10

* Value of RRA/AERE measurement with respect to CEN/SCK value.

It was noted that the ORNL foils which had been supplied to the UK had been irradiated in the same locations as those measured by CEN/SCK Mol, Belgium and reported in (To 82a). Also shown in Table 2.3.1.11 therefore are the comparisons of UK results to CEN/SCK results. The results show a very good agreement and considerably better than that for the copper foils of UK origin. Since the latter does not appear therefore to be due to discrepancies in counting methods, these results would seem to cast considerable doubt on the quality of the UK copper source material used in the RRA/AERE dosimetry packs. However, inspection of Table 2.3.1.10 reveals that in terms of the UK measured reaction rates the $^{63}Cu(n,\alpha)$ activities are nevertheless consistent with the other reaction rates measured. The discrepancy noted in Section 2.3.1 therefore remains unresolved.

2.3.1.7 Acknowledgments

The authors wish to thank Mr. M. Banham and Mr. M. Wilkins of AERE-Harwell (UK) for supplying and counting the dosimetry capsules used in this experiment and Dr. W. H. Taylor, Mr. M. Murphy and Mr. M. Marsh of AERE-Winfrith (UK) for undertaking the intercomparison measurements.

2.3.2 CEN/SCK RESULTS AND ANALYSIS

H. Tourwé and A. Fabry (CEN/SCK)

As stated by Tourwé et al. (To82a), SCK/CEN Mol supplied ORNL with interlaboratory steel and gadolinium capsules and with different sets of foils. The final counting of the SCK/CEN capsules was done at ORNL. Each capsule contained six Ag/Al, six Co/Al, six Nb, six Fe, six Ti, six Ni and two Cu foils. The gadolinium capsules were filled by ORNL with fission detectors supplied by HEDL. Placement information for these sensors in the PSF-SDMF is provided in Table 1, Ref. To82a.

The activation detectors were irradiated in the PSF facility of the ORR reactor during about 18 days. Details of the irradiation histories are given in Table 2 of Ref. To82a.

The interlaboratory capsules were dismantled after irradiation at ORNL. Part of the interlaboratory capsule content was sent to SCK/CEN-Mol, the remaining part being sent to HEDL. Afterwards, SCK/CEN provided ECN-Petten and PTB-Braunschweig each with a detector set of each irradiation location. All detectors were counted by SCK/CEN before shippment to ECN and PTB.

The AERE/RR&A capsules were dismantled by AERL Harwell. The dosimeters from these capsules were counted at AERE-Harwell and AERE-Winfrith.

The Cu foils of the interlaboratory capsules were sent by SCK/CEN in a round robin to all European participants.

The axial fast neutron flux distributions in the different irradiation locations were measured by means of Ni detectors. A cosine function was fitted to the experimental data, see Table 3 (Ref. To82a) and Table 3.15 of Section 3.3.2 of this report.

The counting results (specific activities at the end of irradiation) of the different laboratories, normalized to the SCK/CEN results, are shown in Table 4 (Ref. To82a) and Table 3.14 of Section 3.3.2 of this report; see Section 3.3.2 for a discussion of the results of the comparison of these European results. The Section 3.3.2 discussion was extracted by Gold from the Ref. To82a 4th ASTM-Euratom Symposium paper.

Tourwé et al state that one-dimensional ANISN transport calculations in a 171 energy group structure were performed by ORNL, while two-dimensional discrete ordinate transport DOT calculations in a 17 group structure were performed by SCK/CEN (To82a). They conclude that three-dimensionsal calculations are required to deal with leakage problems. They then discuss the derivation of spectrum averaged cross-sections that are used to determine neutron flux values.

Tourwé et al. conclusions for the European study of the physics-dosimetry results for the 18-day PSF Startup Experiment are:

> *" -- The specific activity results between SCK/CEN, ECN and PTB are excellent; the agreement between AERE-Harwell and AERE-Winfrith results is reasonable.*

-- Neutron flux values, based on countings performed at different European laboratories, were presented. The fast neutron flux > 1 MeV in the SCC and 1/4 T position could be determined with an accuracy better than 10%.

-- The considered ENDF/B-V cross sections are consistent. However, the ENDF/B-V data of 63Cu(n,a) tend to overestimate detector responses. It was also pointed out that more accurate data for the 93Nb(n,n') cross section data are required."

2.3.3 HARWELL SAPPHIRE DAMAGE MONITOR MEASUREMENTS

G. P. Pells, A. J. Fudge and M. J. Murphy (AERE, Harwell, UK)
and S. Watt (Rolls-Royce and Associates, Ltd., UK)

2.3.3.1 Introduction

Detailed information on the use and results of Sapphire Damage Monitor (SDM) measurements is provided in Section 2.6, Ref. Mc87c. The results of the SDM measurements for the 18-day "Startup Experiment" and the "SSC-1 and SSC-2 Experiments" presented in Sections 5.2 and 6.1 are discussed and compared with other test reactor results in Figures 2.6.6 and 2.6.8 of Ref. Mc87c.

The conclusions of the Ref. Mc87c, Section 2.6, study are:

> *"The optical absorption at 400 nm of aluminum vacancy centres produced by neutron irradiation in high-purity, single crystal alpha-Al_2O (sapphire) has been shown to increase in a reproducible manner with damage dose for irradiations at temperatures between 200-310°C in a variety of neutron spectra. The constancy of this behavior has been used to validate the procedures used to calculate the neutron energy spectrum and damage dose in irradiated LWR pressure vessel steels.*
>
> *The thermal stability of the aluminum vacancy centre in sapphire and the fact that sapphire responds to the entire neutron spectrum in a manner similar to that of steels makes it superior to conventional, high-threshold energy, activation monitors in irradiation locations for which a detailed neutron energy spectrum is not available."*

3.0 INTERCOMPARISONS OF RADIOMETRIC NEUTRON DOSIMETRY - SUMMARY

Raymord Gold, L. S. Kellogg, and W. N. McElroy (HEDL)

The PSF startup experiments provided a unique set of benchmarks for comparing RM dosimetry results from many laboratories, both nationally and internationally. The geometrical scale and fluence levels of these PSF startup experiments provided benchmarks considerably closer to LWR power plant environments than were heretofore available. Moreover, because of the unique character of the PSF metallurgical tests (Mc86b), many laboratories around the world participated. Hence, these PSF startup experiments afforded an ideal opportunity for intercomparisons of RM dosimetry.

Three PSF startup experiments were used for these RM intercomparisons:

(RM-I) -- The PSF Surveillance Capsule Perturbation Experiment [also known as the Simulated Dosimetry Measurement Facility Experiment 2 (SDMF2)] (Ba84a,To82).

(RM-II) -- The first PSF metallurgical simulated surveillance capsule (SSC-1) experiment (Mc84b).

(RM-III) -- The PSF 18-day high-power irradiation (SDMF1) (Fa80a).

Including the RM-I, RM-II and RM-III tests, seven test irradiations have been performed in the ORR-PSF Benchmark Facility in support of the NRC LWR-PV Surveillance Dosimetry Improvement Program. These tests are identified in Appendix A of Ref. (Mc87c).

Based on the study of the reported radiometric measurements for the RM-I, RM-II and RM-III tests, it is concluded that:

1) While the agreement among the majority of the laboratories was, most often, satisfactory, with non-fissile dosimeter results generally falling within 5% and the fissionable dosimeter results falling within 10%, improvement is still required in order to routinely meet accuracy goals of LWR-PV surveillance physics-dosimetry.

2) A critical review of both analytical and calculational techniques must be conducted on a periodic basis by all of the laboratories.

3) Each laboratory should review and utilize, where possible, the appropriate ASTM Standard Methods, Guides, and Practices; maintain system calibration and/or control documentation, and continue in this or similar programs using existing benchmark facilities for verifications and direct correlations.

4) Systematic problems can exist with Cu and Nb dosimeters. As previously reported (As87), Co impurity in the Cu sensors can seriously comprise results. As stressed in earlier dosimetry work with Nb (To80), more accurate cross-section data are needed for the 93Nb(n,n') reaction.

5) There is a clear and significant difference in accuracy between fissile and non-fissile RM dosimeters. The higher uncertainties of fissile relative to non-fissile RM dosimeters (by about a factor of two) are just barely acceptable given the goal accuracies of LWR-PVS work.

As stated by Fabry (Fa82), complementary objectives of the RM dosimeter intercalibration studies were to:

" *-- Link PSF and HSST fluence dosimetry to PCA physics benchmarking metrology.*

-- Provide an international neutron metrology and analysis opportunity, including the validation of UK, French, and Belgium damage monitors and of dosimetry cross section data for crucial but less well known long-half life radiometric monitors;

93Nb(n,n') versus 237Np(n,f) and 103 Rh(n,n')

63Cu(n,a) versus 27Al(n,a).

In this regard, it is noted that radiometric measurements were not made by any U.S. participants on the 93Nb(n,n') reaction; only the European participants made such measurements.

3.1 INTRODUCTION

Raymond Gold, L. S. Kellogg, and W. N. McElroy (HEDL)

In light water reactor (LWR) pressure vessel surveillance (PVS) work, it is currently accepted that the accuracy goal for reported neutron exposure parameters [flux and fluence (E < 0.1 and 1.0 MeV) and dpa] is the 5% to 15% (1σ) range (As82,Mc81,Mc82,Ra77,Ra78). To achieve and maintain this level of accuracy, reactor physics calculational and dosimetry measurement results must routinely be in the same accuracy range or better. It has been shown that this level of accuracy can be obtained, but only through careful standardization, which includes interlaboratory program work using benchmark (verification) facilities and extensive interlaboratory comparisons (Fa77, Gr78,Gr78a,Gi78,Mc81a). Through these interlaboratory activities, systematic biases that arise at any one laboratory can be recognized and then (hopefully) resolved.

The use of radiometric (RM) neutron dosimetry for measurement of neutron exposure in LWR-PVS work is virtually universal. RM neutron dosimetry has been used since the inception of LWR-PVS programs, and a number of ASTM standards on this subject have existed for sometime. While two more recent passive neutron dosimetry methods have been proposed and possess unique advantages for LWR-PVS work [namely, solid state track recorder (SSTR) and helium accumulation fluence monitor (HAFM) neutron dosimetry], the use of these two methods in LWR-PVS work is extremely limited to date. Standards for both of these newer methods have only recently been issued [As82b,As83a]. Equally significant is the fact that the number of laboratories with expertise and special facilities required for these two methods is very limited. As a consequence, RM dosimetry is the primary standard for LWR-PVS work and probably will continue to be so for sometime.

The PSF startup experiments provided a unique set of benchmarks for comparing RM dosimetry results from many laboratories, both nationally and internationally. The geometrical scale and fluence levels of these PSF startup experiments provided benchmarks considerably closer to LWR power plant environments than were heretofore available. Moreover, because of the unique character of the PSF metallurgical tests (Mc86b), many laboratories around the world participated. Hence, these PSF startup experiments afforded an ideal opportunity for intercomparisons of RM dosimetry.

Three PSF startup experiments were used for these RM intercomparisons:

(RM-I) -- The PSF Surveillance Capsule Perturbation Experiment [also known as the Simulated Dosimetry Measurement Facility Experiment 1 (SDMF2)] (Ba84a,To82).

(RM-II) -- The first PSF metallurgical simulated surveillance capsule (SSC-1) experiment (Mc84b).

(RM-III) -- The PSF 18-day high-power irradiation (SDMF1)(Fa80a).

Table 3.1 identifies laboratories that participated in each of these three (RM-I, RM-II and RM-III) PSF experiments.

RM dosimetry aspects of these three PSF irradiations are described in Section 3.2. Interlaboratory comparisons are provided in Section 3.3. Conclusions drawn from these intercomparisons are then presented in Section 3.4. Section 3.5 provides information related to NBS radiometric counting and fluence standards. These standards were prepared and made available to assist in the calibration and verification of the accuracy of the participating laboratories' reported radiometric and fluence exposure parameter results.

TABLE 3.1

LABORATORIES PARTICIPATING IN PSF STARTUP EXPERIMENTS

PSF Experiment		Participating Laboratories*
RM-I	SDMF-2	B&W, BMI, CE, GE, HEDL, SwRI, W
RM-II	SSC-1	B&W, BMI, CE, GE, HEDL, SwRI, W
RM-III	SDMF-1	AEEW, AERE, CEN/SCK, ECN, HEDL, PTB

*AEEW = Atomic Energy Establishment Winfrith (UK)
AERE = Atomic Enger Research Establishment Harwell (UK)
B&W = Babcock and Wilcox (US)
BMI = Battelle Memorial Institute (US)
CEN/SCK = Centre d'Etude de'l Energie Nucleaire/Studiecentrum voor Kernenergie (Belg)
CE = Combustion Engineering (US)
ECN = Netherlands Energy Research Foundation, Petten (Neth)
GE = General Electric (US)
HEDL = Hanford Engineering Development Laboratory (US)
PTB = Physikalisch-Technische Bundesanstalt, Braunschweig (FRG)
SwRI = Southwest Research Institute (US)
W = Westinghouse (US)

3.2 DESCRIPTION OF RM NEUTRON DOSIMETRY IN PSF EXPERIMENTS

The PSF startup experiments used for benchmark testing of RM dosimetry in LWR-PVS environments were described at the fourth ASTM-EURATOM Symposium on Reactor Dosimetry, where interlaboratory comparisons of RM results were initially presented (Ke82,To82a). PSF irradiations RM-I, RM-II, and RM-III are described below in Sections 3.2.1, 3.2.2, and 3.2.3, respectively. Special emphasis is given to the RM dosimetry aspects of these PSF startup experiments.

3.2.1 RM-I -- PSF Surveillance Capsule Perturbation Experiment (SDMF2)

The RM-I experiment was included as an integral part of the PSF Surveillance Capsule Perturbation Experiment (Ba84a,To82). RM dosimeter sets fabricated at HEDL included six replicate samples of each dosimeter and were designed to minimize spatial effects. The design of typical capsules is illustrated in Figures 3.1 and 3.2. Capsules of similar design but without the gadolinium shield were also used in the first irradiation.

RM dosimeters were placed in the Thermal Shield Back (TSB) and the Pressure Vessel Face (PVF) simulated surveillance capsules. The location of the two capsules are shown in Figure 3.3. Figures 3.4 shows the dosimetry arrangement in each capsule. Those dosimetry capsules labeled HF and HNF contain the interlaboratory comparison samples. The HF capsules contain bare or Gd covered fissionable and Co/Al monitors, shown in Figure 3.2. The HNF capsules have bare or Gd-covered non-fission wires, as shown in Figure 3.1.

3.2.2 RM-II -- SCC-1 Experiment

The RM-II experiment was included in the first metallurgical simulated surveillance capsule (SSC-1) experiment (Mc84b). Figure 3.5 reveals that the 4/12 configuration was used in the SSC-1 experiment. The location of RM dosimeters within the experiment is shown in Figure 3.6. The HF comparison samples were placed in Hole B-Block 38 and the HNF samples in Hole D-Block 37.

After both the RM-I and RM-II irradiations, the assemblies were dismantled at ORNL and the individual dosimeter capsules shipped to HEDL. The capsules were opened and the individual dosimeters were identified by unloading sequence and dosimeter weight or ID designation. All RM dosimeters were counted at HEDL to determine relative normalization factors between a given RM dosimeter and the corresponding HEDL RM dosimeter. These individual normalization factors could then be used on a dosimeter-by-dosimeter basis to correct for effects that might arise from:

1) Gradients in the neutron exposure.
2) Self-shielding.
3) Uncertainties in dosimeter mass.

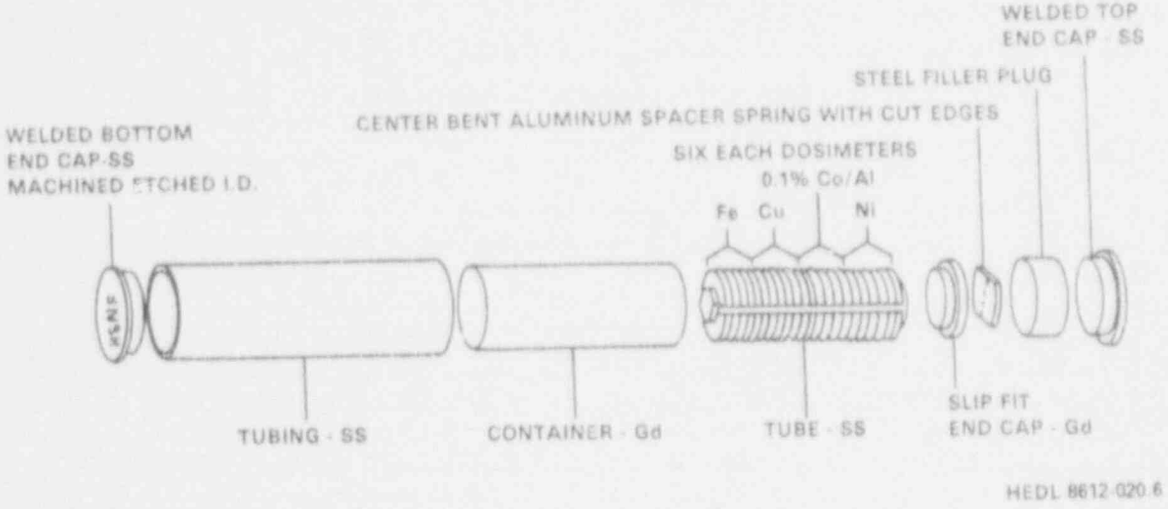

FIGURE 3.1. HEDL Surveillance Capsule - Non-Fissionable Materials (1 Set HEDL/Vendor/Service Laboratory Counting).

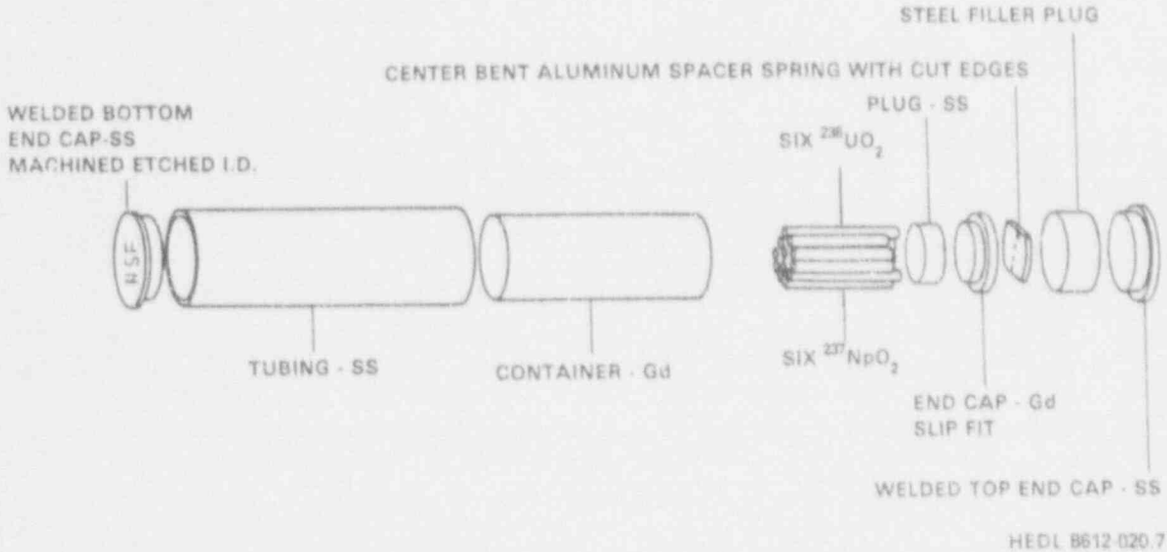

FIGURE 3.2. HEDL Surveillance Capsule - Fissionable Materials (1 Set HEDL/Vendor/Service Laboratory Counting).

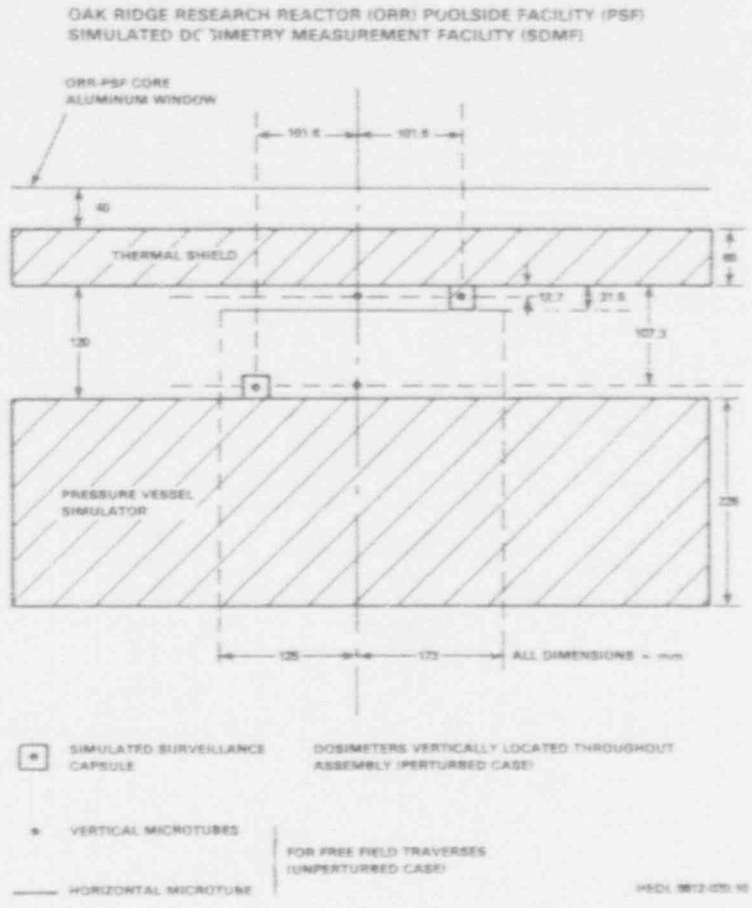

FIGURE 3.3. PSF-SDMF Perturbation Test Experimental Configuration (Horizontal Cut at Maximum Axial Flux).

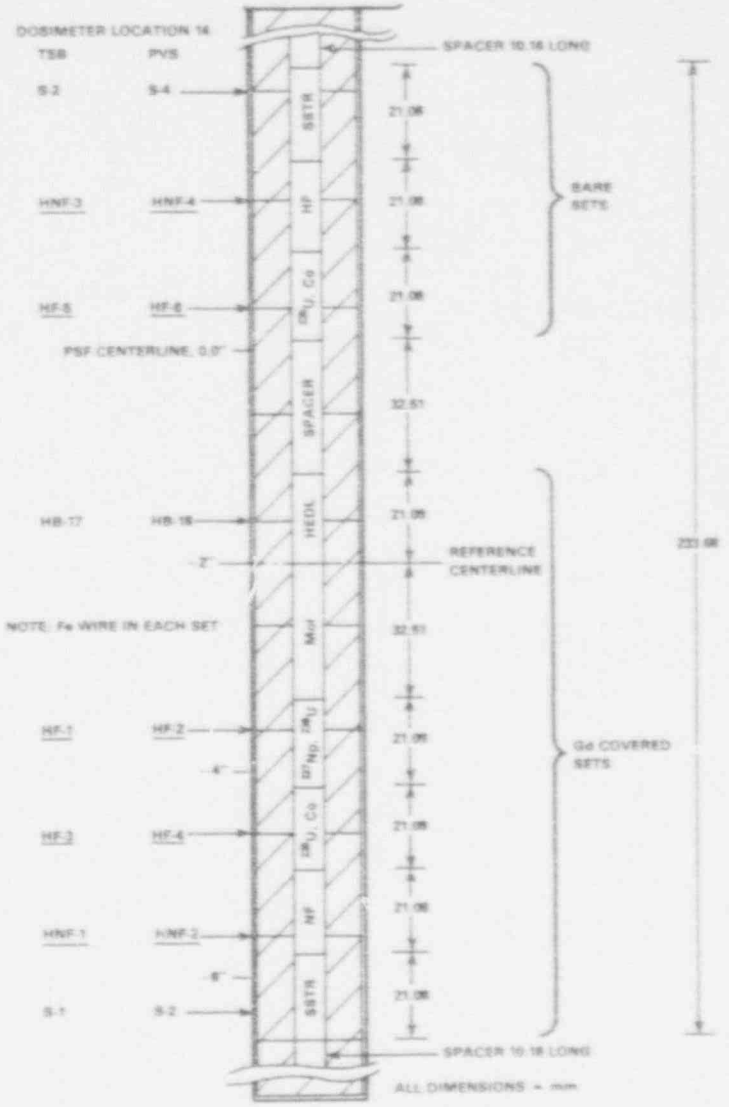

FIGURE 3.4. Axial Distribution of Dosimetry Sets in Simulated Surveillance Capsule.

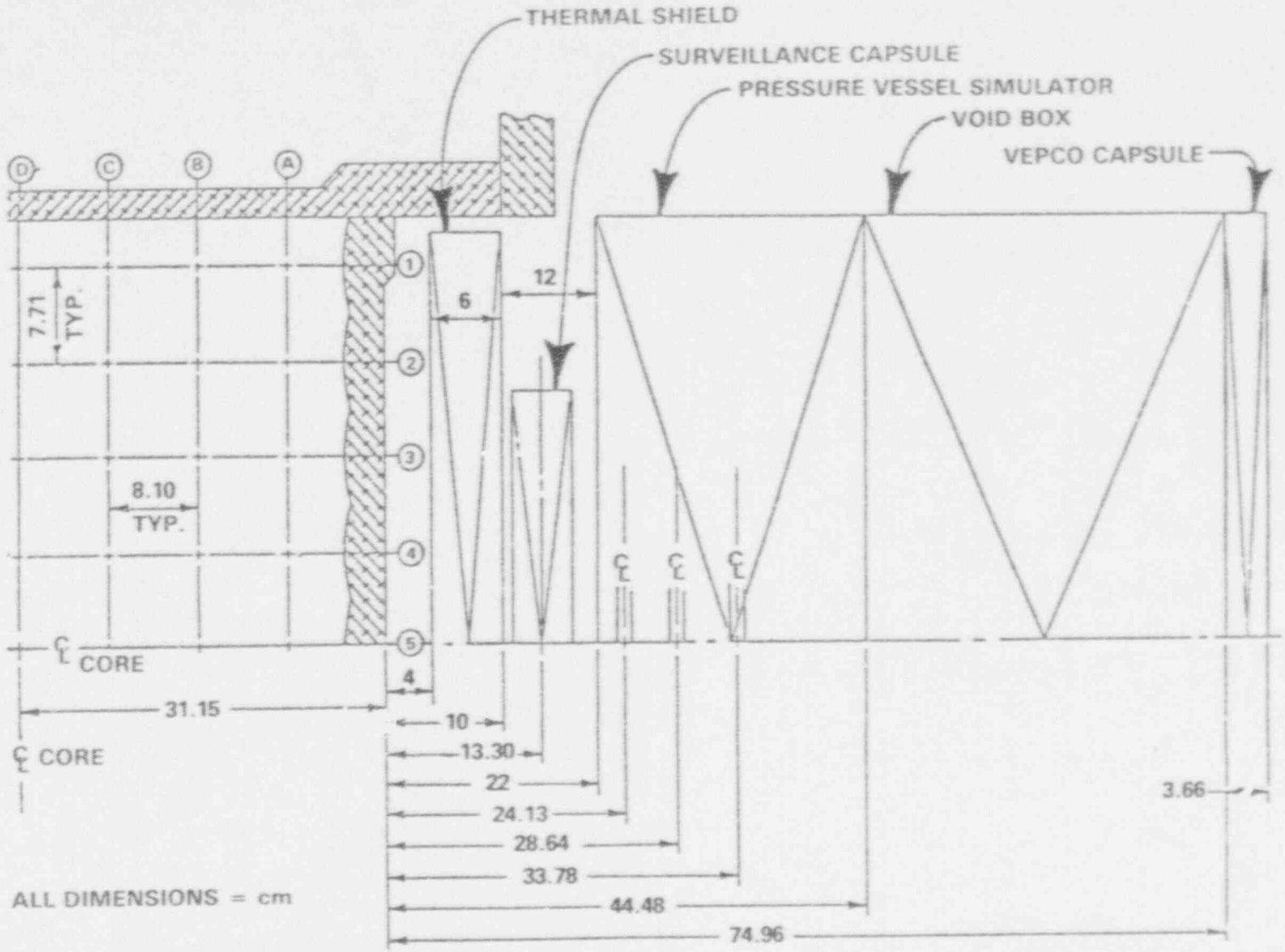

FIGURE 3.5. ORR-SDMF 4/12 Configuration (SSC-1).

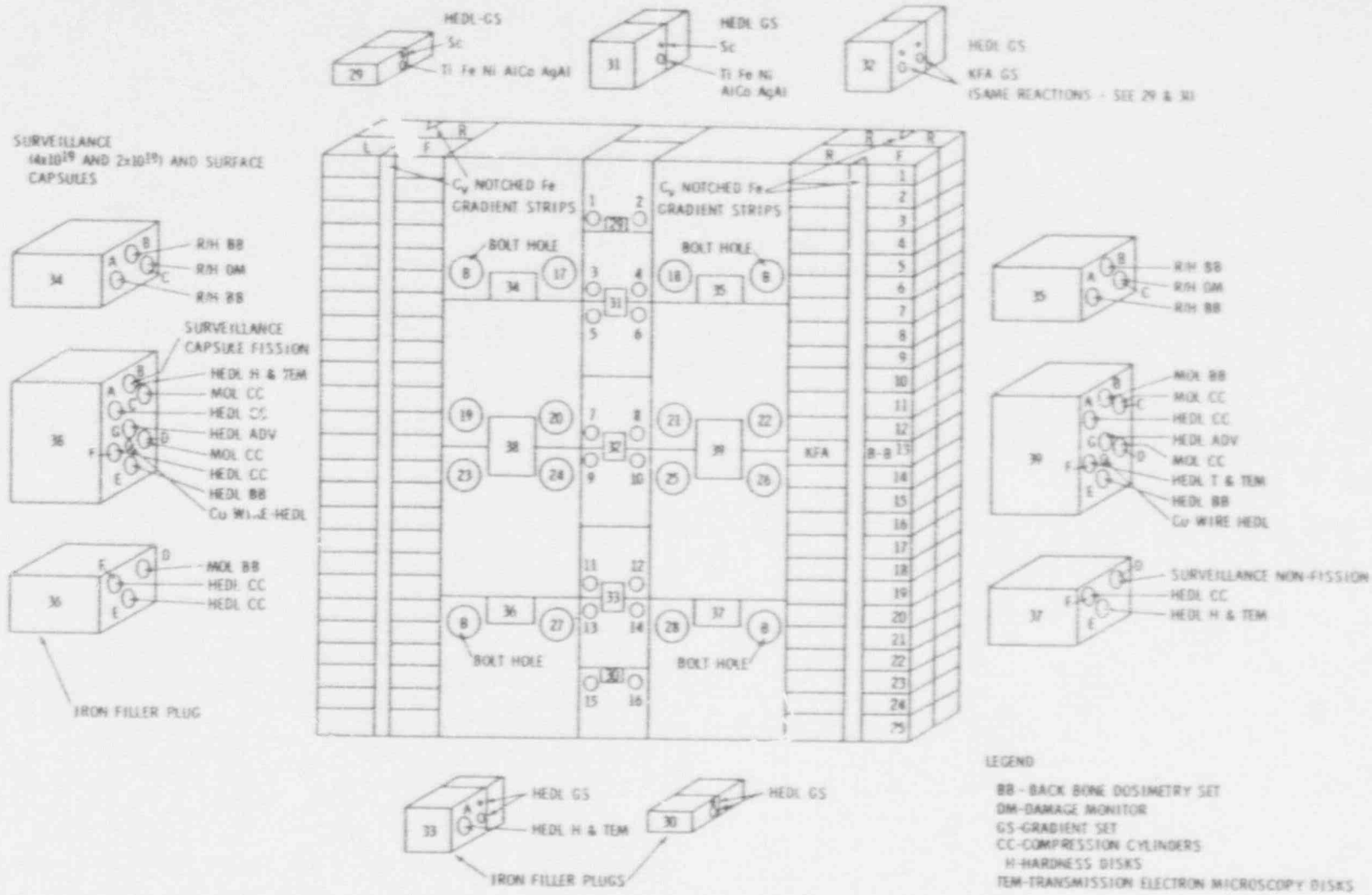

+Fe wire ~0.010-in. OD placed in ~0.020 OD SS Tubing.
**Interlaboratory comparison dosimeters.

FIGURE 3.6. SSC-1 Specimen Configuration.

These normalization factors were determined to an accuracy of better than 1.5% by counting at HEDL.

In addition to the dosimeter sets, laboratory participants were provided all basic information concerning the dosimetry materials, as well as the irradiation information provided by ORNL to allow calculations of both absolute specific activities and reaction rates. These data included the individual dosimetry "as-built" sheets (describing materials, form, and encapsulation), dosimeter (QA) information (Table 3.2), and the individual location and time history information (Table 3.3).

3.2.3 RM-III -- The 18-Day High-Power Experiment (SDMF-1)

For the RM-III experiment, different sources of RM materials were employed. AERE and Rolls-Royce and Associates (RR&A, Derby, UK) supplied ORNL with stainless steel capsules containing Fe, Cu, Ti, Ni, Nb, and Co/Al detectors together with some prototype sapphire damage dosimeters. SCK/CEN Mol supplied ORNL with interlaboratory steel and gadolinium capsules and with different sets of foils. The final mounting of the SCK/CEN capsules was done at ORNL. Each capsule contained 6 Ag/Al, 6 Co/Al, 6 Nb, 6 Fe, 6 Ti, 6 Ni, and 2 Cu foils. The gadolinium capsules were filled by ORNL with fission detectors supplied by HEDL.

These AERE/RR&A and SCK/CEN capsules were located in the PSF 4/12 configuration according to the specifications given in Table 3.4. Table 3.4 considers only those RM capsules that were used for the interlaboratory comparisons by the European laboratories and HEDL.

Table 3.5 provides detailed irradiation histories for each RM capsule. Because of loading and unloading procedures, the irradiation interval was somewhat different for RM capsules at these different locations.

After irradiation, the interlaboratory capsules were dismantled at ORNL. Part of the interlaboratory capsule contents was sent directly to SCK/CEN Mol, the remaining part being sent to HEDL. SCK/CEN counted all the detectors sent to them and then provided both ECN-Petten and PTB-Braunschweig individual detector sets from each irradiation location.

The AERE/RR&A capsules were dismantled by AERE-Harwell, and RM dosimeters from these capsules were counted at both AERE-Harwell and AEE-Winfrith.

After counting, the Cu foils from the interlaboratory capsules were sent by SCK/CEN to all the European participants in a round robin.

TABLE 3.2

DOSIMETRY FOIL QA DATA

Dosimeter	Form	ρ	Batch	Target Element[a,b] (wt.%)	Isotopic Wt. % (a,b) 233	234	235	236	237	238	239
^{235}U	18.6 mil UO_2 Wire	8.68	264C	87.97	<0.005	0.034[1]	99.89[1]	0.025[1]		0.053[2]	
^{238}U	17.5 mil UO_2 Wire	9.62	ES-2	87.75	<0.001	<0.001	0.0012[1]	<0.001		99.999[1]	
^{237}Np	19.7 mil NpO_2 Wire	8.92	HP-28	87.4			<0.0005	<0.0005	99.99[1]	≤0.003	≤0.003

The above foils are encapsulated in 0.035" OD vanadium capsules (~40 ppm Ta impurity) wall thickness <0.006".

Capsule lengths are: ^{235}U - 0.190", ^{238}U [illegible]", ^{237}Np - 0.340".

Dosimeter	Form	Batch	Isotopic	Target Element and Impurity Content (Wt.%) Ni	Fe	Cu	Ti	Co	Al	Ag	Cr	Mg	Si	Mn
Ni[a]	20 mil Wire (0.51 mm)	S.E.	Natural	Balance	<0.0003			<0.4.001		<0.0001		<0.0002	<0.0003	
Fe[c]	20 mil Wire	2	"	0.0041	Balance			<0.0052			0.0018			
Cu[a,d]	20 mil Wire	CPO 3054	"			99.999		<0.0003		0.0002		0.0001	0.0001	
Ti[a]	20 mil Wire	139 W	"		0.008	0.001	99.917		0.0001		0.003	0.001	0.005	0.02
Co/Al[a]	20 mil Wire	SRM 953	"					0.116	Balance					

[a] Elemental, isotopic and/or impurity analysis provided by vendor. Assigned errors, i.e. (1), represents value error in the last significant figures.
[b] QA also performed at HEDL. Values supplied by ORNL were confirmed within the error assignments.
[c] Impurity analysis performed at HEDL utilizing activation analysis. Analysis was not made for impurity products with t 1/2 <~2 hr.
[d] Co analysis was made at HEDL by spark source mass spectrometry.

TABLE 3.3

IRRADIATION HISTORY AND LOCATION

FIRST ORR-SDMF IRRADIATION
(Perturbation Experiment)

Start of Irradiation	1530 EST	1/31/80
End of Irradiation	1530 EST	2/9/80
Total Duration		9.00 days
Nominal Reactor Power		30 MW

Irradiation can be treated as a square wave function.

Sample Locations

X coordinate: ISB - 101.6 mm South of Core C_L

PVS - 101.6 mm North of Core C_L

Y coordinate: Referenced to ORR Core A1 window:

ISB - 112.7 mm

PVS - 207.3 mm

Z coordinate: Approximate location referenced between Reference Core C_L (maximum flux) rather than actual Core C_L and approximate location of mid-point of each replicate sample group. Actual sample position depends on sample location within set and adjustments will be made later if required.

Gadolinium Covered Capsules: HF-1, HF-2, HF-3, HF-4, HNF-1, HNF-2

Bare Capsules: HF-5, HF-6, HNF-3, HNF-4

SECOND ORR-SDMF IRRADIATION
(SSCet Experiment)

Inserted	Retracted or ORR Down
April 30, 1980 13:34	May 8, 1980 7:00
May 8, 1980 16:43	May 14, 1980 13:30
May 16, 1980 9:67	[illegible] 7", 1980 2:17
May 22, 1980 10:49	[illegible], 1980 24:00
June 12, 1980 9:20	[illegible] e 23, 1980 12:53

(All times Eastern Daylight Time)

Nominal Reactor Power 30MW

Sample locations

X coordinate: HSF 388 69.9 mm South of Core C_L

HSNF 37D 47.2 mm North of Core C_L

(individual dosimeter locations vary from this mid point location)

Y coordinate: Referenced to ORR A1 window

HSF 38D 133.0 mm

(individual dosimeters may vary by ± 1.1 cm)

HSNF 37D 139.9 mm

Z coordinate: Referenced to Reference Core C_L (maximum flux) rather than actual Core C_L and mid point of each capsule. Actual position of individual HSF samples may vary by ± 1.1 mm

HSF 388 7.9 mm

HSNF 37D -67.5 mm

TABLE 3.4

LOCATION OF RM CAPSULES IN IRRADIATION RM-III

IRRADIATION LOCATION	SAMPLE	AXIAL HEIGHT ABOVE MIDPLANE (mm)
SSC	INTERLABORATORY CAPSULE	- 51
	AERE/RR & A CAPSULE	- 3.5
1/4 T	INTERLABORATORY CAPSULE	- 75
	AERE/RR & A CAPSULE	-122
	FISSION DETECTORS	0
1/2 T	INTERLABORATORY CAPSULE	- 75
	AERE/RR & A CAPSULE	-122
3/4 T	INTERLABORATORY CAPSULE	- 75
	AERE/RR & A CAPSULE	-122

TABLE 3.5

IRRADIATION HISTORIES FOR THE 18-DAY HIGH-POWER RUN (RM-III)

LOCATION	BEGIN EXPOSURE (LOCAL TIME)	END EXPOSURE (LOCAL TIME)	TOTAL IRRADIATION TIME (s)	EFFECTIVE IRRADIATION TIME AT 30 MW (s)
SSC	OCT. 27, 1979 14h26	NOV. 14, 1979 8h55	$1.5377\ 10^6$	$1.5105\ 10^6$
1/4 T	OCT. 27, 1979 14h26	NOV. 14, 1979 8h43	$1.5370\ 10^6$	$1.5097\ 10^6$
1/2 T	OCT. 27, 1979 21h11	NOV. 14, 1979 8h55	$1.5134\ 10^6$	$1.4902\ 10^6$
3/4 T	OCT. 27, 1979 21h18	NOV. 14, 1979 8h55	$1.5130\ 10^6$	$1.4898\ 10^6$

3.3 INTERLABORATORY COMPARISONS OF RM DOSIMETRY

3.3.1 Comparison of RM Results from Irradiations RM-1 and RM-II

In the RM-I and RM-II experiments, all participating laboratories used high-resolution Ge or GeLi detectors in conjunction with 2048 to 8196 multichannel analyzer systems for analysis of the dosimeter gamma spectra. A few of the participants also analyzed low-activity reactors [e.g., $^{63}Cu(n,\alpha)$ ^{60}Co] using NaI(Tl) detectors. All non-fissile dosimeters were analyzed nondestructively, but some of the participating laboratories destructively analyzed the fissionable dosimeters in accordance with their routine surveillance of the participants due to the much higher activities of some of the ...ters than the routine surveillance sample activities normally ...ered.

...al review of the individual preliminary results from RM-I and RM-II ...ucted. Outlying values were anticipated, but consistent discrepan... large as 60% were observed. Individual discussions were held with ...boratory participant concerning these data and the possible discre...s that existed. Analytical and calibration techniques, nuclear param...ers being used, and corrections applied to the observed counting data were reviewed. In almost all cases, one or more problems were identified, though some were relatively insignificant. Some of the more important problems identified, and their effects on the reported RM data, are shown in Table 3.6.

Final reported specific activities for the RM-I irradiation calculated to end of irradiation (EOI) are listed in Tables 3.7 and 3.8 (not all participants reported all reaction rates). To determine the range of values that might be expected from the laboratories performing the analysis, the participants' data were first scaled by the individual HEDL normalization factor. The average value of this normalized set of data was obtained. Maximum and minimum values were then determined relative to this average. The maximum-to-minimum ratio is used as a range evaluation and is presented in Table 3.9. Since absolute HEDL values are not given in Table 3.9, the deviation between individual participant-measured activities and HEDL measured activities are presented separately in Table 3.10.

A comparison of the relative ratios listed in the vertical columns of Table 3.10 demonstrates whether a particular laboratory appears to be consistently biased. It would appear that Laboratory B is generally biased low by ~6% to 10% for non-fissile RM dosimeters. However, Laboratory C appears to be generally biased high by ~4% to 7% for non-fissile RM dosimeters, and at the same time Laboratory C appears to be generally biased low by ~5% to 10% for fissile RM dosimeters. By reading across this table, one can observe whether an apparent bias exists in the analysis of a particular dosimeter reaction. It appears that the HEDL analysis of both the $^{63}Cu(n,\alpha)$ and $^{46}Ti(n,p)$ reactions appear biased low by ~2% relative to the other participants.

TABLE 3.6

IDENTIFIED PROBLEMS AND ESTIMATED EFFECT

Problem	Effect on Data
1. Faulty calibration standards	10% to 100% depending on energy region
2. Faulty nuclear parameter data	0% to 2%, depending on specific results
3. No correction for external or self shielding	0% to 4% depending upon reaction and analysis technique
4. Error in conversion of specific activity to reaction rate	0% on specific activity up to 4% on specific reaction rates
5. Coincidence loss corrections for high count rate samples not applied	Estimated at up to 6%

The RM results from participant laboratories from irradiation RM-II are given ir Tables 3.11 and 3.12. Unfortunately, only three of the six participating laboratories reported results. Two separate sets of results are reported by Laboratory C from measurements performed by two different individuals in Laboratory C. Since a difference was observed, both sets of results were reported and are treated separately in the comparisons. It was anticipated that the RM-II test would show improved correlations; and indeed the deviations relative to HEDL (Table 3.13) indicate better agreement. All comparisons with two of the three reporting participants fall within $\sim\pm4\%$. Laboratory C still appears to be biased, though this time a low bias is indicated for the non-fissile RM dosimeters, while the RM-I irradiation indicates a high bias.

3.3.2 Comparison of RM Results from Irradiation RM-III

RM dosimetry results (Fa80a) for irradiation RM-III (specific activities at the end of irradiation) from the participating laboratories are shown in Table 3.14. All these RM results have been normalized to the CEN/SCK RM data. In addition, all RM results were corrected for the axial fast neutron intensity gradient.

An empirical correction for this axial gradient was determined using an axial array of Ni RM dosimeters at each of the RM-III irradiation positions, namely the SSC, 1/4 T, 1/2 T, and 3/4 T locations of the 4/12 configuration in the PSF.

TABLE 3.7

INTERLABORATORY COMPARISON OF RADIOMETRIC (RM) DATA
FROM IRRADIATION RM-I
[Non-Fission Foil Sets (DPS/mg @ EOI)](a)

Dosimeter Set / Reaction	Laboratory	HNF-1		HNF-3		HFN-2		HNF-4	
		[E+5]		[E+5]		[E+4]		[E+4]	
$^{58}Ni(n,p)$	A	4.60	4.491	4.26	4.170	8.17	7.984	7.73	7.480
	B	4.18	4.497	3.90	4.164	7.30	7.986	6.78	7.470
	C	4.33	4.510	4.04	4.192	7.98	7.968	7.43	7.493
	D	4.58	4.486	4.22	4.163	7.97	8.045	7.50	7.465
	E(b)	4.44	4.512	4.05	4.158	7.79	8.016	7.32	7.472
	F	4.430	4.510	4.187	4.177	8.243	8.027	7.728	7.438
		(E+3)		(E+3)		(E+3)		(E+3)	
$^{46}Ti(n,p)$	A	5.72	5.59(c)	5.43	5.37	1.22	1.154	1.17	1.119
	B	5.00	5.59	4.65	5.40	1.07	1.157	1.11	1.125
	C	5.75	5.55	5.55	5.30	1.24	1.159	1.21	1.122
	D	5.68	5.60	5.49	5.37	1.23	1.163	1.17	1.119
	E(b)	5.56	5.60	5.23	5.343	1.16	1.170	1.11	1.107
	F	5.677	5.557	5.427	5.33	1.206	1.141	1.175	1.130
		(E+1)		(E+1)		(E+1)		(E+1)	
$^{63}Cu(n,\alpha)$	A	8.19	8.048	7.89	7.688	1.90	1.880	1.91	1.825
	B	7.98	8.166	7.63	7.509	1.88	1.854	1.82	1.787
	C	8.56	8.031	8.11	7.870	2.02	1.864	1.90	1.784
	D	8.06	8.069	7.87	7.730	1.92	1.864	1.82	1.814
	E(b)	7.82	8.002	7.56	7.714	1.84	1.851	1.78	1.819
	F	8.444	7.815	7.948	7.789	1.994	1.886	1.935	1.811
		(E+3)		(E+3)		(E+3)		(E+3)	
$^{54}Fe(n,p)$	A	6.86	6.659	6.67	6.633	1.26	1.233	1.23	1.155
	B	6.27	6.692	5.93	6.608	1.15	1.245	1.08	1.168
	C	6.89	6.758	6.58	6.573	1.27	1.248	1.25	1.194
	D	6.79	6.646	6.45	6.600	1.25	1.234	1.20	1.182
	E(b)	6.70	6.674	6.40	6.622	1.21	1.260	1.18	1.172
	F	6.650	6.628	6.289	6.560	1.242	1.239	1.160	1.183
		(E+3)		(E+4)		(E+3)		(E+4)	
$^{58}FE(n,\gamma)$	A	6.45	6.352	6.71	6.688	8.32	8.748	2.29	2.246
	B		6.530		6.630		9.067		2.241
	C		6.569		6.627		9.104		2.240
	D		6.517		6.654		8.950		2.244
	E(b)	6.62	6.542	6.62	6.674	8.78	9.049	2.32	2.247
	F		6.610		6.540		8.948		2.249

(a) The first column under each heading are those data reported by the participants, with any subsequent corrections made by HEDL. The second column of data is the corresponding HEDL analysis. Results are to exponent in parenthesis [e.g., 4.60 (E+5) reads 4.60×10^5].

(b) The participant reported the specific activity as per mg target isotope. For comparison with the other reported values, the reported numbers were multiplied by the atom fraction used by the participant.

(c) Only two absolute counts were made on these sets. All of the samples in these sets were counted on a non-calibrated system for determination of the relative ratios. Correlations were made between those samples counted on both systems and absolute values were than calculated for the remaining samples in the sets.

TABLE 3.8

INTERLABORATORY COMPARISON OF RADIOMETRIC (RM) DATA FROM IRRADIATION RM-I
[Fission Foil Sets (DPS/mg @ EOI)]

		$^{235}U(n,f)$ (a)									
		^{140}Ba		^{103}Ru		^{95}Zr		^{137}Cs	$^{59}Co(n,\gamma)$	
Dosimeter Set	Laboratory	(E+5)		(E+5)		(E+5)		(E+3)	(E+5)	
MF-3	A	25.2	25.20	51.3	48.73	64.0	63.52		34.0	33.06
	B (b)		25.82		49.71	64.5	64.50		32.3	32.81
	C (b)		29.58	40.9	47.06	53.4	61.73	31.6	35.5	33.09
	D (c)	24.8	25.51	46.9	48.99	67.0	63.81	35.5	31.5	31.26
	E	23.2	24.85	48.1	47.68	60.6	62.37	35.9	33.9	33.29
	F		24.94		47.95		62.92		30.6	30.93
MF-5	A	361	329.8	651	601.3	858	812.0		172	171.9
	B (b)		326.5		588.7	668	780.9		161	173.9
	C (b)		330.9	840	602.6	875	800.6	470	184	173.0
	D (c)	294	324.5	528	580.2	788	770.6	535	148	169.7
	E	321	335.3	605	595.8	787	810.8	462	165	167.7
	F		327.2		586.1		781.9		172	172.9
MF-4	A	3.38	3.409	6.72	6.505	8.49	8.699		4.08	3.989
	B (b)		3.555		6.543	8.50	9.101		3.90	3.973
	C (b)		3.497	6.15	6.521	8.02	9.059	4.57	4.33	4.019
	D (c)	3.32	3.586	6.47	6.641	9.25	9.259	4.69	4.04	3.978
	E	3.37	3.561	6.77	6.562	8.39	9.155	4.87	3.98	3.871
	F		3.670		6.666		9.322		4.110	4.058
MF-6	A	123.	126.7	228	214.3	304	294.7		52.9	51.89
	B (b)		121.9		202.9	267	274.9		48.8	53.75
	C (b)		121.9		204.0	250	277.9	156	58.0	54.33
	D (c)	106	124.4	193	210.2	290	285.6	152	57.2	55.15
	E	111	127.7	215	212.9	278	293.3	167	52.8	53.06
	F		130.3		214.7		296.8		58.8	57.45

		$^{237}Np(n,f)$							
		(E+5)		(E+4)		(E+4)		(E+2)	
MF-1	A	11.2	11.08	44.5	43.18	27.1	27.27		
	B (b)		11.80		44.12	30.7	27.76		
	C (b)		11.67	39.6	43.10	24.8	27.26	16.9	
	D	11.0	11.75	41.8	43.71	28.8	27.66	18.6	
	E	10.3	11.61	43.2	43.60	26.1	27.30	17.6	
	F	10.5	11.12	39.7	41.38	25.6	25.98	18.5	
MF-2	A	1.35	1.307	5.24	5.053	3.23	3.167		
	B (b)		1.375		5.032	3.41	3.236		
	C (b)		1.406	4.79	5.147	3.16	3.318	2.16	
	D	1.31	1.322	5.12	4.975	3.52	3.185	2.00	
	E	1.20	1.382	4.99	5.159	3.12	3.210	2.13	
	F	1.27	1.310	4.92	5.040	3.18	3.229	2.27	

		$^{238}U(n,f)$						
		(E+8)		(E+8)		(E+8)		(E+1)
MF-1	A	17.8	16.90	7.06	6.693	35.5	34.98	
	B (b)		16.98		6.823	35.9	34.99	
	C (b)		17.67	6.71	7.011	34.4	36.52	29.8
	D	16.8	16.46	6.46	6.587	36.3	33.44	23.6
	E	16.0	16.95	6.79	6.759	34.2	35.10	25.8
	F	17.1	17.16	6.51	6.865	34.1	35.64	25.4
MF-2	A	2.79	2.722	1.11	1.070	0.572	0.5812	
	B (b)		2.740		1.056	0.596	0.5708	
	C (b)		2.695	0.922	1.033	0.558	0.5802	3.74
	D	2.65	2.792	1.08	1.057	0.616	0.5847	4.15
	E	2.49	2.679	1.01	1.036	0.530	0.5676	3.81
	F	2.74	2.777	1.09	1.059	0.555	0.5750	4.02

(a) The first column under each heading are those data reported by the participant with any necessary corrections. The second column is the corresponding NEDL data. The value in parens (E+5) is the exponent for the data following it ((E+5) 25.2 should read 25.2×10^5).

(b) Corrections were made for elemental and isotopic composition.

(c) Correction made for Co alloy content

TABLE 3.9

RANGE EVALUATION (MAXIMA/MINIMA) OF RESULTS FROM IRRADIATION RM-I

Sensor[b] Set No.	$^{58}Ni(n,p)$ Ratio 1	Ratio 2	Ratio 3	Labs	$^{46}Ti(n,p)$ Ratio 1	Ratio 2	Ratio 3	Labs	$^{54}Fe(n,p)$ Ratio 1	Ratio 2	Ratio 3	Labs	$^{54}Fe(n,p)$ Ratio 1	Ratio 2	Ratio 3	Labs
HNF - 1	1.34 C/B	1.10 A/B	1.07 A/C	6	1.35 C/B	1.18 C/B	1.04 C/E	6	1.13 F/B	---	1.09 F/E		1.38 C/B	1.10 A/B	1.03 A/F	6
HNF - 3	1.24 C/B	1.09 A/B	1.05 A/C	6	1.48 C/B	1.21 C/B	1.07 C/E	6	1.05 C/E	1.06 C/F	---		1.27 C/B	1.12 A/B	1.06 A/F	6
HNF - 2	1.35 C/B	1.13 F/B	1.06 F/E	6	1.42 C/B	1.14 A/B	1.07 A/E	6	1.06 C/E	1.09 C/E	---		1.46 C/B	1.11 A/B	1.07 A/E	6
HNF - 4	1.28 C/B	1.14 F/B	1.06 F/E	6	1.41 C/B	1.09 C/B	1.00 C/E	6	1.08 C/E	1.09 F/E	---	6	1.43 C/B	1.15 A/B	1.09 A/E	6

Sensor Set No.	$^{58}Fe(n,\gamma)$ Ratio 1	Ratio 2	Ratio 3	Labs
HNF - 1	1.35 C/A	1.03 E/A	1.01 E/A	3[c]
HNF - 3	1.07 C/E	1.02 A/E	1.02 A/E	3
HNF - 2	1.23 C/A	1.04 E/A	1.04 E/A	3
HNF - 4	1.12 C/E	1.01 A/E	1.01 A/E	3

Sensor Set No.	$^{59}Co/^{63}Cu(n,\gamma)$ Ratio 1	Ratio 2	Ratio 3	Labs
HF - 3	1.15 C/B	1.04 C/B	1.04 A/F	6
HF - 5	1.15 C/B	1.15 C/B	1.06 C/E	6
HF - 4	1.06 F/B	1.10 C/B	1.06 C/F	6
HF - 6	1.23 C/B	1.17 C/B	1.07 C/E	6

	$^{235}U(n,f)^{140}Ba$ Ratio 1	Ratio 2	Ratio 3	Labs	$^{235}U(n,f)^{103}Ru$ Ratio 1	Ratio 2	Ratio 3	Labs	$^{235}U(n,f)^{95}Zr$ Ratio 1	Ratio 2	Ratio 3	Labs	$^{235}U(n,f)^{137}Cs$ Ratio 1	Ratio 2	Ratio 3	Labs
HF - 3	1.03 A/E	---	---	3	1.19 C/D	1.21 A/E	1.09 A/D	4	1.09 D/E	1.17 A/E	1.04 A/F	5	---	1.11 E/E	---	3
HF - 5	1.29 A/D	---	---	3	1.73 C/D	1.19 A/D	1.05 A/E	4	1.51 C/B	1.28 C/B	1.09 D/E	5	---	1.14 C/D	---	3
HF - 4	1.07 A/D	---	---	3	1.30 C/D	1.09 E/E	---	4	1.11 D/E	1.14 D/E	1.09 D/E	5	---	1.05 E/E	---	3
HF - 6	1.13 A/D	---	---	3	1.63 C/D	1.14 A/D	---	4	1.15 C/E	1.14 A/E	1.09 A/E	5	---	1.07 E/D	---	3

	$^{237}Np(n,f)^{140}Ba$ Ratio 1	Ratio 2	Ratio 3	Labs	$^{237}Np(n,f)^{103}Ru$ Ratio 1	Ratio 2	Ratio 3	Labs	$^{237}Np(n,f)^{95}Zr$ Ratio 1	Ratio 2	Ratio 3	Labs	$^{237}U(n,f)^{137}Cs$ Ratio 1	Ratio 2	Ratio 3	Labs
HF - 1	1.14 A/F	---	1.08 A/D	4	1.37 C/F	1.11 A/C	1.08 A/E	5	1.16 A/E	1.21 B/C	1.04 A/E	6	---	1.15 F/C	1.09 D/C	4
HF - 2	1.19 A/E	---	1.06 A/F	4	1.37 C/F	1.12 A/C	1.08 A/F	5	1.16 D/C	---	---	6	---	1.12 F/D	1.03 E/D	4

	$^{238}U(n,f)^{140}Ba$ Ratio 1	Ratio 2	Ratio 3	Labs	$^{238}U(n,f)^{103}Ru$ Ratio 1	Ratio 2	Ratio 3	Labs	$^{238}U(n,f)^{95}Zr$ Ratio 1	Ratio 2	Ratio 3	Labs	$^{238}U(n,f)^{137}Cs$ Ratio 1	Ratio 2	Ratio 3	Labs
HF - 1	1.00 A/E	---	1.04 A/F	4	1.44 C/F	1.11 A/F	1.06 E/F	5	1.16 C/F	1.15 D/C	1.04 A/E	6	---	1.08 E/C	---	4
HF - 2	1.09 A/E	---	---	4	1.27 C/F	1.16 A/C	1.06 A/E	5	1.13 D/E	1.08 B/C	---	6	---	1.09 D/C	---	4

(a) Four vendors and two service laboratories participated in this test. All laboratories remain anonymous for these intercomparisons and are identified only as Laboratories A, B, C, D, E and F. The table evaluation shows the present laboratory-to-laboratory comparative status but also shows the improvement in the data comparisons (Ratios 2 and 3) as a result of interim evaluations and discussions with participants. Ratio 1 represents the initial review of RM results. Ratio 2 was obtained after discussions with participants and subsequent reworking of data by participants. For Ratio 3, and for the case of non-fissile sensors, the results from Laboratory B appeared to be consistently biased low and were, therefore, not used. In the case of the fissile sensors, if a participant appeared to be definitely biased, those results were not used in Ratio 3.

(b) HNF-X and HF-X are sensor set identification numbers for specific perturbed locations in 1-in. x 1-in. stainless steel simulated surveillance capsules for this first PSF-SDMF test.

(c) Results for the $^{58}Fe(n,\gamma)$ reaction were not reported by one laboratory after preliminary recalibration of their counting system.

TABLE 3.10

DEVIATIONS OF RM RESULTS FROM IRRADIATION RM-I*

Set ID	Reaction	LABORATORY A	B	C	D	E	F
HMF-1	$^{58}Ni(n,p)$	2.38	- 7.05	-3.99	2.10	-1.60	-1.77
-3		2.16	- 6.34	-3.63	1.37	-2.60	0.24
-2		2.33	- 8.59	0.15	-0.93	-2.12	2.69
-4		3.34	- 9.24	-0.84	0.47	-2.03	3.90
HMF-1	$^{46}Ti(n,p)$	2.33	-10.6	3.60	1.43	-0.71	2.16
-3		1.10	-13.9	4.72	2.23	-2.11	1.82
-2		5.72	-7.52	6.98	5.76	-0.85	5.26
-4		4.56	-1.33	7.84	4.56	0.27	3.98
HMF-1	$^{63}Cu(n,\alpha)$	1.76	-3.38	8.59	-1.12	-2.27	8.05
-3		2.63	1.61	3.05	1.81	-2.00	2.01
-2		1.06	1.40	8.37	3.00	0.59	5.73
-4		4.66	1.85	6.50	2.00	2.14	6.85
HMF-1	$^{54}Fe(n,p)$	3.02	-6.31	1.95	-3.73	0.39	-5.37
-3		0.56	-10.26	0.11	-2.27	-3.35	-4.13
-2		2.19	-7.63	1.76	1.30	-3.96	0.24
-4		6.49	-7.53	4.69	1.52	0.68	-1.94
HMF-1	$^{58}Fe(n,\gamma)$	1.54				1.19	
-3		3.29				0.81	
-2		-4.87				-2.97	
-4		1.96				3.25	
HMF-3	$^{59}Co(n,\gamma)$	2.84	-1.55	7.45	1.09	1.83	-1.07
-5		0.06	-7.42	6.36	-1.00	-1.61	-0.52
-4		2.28	-1.84	7.74	1.56	2.82	1.28
-6		1.95	-9.21	6.76	3.72	-0.49	2.35

Set ID	Reaction	LABORATORY A	B	C	D	E	F
HF-3	$^{235}U(n,f)^{140}Ba$	0.00			- 4.35	- 6.68	
HF-5		9.46			- 9.40	- 4.26	
HF-4		9.39			- 7.42	- 5.36	
HF-6		-2.92			-14.79	-13.08	
HF-3	$^{235}U(n,f)^{103}Ru$	5.27		-13.09	- 3.18	0.88	
HF-5		8.27		6.21	- 9.00	1.54	
HF-4		3.31		- 5.59	- 2.57	3.17	
HF-6		6.39		- 6.37	- 8.18	0.99	
HF-3	$^{235}U(n,f)^{95}Zr$	0.76	0.00	-13.49	4.99	- 2.84	
HF-5		5.67	-14.40	9.29	2.26	- 3.31	
HF-4		-2.40	- 6.49	-11.47	- 0.10	- 8.36	
HF-6		3.16	- 1.78	- 6.39	1.54	- 5.22	
HF-1	$^{237}Np(n,f)^{140}Ba$	1.27			- 6.38	-11.28	-5.58
HF-2		3.29			- 0.91	-13.29	-3.05
HF-1	$^{237}Np(n,f)^{103}Ru$	3.06		-31.26	- 4.37	- 0.92	-4.06
HF-2		4.11		- 6.94	2.91	- 3.28	-2.38
HF-1	$^{237}Np(n,f)^{95}Zr$	-0.22	10.59	- 9.06	4.12	- 4.40	-1.46
HF-2		1.99	5.38	- 4.76	10.83	- 2.80	-1.24
HF-1	$^{238}U(n,f)^{140}Ba$	2.96			- 2.19	- 5.60	-0.35
HF-2		0.65			- 0.40	- 7.05	-1.33
HF-1	$^{238}U(n,f)^{103}Ru$	5.48		- 4.29	- 1.93	0.46	-5.17
HF-2		3.74		1.65	2.08	- 2.51	-1.79
HF-1	$^{2}U(n,f)^{95}Zr$	1.72	2.60	- 5.81	8.55	- 2.56	1.37
HF-2		-1.58	4.41	- 3.83	5.35	- 6.62	-3.48

*The deviation cited is (X/HEDL-1) given in percent, where X represents the participant laboratory RM result and HEDL represents the RM result obtained by HEDL.

TABLE 3.11

INTERLABORATORY COMPARISON OF RADIOMETRIC (RM) DATA FROM IRRADIATION RM-II [Fission Foil Sets (DPS/mg @ EOI)](a)

Dosimeter Set	Laboratory	$^{238}U(n,f)$ $^{140}Ba(n,f)$ (E+5)	$^{103}Ru(n,f)$ (E+5)	$^{95}Zr(n,f)$ (E+5)	$^{137}Cs(n,f)$ (E+2)
HNF-3B8	A	3.064	2.05 2.003	.15 1.159	10.95
	B	3.153	2.053	1.207	10.92
	C-1[b]	2.863	1.74 1.575	1.01 1.142	9.40 11.30
	C-2		1.80	1.05 (1.16)	9.68 (10.4)
	D	3.093	1.998	1.163	10.3 10.16
	E	3.089	2.034	1.183	10.96
	F	2.989	2.022	1.174	10.50

Dosimeter Set	Laboratory	$^{237}Np(n,f)$ $^{140}Ba(n,f)$ (E+6)	$^{103}Ru(n,f)$ (E+5)	$^{95}Zr(n,f)$ (E+5)	$^{137}Cs(n,f)$ (E+3)
HNF-3B8	A	2.017	1.36 1.315	9.42 9.571	8.368
	B	1.956	1.287	9.325	8.156
	C-1[b]	2.097	1.22 1.351	8.72 9.793	7.82 8.484
	C-2		1.21	8.65 (9.24)	7.73 (8.37)
	D	2.005	1.302	9.431	8.31 8.169
	E	2.081	1.310	9.456	8.591
	F	2.088	1.332	9.602	9.308

(a) The first column listed under each heading are those data reported by the participants, the second column is the HEDL data. Result exponents are given in parens [eg. 3.064 (E+5) should read 3.064×10^5].

(b) Two individuals ran separate analyses for this laboratory and both values are reported. The values in parens are from recent counts.

TABLE 3.12

INTERLABORATORY COMPARISON OF RADIOMETRIC (RM) DATA FROM IRRADIATION RM-II [Non-Fission Foil Sets (DPS/mg @ EOI)](a)

Dosimeter Set	Laboratory	Reaction $^{58}Ni(n,p)$ (E+6)	$^{63}Cu(n,\gamma)$ (E+2)	$^{54}Fe(n,p)$ (E+4)
HSNF	A	1.16 1.144	2.41 2.389	2.06 2.020
	B	1.137	2.377	2.016
	C-1[b]	1.03 1.138	2.31 2.399	1.87 2.019
	C-2	1.06	2.35	1.95
	D	.13 1.141	2.43 2.386	2.01 1.995
	E	1.141	2.400	2.011
	F	1.132	2.384	2.003

Dosimeter Set	Laboratory	$^{58}Fe(n,\gamma)$ (E+4)	$^{59}Co(n,\gamma)$ (E+4)
HSNF	A	1.82 1.818	1.40 1.382
	B	1.825	1.381
	C-1[b]	1.79 1.836	1.33 1.390
	C-2	1.84	1.37
	D	1.84 1.801	1.42 1.397
	E	1.828	1.383
	F	1.836	1.834

(a) The first column listed under each heading are those data reported by the participants, the second column is the HEDL data. The number in parens is the exponent for those numbers following [eg. 1.16 (E+6) should read 1.16×10^6].

(b) Two individuals ran separate analyses for this laboratory and both values are reported.

TABLE 3.13

DEVIATIONS OF RM RESULTS FROM IRRADIATION RM-II*

Reaction	Laboratory						
	A	B	C-1	C-2	D	E	F
$^{58}Ni(n,p)$	1.40		-9.57	-6.85	-0.96		
$^{63}Cu(n,\alpha)$	0.88		-3.71	-2.04	1.84		
$^{54}Fe(n,p)$	1.98		-7.38	-3.42	0.75		
$^{58}Fe(n,\gamma)$	0.11		-2.51	0.22	2.17		
$^{59}Co(n,\gamma)$	1.30		-4.32	-1.44	1.65		
$^{237}Np(n,f)^{103}Ru$	3.42		-9.70	-10.4			
^{95}Zr	-1.58		-10.9	-5.6			
^{137}Cs			-7.83	-1.34	1.73		
$^{238}U(n,f)^{103}Ru$	2.09		-11.9	-8.86			
^{95}Zr	-0.78		-11.6	1.58			
^{137}Cs			-16.8	-7.96	1.38		

*The deviation cited is (X/HEDL-1) given in percent, where X represents the participant laboratory RM result and HEDL represents the RM result obtained by HEDL.

These axial Ni RM results were fit by a cosine buckling term of the form $\cos[B(y - C)]$, where y is axial distance in mm from reactor midplane. Table 3.15 summarizes the B and C parameters obtained from these fits. The axial distribution becomes flatter when penetrating into the vessel wall, while the axial maximum shifts from negative to positive values.

Small radial flux corrections were applied to the detectors from the RM-III interlaboratory capsules, since the detectors in these capsules were not all positioned on the same vertical axis. Somewhat different decay scheme parameters were used by the RM-III participants. In order to intercompare results, all reported data were rescaled using decay scheme parameters taken from Zijp and Baard (Zi79).

TABLE 3.14

SPECIFIC ACTIVITIES MEASURED BY THE PARTICIPATING LABORATORIES IN IRRADIATION RM-III

	REACTION	SPECIFIC ACTIVITIES RELATIVE TO SCK/CEN				RECOMMENDED SPECIFIC ACTIVITIES ($Bq\ g^{-1}$)	σ (%)
		INTERLABORATORY CAPSULE		AERE/RR & A CAPSULE[1]			
		ECN	PTB	$(AERE)_1$ [2]	$(AERE)_2$ [2]		
SSC	$^{93}Nb(n,n')$	1.17			1.02	$2.062\ 10^7$	9.0
	$^{58}Ni(n,p)$		1.01	1.09	1.05	$7.242\ 10^8$	3.9
	$^{54}Fe(n,p)$	1.01	1.00	1.07	1.10	$1.103\ 10^7$	4.3
	$^{46}Ti(n,p)$	0.99	1.02	1.12	1.07	$8.508\ 10^6$	5.3
	$^{63}Cu(n,\alpha)$	1.02	1.01	0.99[3] (1.89)	(1.05)	$1.201\ 10^5$	1.4
1/4 T	$^{237}Np(n,f)\ \{^{95}Zr$	0.97	0.98			$3.437\ 10^7$	1.6
	$^{237}Np(n,f)\ \{^{137}Cs$	0.96	0.98			$2.522\ 10^5$	2.0
	$^{238}U(n,f)\ \{^{95}Zr$	0.95	0.98			$3.508\ 10^6$	2.6
	$^{238}U(n,f)\ \{^{137}Cs$	0.99	0.97			$2.738\ 10^5$	1.4
	$^{93}Nb(n,n')$				1.00	$1.330\ 10^6$	0.3
	$^{58}Ni(n,p)$	1.00	1.00	1.07	1.03	$4.472\ 10^7$	3.1
	$^{54}Fe(n,p)$	1.00	0.98	1.11	1.09	$6.956\ 10^5$	6.0
	$^{46}Ti(n,p)$	1.00	1.01	1.12	1.04	$5.851\ 10^5$	4.9
	$^{63}Cu(n,\alpha)$	1.01	1.01	1.01[3] (1.15)	(1.08)	$9.206\ 10^3$	0.5
1/2 T	$^{93}Nb(n,n')$				0.85	$6.643\ 10^5$	11.8
	$^{58}Ni(n,p)$	0.99		1.09	1.02	$1.721\ 10^7$	4.4
	$^{54}Fe(n,p)$	0.97	1.00	1.10	1.10	$2.606\ 10^5$	6.0
	$^{46}Ti(n,p)$	0.98	1.02	1.13	1.07	$2.161\ 10^5$	5.8
	$^{63}Cu(n,\alpha)$	1.03	1.02	1.02[3] (1.37)	(1.30)	$3.465\ 10^3$	1.0
3/4 T	$^{93}Nb(n,n')$				0.84	$3.338\ 10^5$	11.9
	$^{58}Ni(n,p)$	1.00	0.99	1.07	1.00	$6.310\ 10^6$	3.3
	$^{54}Fe(n,p)$	1.00	1.00	1.10	1.07	$9.306\ 10^4$	4.7
	$^{46}Ti(n,p)$	0.96	0.98	(0.76)	1.01	$7.566\ 10^4$	2.2
	$^{63}Cu(n,\alpha)$	1.00	1.01	1.02[3] (1.46)	(1.27)	$1.245\ 10^3$	0.9

(1) RR&A: Rolls Royce and Associates.
(2) $(AERE)_1$: Measurements performed at Harwell; $(AERE)_2$: Measurements performed at Winfrith.
(3) Cu foil from interlaboratory capsule.

TABLE 3.15

PARAMETERS B AND C OBTAINED FROM FITTING
AXIAL Ni RM DOSIMETRY DATA

IRRADIATION LOCATION	B (mm^{-1})	C (mm)
SSC	$4.42\ 10^{-3}$	- 45.4
1/4 T	$3.34\ 10^{-3}$	- 20.6
1/2 T	$2.82\ 10^{-3}$	- 4.9
3/4 T	$2.80\ 10^{-3}$	3.2

The agreement between SCK/CEN, ECN, and PTB is excellent -- in general, better than 2% for all non-fission detectors and better than 5% for the fission detectors. The agreement between the $(AERE)_1$ and $(AERE)_2$ results is reasonable: the $(AERE)_1$ results are, on the average, 4% to 5% higher than the $(AERE)_2$ results, while the average difference for the Cu detectors is about 10%. The observed differences for $^{93}Nb(n,n')$ are somewhat larger than could be expected, taking into account the results from a recent niobium intercomparison (To82).

The specific activities deduced from the detectors in the AERE/RR&A capsules are systematically higher (except for Nb) than the specific activities deduced from the detectors in the interlaboratory capsules: 5% to 10%, on the average, for the $^{58}Ni(n,p)$, the $^{54}Fe(n,p)$, and the $^{46}Ti(n,p)$ reactions, while a difference of ~25% is noted for $^{63}Cu(n,\alpha)$ reactions. These ^{63}Cu differences are apparently not due to a bias in the calibration of the counting equipment of the participants, since a round robin of Cu detectors of the interlaboratory capsules resulted in an excellent agreement -- better than 3% (see Table 3.14). Preliminary investigations indicate also that local fast neutron flux perturbations, created by the dosimetry capsules, can be excluded, so that a major reason for the observed 5% to 10% differences could not be identified. The high specific activities from the $^{63}Cu(n,\alpha)^{60}Co$ reaction in the AERE/RR&A capsules are probably due to Co impurities in the Cu material.

The overall uncertainties on the measured specific activities, as quoted by the different laboratories, are given in Table 3.16. The uncertainties are on the order of 1.5% to 3% for most reactions, except 93Nb(n,n').

The recommended specific activities (Table 3.14) at the end of the irradiation were calculated by averaging the available results. The Cu results of the AERE/RR&A dosimeter capsules were not considered in the calculation of the recommended specific activities (values given between brackets in Table 3.14).

TABLE 3.16

OVERALL UNCERTAINTIES ON THE MEASURED SPECIFIC ACTIVITIES

REACTION	UNCERTAINTY (1 σ) IN %			
	ECN	PTB	AERE	SCK/CEN
$^{237}Np(n,f)\{^{95}Zr$	2.9	1.7		2.1
^{137}Cs	2.9	1.4		2.0
$^{238}U(n,f)\{^{95}Zr$	2.9	2.5		2.1
^{137}Cs	2.9	1.4		2.0
$^{93}Nb(n,n')$	5.6		4.6	4.5
$^{58}Ni(n,p)$	2.6	1.5	3.4	1.9
$^{54}Fe(n,p)$	2.2	1.5	2.4	1.9
$^{46}Ti(n,p)$	2.3	1.5	3.2	1.9
$^{63}Cu(n,\alpha)$	2.7	1.5	3.2	1.9

The results of the thermal dosimeters are not discussed in this paper since they are of less importance to the PCA/PSF program. These thermal RM results were only used to determine minor corrections such as the ^{58}Co and ^{58m}Co burnup of the Ni detectors.

3.4 CONCLUSIONS

While the agreement among the majority of the laboratories participating in the RM-I and RM-II interlaboratory comparisons is generally satisfactory, with non-fissile dosimeter results generally falling within ±5% and the fissionable dosimeter results falling within ±10%, improvement is still required in order to routinely meet accuracy goals of LWR-PVS surveillance dosimetry. Improved agreement was attained in the RM-III experiment, wherein non-fissile RM monitors generally agreed better than 2% and fission monitors generally agreed to better than 5%. The results obtained from these tests along with the subsequent corrections indicate that a critical review of both analytical and calculational techniques must be conducted on a periodic basis by all of the laboratories. In addition, it is recommended that each laboratory review and utilize, where possible, the appropriate ASTM Standard Methods and Guides, maintain system calibration and/or control documentation, and continue in this or similar programs using existing benchmark facilities for verifications and direct correlations.

In the RM-I and RM-II experiments, intercomparisons of dosimetry results from six service laboratories have provided experimental estimates of measured reaction rates accuracies. Preliminary results were distributed over a range of relative values as large as 60%. Had results from a single laboratory been used to derive surveillance capsule fluence values (often based on only one or two reactions), a bias of 40% or more could easily have been introduced. Following discussions of the preliminary analysis results and identification of existing problems, these biases were generally reduced to below 15%.

In the RM-III experiment, systematic problems were uncovered with Cu and Nb dosimeters. Any Co impurity in copper can seriously compromise results. Also, and as stressed in earlier dosimetry work with Nb (To80), more accurate cross-section data are needed for the Nb(n,n′) reaction; see Sections 2.3.1 and 5.2.2.

An important distinction between the RM-I and RM-II intercomparisons and the RM-III intercomparison must be stressed. The use of HEDL- determined normalization factors reduces the RM-I and RM-II tests to essentially an interlaboratory comparison of absolute gamma-ray counting measurements. However in RM-III, factors that arise in the use of dosimetry materials from different suppliers, such as mass and impurities, were included along with absolute gamma-ray counting measurements. Both types of tests are clearly needed. In fact, interlaboratory RM dosimetry results from the long-term PSF two year metallurgical irradiations could be used to obtain an additional intercomparison of the type treated here in the RM-III test. The reader is referred to the NUREG/CR-3320, Volume 3 (Mc87c) report on the PSF Physics-Dosimetry Program.

Finally, these tests and intercomparisons establish a clear and significant difference in accuracy between fissile and non-fissile RM dosimeters. The important contribution of fast neutrons to PV embrittlement, especially in the region from roughly 0.1 up to 1.0 MeV, makes the use of the threshold

fission monitors ^{238}U and ^{237}Np crucial in LWR-PVS dosimetry. The higher uncertainties of fissile RM dosimeters relative to non-fissile RM dosimeters (by about a factor of two) are just barely acceptable given the goal accuracies of LWR-PVS work. Indeed, there is no fundamental reason that fissile RM dosimeters must possess such considerably higher uncertainties. If anything, these two threshold RM fissile dosimeters generally possess as accurate or more accurate integral cross sections in standard neutron fields than do the fast neutron non-fissile RM dosimeters (Fa76,Gi85,Ma82). Consequently, additional work is clearly needed to resolve systematic effects that are adversely impacting the accuracy of RM dosimetry with fissile monitors.

3.5 NBS RADIOMETRIC COUNTING AND FLUENCE STANDARDS

E. D. McGarry (NBS)

In addition to the benchmark referencing requirements discussed in Section 2.1, it was considered necessary to have HEDL radiometric counting procedures benchmarked (re-validated) because of the interlaboratory comparisons conducted by HEDL in support of the international participation in the PSF benchmarks. Because HEDL performed the analyses of the comparisons (Ke82), all results are reported relative to the HEDL results. These comparisons made available an assessment of the quality of the world-wide status of radiometric dosimetry for LWR surveillance, Section 3; consequently, a permanent record of these LWR-PV-SDIP benchmark efforts involving HEDL radiometric analysis has additional meaning.

Table 3.5.1 specifies the certified fluence standards supplied to HEDL by NBS to benchmark reference radiometric counting for the PSF.

Table 3.5.2 gives the HEDL measured activities of the fluence standards at the end of irradiation (EOI) and the derived average reaction rate per nucleus.

Table 3.5.3 gives an analysis of HEDL's evaluation of the NBS fluence standards. The quantities reported by NBS for each standard are a certified neutron fluence and an irradiation time in a fission spectrum (see Table 3.5.1). The quantities reported by HEDL for each fluence standard are specific radioactivity and a saturated reaction rate, because the HEDL gamma spectroscopy system (energy selective counting system) is calibrated, in a absolute sense, in terms of its measured response to various NBS and IAEA gamma standards. The reaction rates derived by HEDL are in the form of the measured dosimetry data that are needed as input to spectrum adjustment codes which, in turn, provide dosimetry adjusted transport calculations; i.e., to locally measured dosimetry conditions.

Performing an analysis without modifying the information reported in Tables 3.5.2 and 3.5.3, is best accomplished by deriving ^{235}U fission-spectrum-averaged cross section information.

Part I Table 3.5.3 gives two values for both the iron and nickel (n,p) reactions and four values of the ^{238}U fission cross section. The Table 3.5.2 uncertainties listed adjacent to the columns of values are one-sigma results and the NBS uncertainties are not incorporated in the HEDL results. However, there is considerable uncertainty correlation among the various isotopic results. This is a result of interdependencies such as multiple results from selectively counting various isotopes from a fission foil, or iron and nickel results from an alloy, and uncertainties common to the same counting system.

In Part II of Table 3.5.3, the as-derived ^{235}U cross sections are compared with evaluated experimental (EXP'MTL) results, taken from Ref (Gr86a), and with calculated results which come from integrating the ENDF/B-V form of the ^{235}U fission spectrum with the cross sections from the ENDF/B-V dosimetry-A file. As is frequently the case for well calibrated gamma counting systems, the derived cross sections agree better with the evaluated experimental results. However, the bias with calculation is important because measured dosimetry reaction rates are almost always compared with those calculated from neutron-

transport-generated spectra. In this comparison, an analysis should take into account the known existing biases between benchmarked measurement and calculation. How this is generally accomplished is not known. Even if all the difficulty is attributed to errors associated with the differential cross section data in the ENDF files, it is not clear how uncertainty correlations in adjustment procedures account or compensate for the mentioned biases.

In any event, the processed fluence standard data shown in Part II, Table 3.5.3, tends to confirm the adequacy of the HEDL radiometric-dosimeter gamma-counter calibration (at a variety of gamma energies) that existed in the 1982-1984 time interval.

TABLE 3.5.1

CERTIFIED FLUENCE STANDARDS SUPPLIED TO HEDL BY NBS TO BENCHMARK REFERENCE RADIOMETRIC COUNTING OF LWR-PV-SDIP DOSIMETRY

Foil I.D.	^{235}U Irrad.	EOI	Exposure Time (Hours)	NBS Fluence	Fluence Uncert.	Time (Seconds)
Ni-R	Fe/Ni-1	02/06/83	72.3	4.425E+15	2.1%	2.604E+05
Fe-GD	Ti/Fe-1	03/01/83	93.5	5.980E+15	2.4%	3.367E+05
Fe/Ni-C	U/Fe-2	11/20/83	97.8	6.056E+15	2.2%	3.520E+05
U8-5-27	"	"	97.8	6.056E+15	2.2%	3.520E+05
U8(Nat)-5	U/Fe-3	08/30/84	149.0	9.070E+15	2.5%	5.364E+05

TABLE 3.5.2

MEASURED ACTIVITY AT END OF IRRADIATION AND DERIVATION OF TIME-AVERAGED REACTION RATES

I.D.	Foil Reaction	Time (Seconds)	Activity (dps/mg)	Uncert. on Activity	<R> Derived Reaction Rate
Ni-R	$^{58}Ni(n,p)^{58}Co$	260424	3.717E+02	2.7%	1.849E-15
Fe-GD	$^{54}Fe(n,p)^{54}Mn$	342000	7.595E+00	2.1%	1.443E-15
Fe/Ni-C	$^{54}Fe(n,p)^{54}Mn$	352020	7.174E+00	3.3%	1.397E-15
"	$^{58}Ni(n,p)^{58}Co$	352020	3.738E+02	2.6%	1.878E-15
U8-5-27	$^{238}U(n,f)^{140}Ba$	352020	1.495E+02	3.8%	5.416E-15
"	$^{238}U(n,f)^{103}Ru$	352020	5.782E+01	2.8%	5.411E-15
"	$^{238}U(n,f)^{95}Zr$	352020	2.899E+02	2.9%	5.325E-15
"	$^{238}U(n,f)^{137}Cs$	352020	2.065E-01	3.6%	5.463E-15

TABLE 3.5.3

DERIVATION OF OBSERVED ^{235}U SPECTRUM-AVERAGED CROSS SECTIONS FOR NEUTRON FLUENCE STANDARDS AND COMPARISON OF RESULTS WITH PUBLISHED EXPERIMENTAL VALUES AND WITH CALCULATED VALUES.

PART I -- Cross Section Derivation:

Foil I.D.	Reaction	<Ø> NBS Fluence Rate	<R> HEDL Reaction Rate	Cross Section From <R>/<Ø> (mb)
Ni-R	$^{58}Ni(n,p)^{58}Co$	1.699E+10	1.8490E-15	108.8
Fe-GD	$^{54}Fe(n,p)^{54}Mn$	1.766E+10	1.4430E-15	81.7
Fe/Ni-C	$^{54}Fe(n,p)^{54}Mn$	1.720E+10	1.3970E-15	81.2
"	$^{58}Ni(n,p)^{58}Co$	1.720E+10	1.8780E-15	109.2
U8-5-27	$^{238}U(n,f)^{140}Ba$	1.720E+10	5.4160E-15	314.9
"	$^{238}U(n,f)^{103}Ru$	1.720E+10	5.4110E-15	314.6
"	$^{238}U(n,f)^{95}Zr$	1.720E+10	5.3250E-15	309.6
"	$^{238}U(n,f)^{137}Cs$	1.720E+10	5.4630E-15	317.6

PART II -- Comparison with Experimental and Calculated Results:

Foil I.D.	Reaction	Measured Cross Section <R>/<Ø> (mb)	Exp'mtl Value NBS (mb)	Exp'mtl Versus Measured (%)	Calc. Cross Section (mb)	Calc. Versus Measured (%)
Ni-R	$^{58}Ni(n,p)^{58}Co$	108.8	111	2.022	105.00	-3.492
Fe-GD	$^{54}Fe(n,p)^{54}Mn$	81.7	81.7	-0.988	81.00	-0.856
Fe/Ni-C	$^{54}Fe(n,p)^{54}Mn$	81.2	81.7	0.615	81.00	-0.856
"	$^{58}Ni(n,p)^{58}Co$	109.2	111	1.016	105.00	-3.846
U8-5-27	$^{238}U(n,f)^{140}Ba$	314.9	312	-0.921	305.20	-3.080
"	$^{238}U(n,f)^{103}Ru$	314.6	312	-0.826	305.20	-2.989
"	$^{238}U(n,f)^{95}Zr$	309.6	312	1.007	305.20	-1.421
"	$^{238}U(n,f)^{137}Cs$	317.6	312	-1.763	305.20	-3.904

4.0 TRANSPORT CALCULATION RESULTS - SUMMARY

L. F. Miller (ORNL) and A. F. Thomas (RR&A)

The Poolside Facility (PSF) and the Pool Critical Assembly Pressure Vessel Facility (PCA-PVF) have been used extensively for evaluating measurement techniques and computational methods. Differences among measurements and calculations for the PCA-PVF and PSF (St81c,Mc81b,Ma80c,Ma81f,Ma82a) have generally been in the 10% to 20% range. Somewhat larger differences between measurements and calculations have been noted for comparisons that include transport through several inches of iron and for particular dosimeters.

Results reported herein are relative to the startup experiments at the PSF and are reported in detail by Maerker and Williams (Ma82i) and by Maerker and Worley (Ma84a). Results by Maerker and Worley (Ma84a) are revisions of those by Maerker and Williams (Ma82i) and are about 5% better than the original calculations. The geometry and components used for this experiment are essentially equivalent to the PSF described in Section 1.1. Details relative to calculations are included in Section 4.1.

The neutron transport calculations utilized a flux-synthesis technique based on three calculations (two two-dimensional and one one-dimensional). The source term was obtained from a three-dimensional diffusion theory calculation (Vo81) and is reported in Section 1.2. Ratios of calculated-to-experimental values for the revised calculations range from 0.75 [at the 3/4-T position for $^{46}Ti(n,p)$] to 0.93 [at the 1/4-T position for $^{237}Np(n,f)$]. Discrepancies between measurements and calculations relative to the startup experiment are within expected ranges based on previous evaluations (i.e., PCA-PVF), known uncertainties associated with nuclear data, measurements, and applicable computational methodology.

Details are provided elsewhere (Mc87c) of the calculational methods and data used and the results obtained by RR&A in the successful validation of the ANISN methodology and the subsequent calculation of the PSF 4/12 irradiation facility using both the ANISN and MCBEND techniques. These RR&A (1-D) and MCBEND (3-D Monte Carlo) results provide a further basis for comparison and verification of the overall reliability of the ORNL and RR&A calculational results. The RR&A calculational results are used in Section 5.2 for a consistency analysis of the measured reaction rates in the UK dosimetry for the 18 day startup and the SSC-1 and SSC-2 experiments. They are also used in Section 6.2 in the derivation of recommended exposure parameter values for these experiments.

4.1 ORNL ANALYSIS

L. F. Miller

Dosimeter irradiations for the startup experiment were conducted during the last 18 days of ORR cycle 151-A at locations depicted by Figures 1.1.13 and 1.1.14. Middle-of-cycle (MOC) burnup and control-rod conditions are utilized to define input data for the three-dimensional (3-D) diffusion code VENTURE (Vo81) used for determining the source distribution (see Section 1.2). An ancillary code, VIPOR, was used for preparation of input data to VENTURE. The 3-D neutron source distribution was integrated in appropriate transverse directions to obtain x,y-, y,z-, and y-source distributions for the associated discrete ordinates transport calculations. The DOT-IV (Rh79) computer program was used for the two two-dimensional (2-D) transport calculations (XY and YZ), and ANISN (En67) was used for the one-dimensional (1-D) transport calculation (Y).

Results from the 2-D and 1-D transport calculations were combined as shown below to synthesize the 3-D fluxes. In particular,

$$\phi(x,y,z) = \phi(x,y)\phi(y,z)/\phi(y) \qquad (1)$$

where $\phi(x,y,z)$ represents the 3-D flux distribution. Coordinates (x,y,z) are identified on Figures 1.1.13 and 1.1.14. The motivation for this method to synthesize the 3-D fluxes and explanations relative to conditions when the synthesis results should be essentially exact are described by Maerker and Williams (Ma82i). Comparisons of measurements with calculations are given by Table 4.1.1 and are provided by Maerker and Worley (Ma84a). The overall comparisons indicate agreement in the first three locations to within approximately 15% and approximately 20% for the 3/4-T location. These results, as well as others (Wa80,Ma81), suggest that the ENDF/B-IV inelastic cross section for iron may be too high by approximately 8%. In addition, there are expected uncertainties in the source normalization due to reactor power measurements and to within-cycle time-dependent source distributions.

TABLE 4.1.1

COMPARISON OF SOME CALCULATED AND MEASURED* SATURATED ACTIVITIES IN THE STARTUP EXPERIMENT IN Bq PER NUCLEUS AT 30 MW

	SSC	1/4-T	1/2-T	3/4-T
Calculated $^{63}Cu(n,\alpha)$	2.58-15**	1.90-16	7.05-17	2.46-17
Measured $^{63}Cu(n,\alpha)$	3.07-15	2.10-16	7.97-17	2.81-17
C/E	0.84	0.90	0.88	0.87
Calculated $^{46}Ti(n,p)$	5.00-14	3.31-15	1.19-15	4.00-16
Measured $^{46}Ti(n,p)$	6.12-14	4.04-15	1.47-15	5.30-16
C/E	0.82	0.82	0.81	0.75
Calculated $^{54}Fe(n,p)$	4.07-13	2.44-14	8.84-15	2.97-15
Measured $^{54}Fe(n,p)$	4.67-13	2.75-14	1.02-14	3.74-15
C/E	0.87	0.89	0.87	0.80
Calculated $^{58}Ni(n,p)$	5.57-13	3.36-14	1.25-14	4.30-15
Measured $^{58}Ni(n,p)$	6.45 13†	3.90-14	1.49-14	5.56-15
C/E	0.86	0.86	0.84	0.77
Calculated $^{238}U(n,f)$		1.39-13		
Measured $^{238}U(n,f)$		1.56-13†		
C/E		0.89		
Calculated $^{237}Np(n,f)$		1.30-12		
Measured $^{237}Np(n,f)$		1.40-12†		
C/E		0.93		

*All measurements, except the $^{58}Ni(n,p)$ measurement in the SSC, are taken from (Ke80,Ke81). The $^{58}Ni(n,p)$ measurement is provided by A. Fabry. The vertical locations vary between 50.8 and 76.2 mm below the reactor midplane.

**Read 2.69×10^{-15} etc.

†Average of the ^{137}Cs and ^{95}Zr fission product results only; the ^{144}Ce fission product results were ignored because they seemed less consistent with the others.

4.2 RR&A ANALYSIS

A.F. Thomas, S.P. Walley (Rolls-Royce and Associates Limited, U.K.)

4.2.1 Discussion

As part of the USNRC-LWR-PV- .P, neutronics calculations of the experimental facilities were required .. support of the dosimetry analysis of the metallurgical specimens. Detailed calculational and experimental data had previously been generated on the low power Pool Critical Assembly (PCA) mock up of the high-power Oak Ridge Reactor Poolside Facility (PSF) which simulates the core/thermal shield/pressure vessel/cavity of a typical civil LWR. These included 3D MCBEND Monte Carlo calculations carried out by RR&A which generally proved successful in predicting the experimentally determined neutron reaction rates (Mc81).

In order to facilitate the analysis of the dosimetry measurements from the PSF metallurgical irradiations (including the 18-day full-power thermal and physics "Start-Up" experiment) which took place in an optimised but di'ferent configuration from that of the PCA, neutron spectral shape information throughout the PSF array was required, as well as best estimates of calculated parameters at locations of particular importance in the SSC and PVS. In order to achieve this a calculational methodology was defined which incorporated both a 1-D deterministic neutron transport calculational technique (ANISN) and a 3-D Monte Carlo neutron transport calculational technique (MCBEND). Initially the use of the 1-D ANISN method was considered to be a simple and cheap way of achieving the objective of providing systematic spectral information providing it could be shown that the methodology and data used could be validated against a reliable and relevant benchmark, such as the PCA experiments. In contrast, the 3-D MCBEND method is much more expensive but allows a more exact representation of the problem, and is capable of providing accurate estimates of both neutron spectrum shapes and flux intensities within predefined error targets. However since economics dictate that only a few specific locations can be characterised, the ANISN and MCBEND methods were, in effect, considered to be complementary.

Details are provided elsewhere (Mc87c) of the calculational methods and data used and the results obtained by RR&A in the successful validation of the ANISN methodology and the subsequent calculation of the PSF 4/12 irradiation facility using both the ANISN and MCBEND techniques. These RR&A (1-D) and MCBEND (3-D Monte Carlo) results provide a further basis for comparison and verification of the overall reliability of the ORNL and RR&A calculational results. The RR&A calculational results are used in Section 5.2 for a consistency analysis of the measured reaction rates in the UK dosimetry for the 18 day startup and the SSC-1 and SSC-2 experiments. They are also used in Section 6.2 in the derivation of recommended exposure parameter values for these experiments.

5.0 COMPARISON AND EVALUATION OF PHYSICS-DOSIMETRY DATA - SUMMARY

W. N. McElroy and R. Gold (HEDL)

Physics-dosimetry analyses of the PCA and PCA Replica and the PSF experiments followed by the application of neutron flux-spectral adjustment procedures and sensitivity analyses have been perform at HEDL, ORNL, CEN/SCK, RR&A, AERE-Winfrith and other participating laboratories.

Under idealized environmental conditions (benchmark), modern computational techniques are currently capable of predicting absolute in-vessel neutron reaction rates per unit of reactor power to within 15% (one-sigma), but generally, not to within 5% (one-sigma). This is a great improvement compared with the situation prevailing a few years ago, before the PCA and PSF experiments were undertaken, where factors of two or more differences between FSAR predictions and surveillance capsule measurements were not uncommon. The achievable accuracy will be markedly less, however, in applications to actual nuclear power plants.

For the PCA, the results of the consistency analyses by HEDL, ORNL and RR&A indicate that the reactor physics calculations appear to be biased on the low side and differences outside the derived one-sigma uncertainties were observed in some cases. Comparisons of derived exposure parameter values in the PV block show differences between the three laboratories of up to 12%. No consistent bias between the results exists, when all the PCA configurations are considered.

For ORNL studies, differences among measurements and calculations for the PCA and PSF have generally been in the 10% to 20% range. Somewhat larger differences between measurements and calculations have been noted for comparisons that include transport through several inches of iron and for particular dosimeters. Discrepancies between measurements and calculations relative to the PSF startup experiment are within expected ranges based on previous PCA evaluations, known uncertainties associated with nuclear data, measurements, and applicable computational methodology.

For RR&A studies, overall the results obtained by both the ANISN and MCBEND calculations achieved two of their main objectives: To provide (a) accurate neutron spectra for the analysis of dosimetry measurements made on the metallurgical PSF 4/12 irradiations and (b) scoping values of reaction rates and neutron fluxes throughout the experimental array. The underprediction by about 10% of reaction rates using the MCBEND technique was, however, something of a disappointment, given the success of the recent reanalysis of the PCA 12/13 "Blind Test" using the same technique. Nevertheless, these results were <u>not</u> inconsistent with the level of stochastic uncertainty achieved, which was necessarily limited by economic considerations. In that sense the MCBEND technique does provide more realistic and reliable estimates of reaction rates and fluxes than can be achieved by purely deterministic (i.e., ANISN and DOT) transport calculations whose uncertainty is entirely unquantified and where good agreement can often only be achieved after a judicious amount of 'a priori' benchmarking and 'ad hoc' synthesis.

To advance PV neutron transport methodology, more complete answers must be found for a number of existing inconsistencies between measured and calculated reactor physics parameters for the PCA, PSF, VENUS, NESDIP and PWR and BWR cavity and surveillance capsule experiments. These inconsistencies are identified.

With regard to C/E inconsistencies for the NESDIP2 and NESDIP3 benchmarks, ORNL has found that if one folds the AERE-Winfrith measured spectrum with the reaction cross sections used in obtaining the calculated activities, the resulting agreement with the measured activities is excellent; this lends great credibility to the measured spectrum, measured activities, and the dosimetry cross-sections.

In helping to establish a better understanding of the reasons for some of the inconsistencies between calculated and measured "through PV wall" quantities for the PCA and PSF benchmarks, HEDL has fit an exponential function [of the form $(\phi t)_r = (\phi t)_0 \exp(-br)$] to PCA, PSF, and Gundremmingen through wall dosimetry derived flux and/or fluence results. The least-squares derived exponential b-value for the PCA is about 6.3% higher than that observed for the PSF. Some differences between the PSF and PCA results should be anticipated because of differences that exit in these two PV mockups.

For Gundremmingen, a very preliminary b-value was obtained using fission spectrum derived values of fluxes that are based on EG&G-Idaho 54Fe(n,p)54Mn through wall activation measurements. Here again, an exponential representation is found to be an excellent fit to these data. It would be of considerable interest to repeat the Gundremmingen analysis using dosimetry adjusted flux ($E > 1$ MeV) values and to perform a similar analysis on measured 54Mn activation results from trepans that might be removed from the Shippingport PWR reactor vessel; presently, the only Shippingport steel specimens that are available are those that have been taken from trepans that were removed from the reactor shield tank.

A study of the consistency of the b-values for the PCA Replica, the other five PSF experiments and Gundremmingen should be accomplished. Such a study is needed to determine if there are any benchmark-to-benchmark undefined systematic differences that might be detected by differences in the b-values between the results of the PCA, PCA Replica, the seven PSF experiments and Gundremmingen.

5.1 CONSISTENCY OF PCA, PSF, VENUS, NESDIP, PWR AND BWR DATA

W. N. McElroy and R. Gold (HEDL)

Physics-dosimetry analyses of the PCA and PCA Replica (Ka83,Mc81,Bu84,Mc84i, Au85) and the PSF (Fa80a,Ke82,Ma82e,To82,To82a,Wi82,Ka83,To83,Ba84a,Gu84d,Ma84a, Ma84b,St84,St84b,Mc87c,Mc87d) experiments followed by the application of neutron flux-spectral adjustment procedures and sensitivity analyses have been perform at HEDL, ORNL, CEN/SCK, RR&A, AERE-Winfrith and other participating laboratories.

The PCA (Mc81,Mc84i) and PCA Replica (Bu84) Experiments and PCA Blind Test computational results support the statement (Fa79) that under idealized environmental conditions (benchmark), modern computational techniques are currently capable of predicting absolute in-vessel neutron reaction rates per unit of reactor power to within 15% (one-sigma), but generally, not to within 5% (one-sigma). This is a great improvement compared with the situation prevailing a few years ago, before the PCA and PSF experiments were undertaken, where factors of two or more differences between FSAR predictions and surveillance capsule measurements were not uncommon. The achievable accuracy will be markedly less, however, in applications to actual nuclear power plants because of new low-leakage neutron core fuel management schemes, geometrical complexities and other factors; all of which will continue to require careful study and evaluation for specific PWR and BWR plants.

For the PCA, the results of the consistency analyses by HEDL (Lippincott), ORNL (Stallmann) and RR&A (Thomas) indicate that the reactor physics calculations appear to be biased on the low side, and that the recommended experimental data are self-consistent within assigned uncertainties. Although all three laboratories used a least-squares procedure to derive the exposure parameters from a calculated neutron flux spectrum and the same integral data, differences outside the derived one-sigma uncertainties were observed in some cases. Comparisons of derived exposure parameter values in the PV block show differences between the three laboratories of up to 12%. No consistent bias between the results exists, when all the configurations are considered. RR&A has the largest range of uncertainty values; for example, for $\Phi(E > 1\ MeV)$, the RR&A uncertainties range from 5% to 16% in the block compared to HEDL values of 6% to 9% and ORNL values of 4% to 7%.

As stated by Miller in Section 4.0:

> *"The PSF (Poolside Facility; for high power studies) and PCA (Pool Critical Assembly; for low power studies) have been used extensively for evaluating measurement techniques and computational methods. Differences among measurements and calculations for the PCA-PVF and PSF (St81c,Mc81b,Ma80c, Ma81f,Ma82a) have generally been in the 10% to 20% range. Somewhat larger differences between measurements and calculations have been noted for comparisons that include transport through several inches of iron and for particular dosimeters."*

He further states:

"The neutron transport calculations utilized a flux-synthesis technique based on three calculations (two two-dimensional and one one-dimensional). The source term was obtained from a three-dimensional diffusion theory calculation (Vo81) and is reported in Section 1.2. Ratios of calculated-to-experimental values for the revised calculations range from 0.75 [at the 3/4-T position for 46Ti(n,p)] to 0.93 [at the 1/4-T position for 237Np(n,f)]. Discrepancies between measurements and calculations relative to the startup experiment are within expected ranges based on previous evaluations (i.e., PCA), known uncertainties associated with nuclear data, measurements, and applicable computational methodology."

As stated by Thomas and Walley (Section 3.27, Ref. Mc87c):

"Overall the results obtained by both the ANISN and MCBEND calculations achieved two of their main objectives: To provide (a) accurate neutron spectra for the analysis of dosimetry measurements made on the metallurgical PSF 4/12 irradiations and (b) scoping values of reaction rates and neutron fluxes throughout the experimental array. The underprediction by about 10% of reaction rates using the MCBEND technique was, however, something of a disappointment, given the success of the recent reanalysis of the PCA 12/13 "Blind Test" using the same technique (Au85). Nevertheless, these results were <u>not</u> inconsistent with the level of stochastic uncertainty achieved, which was necessarily limited by economic considerations. In that sense the MCBEND technique does provide more realistic and reliable estimates of reaction rates and fluxes than can be achieved by purely deterministic (i.e., ANISN and DOT) transport calculations whose uncertainty is entirely unquantified and where good agreement can often only be achieved after a judicious amount of 'a priori' benchmarking and 'ad hoc' synthesis. However, it is finally worth pointing out that recent experience in running Monte Carlo physics codes on dedicated micro-computers at RR&A has shown that such calculations can be made much more cheaply and hence more competitively with deterministic calculations than the work reported here."

To advance PV neutron transport methodology, more complete answers must be found for a number of existing inconsistencies between measured and calculated reactor physics parameters for the PCA, PSF, VENUS, NESDIP and PWR and BWR cavity and surveillance capsule experiments (Mc88). Among these discrepancies are: 1) the under-prediction of exposure and dosimetry sensor reaction rates with increasing penetration within the PV wall, 2) the consistently low C/E ratios (in the range of 0.6 to 0.9) for the 238U(n,f), 237Np(n,f), 58Ni(n,p), 54Fe(n,p), and 63Cu(n,a) and other threshold reactions in surveillance capsule and ex-vessel cavity locations, 3) differences (up to 20%) associated with the use of the reactor total power level instead of the actual local flux level for calculating sensor reaction rate saturation factors (Ma85d), and 4) the deterioration of the C/E agreement for the 1H(n,p) reaction from near unity in the core region to values in the 1.2 to 1.7 range as one approaches the edge of the core corner and certain locations in the core barrel and outer baffle for the VENUS experiment.

With regard to ORNL reported C/E inconsistencies for the NESDIP2 and NESDIP3 benchmarks (Ma87), Maerker has stated:

"If one folds the AERE-Winfrith measured spectrum with each of the three reaction cross sections [(32S(n,p), 115In(n,n'), 103Rh(n,n')] used in obtaining the calculated activities, the resulting agreement with the measured activities is excellent (C/E = 0.97, 1.05, and 1.025, respectively). This lends great credibility to the measured spectrum, measured activities, and the dosimetry cross-sections."

In helping to establish a better understanding of the reasons for some of the inconsistencies between calculated and measured "through PV wall" quantities for the PCA (Mc81,Mc84i) and PSF (two-year metallurgical experiment; SPVC-SVBC, Section A2.5, Ref. Mc87c) benchmarks, Gold and McElroy (Go87i) fit an exponential function of the form

$$(\phi t) = (\phi t)_0 \exp(-br). \qquad (1)$$

Here, (ϕt) represents the fluence of neutrons having energy > 1 MeV within the PV wall and r is the radial distance (in inches) from the front surface of the PV. The two parameters in Eq. (1), namely $(\phi t)_0$ and b, are generated by the least-squares analysis. The parameter $(\phi t)_0$ is the fluence value at the surface of the PV. The parameter b represents the reciprocal of the fluence relaxation length within the PV. Using available dosimetry adjusted values of fluence (E > 1 MeV) at 0 T, 1/4 T, 1/2 T and 3/4 T PV wall locations, values of b = 0.347 ± 0.0097 (2.8%) for the PSF and b = 0.369 ± 0.0062 (1.7%) for the PCA were derived. The ratio of these two b-values is 1.0634. Thus, the PCA value is about 6.3% higher than that observed for the PSF. Some differences between the PSF and PCA results should be anticipated because of differences that exist in these two PV mockups. In particular, the metallurgical tests in the PSF necessitated temperature-control apparatus. As a consequence of this temperature-control apparatus, perturbations were introduced into the PSF mockup of the PV. For example, electrical heaters as well as gas and water cooling were employed within the PSF mockup in an effort to maintain constant irradiation temperature. No such apparatus was entailed in the PCA (Ka83).

In Ref. Go87c, Gold and McElroy obtained some very preliminary results using data from a decommissioned BWR, namely the KRB-A Gundremmingen reactor. Fast fluence (E > 1 MeV) data has been obtained by measuring the 54Mn activity in trepans cut through the Gundremmingen PV. These very preliminary data (kindly supplied by J. W. Rogers of EG&G, Idaho) are based on the fission spectrum average cross section of the 54Fe(n,p)54Mn reaction. As can be seen from the least-squares fit in Figure 5.1.1, an exponential representation is an excellent fit of these preliminary Gundremmingen data. This least-squares analysis yields a preliminary b-value of 0.4183 for Gundremmingen, which is approximately 13% higher than the PCA benchmark b-value. While this Gundremmingen result is very preliminary, it is most encouraging and obviously merits refinement through an in-depth spectral adjustment analysis of physics-dosimetry results for the Gundremmingen trepans. It would be of considerable interest to perform a similar study on measured 54Mn activation results from trepans that might be removed from the Shippingport PWR reactor vessel; presently, the only Shippingport steel specimens that are available are those that have been taken from trepans that were removed from the reactor shield tank (Sh88).

A study of the consistency of the b-values for the PCA Replica, the other five PSF experiments (which includes the 18-day Startup Experiment; see Appendix A, Ref. Mc87c) and Gundremmingen should be accomplished. Such a study is needed to determine if there are any benchmark-to-benchmark undefined systematic differences that might be detected by differences in the b-values between the results of the PCA, PCA Replica, the seven PSF experiments and Gundremmingen.

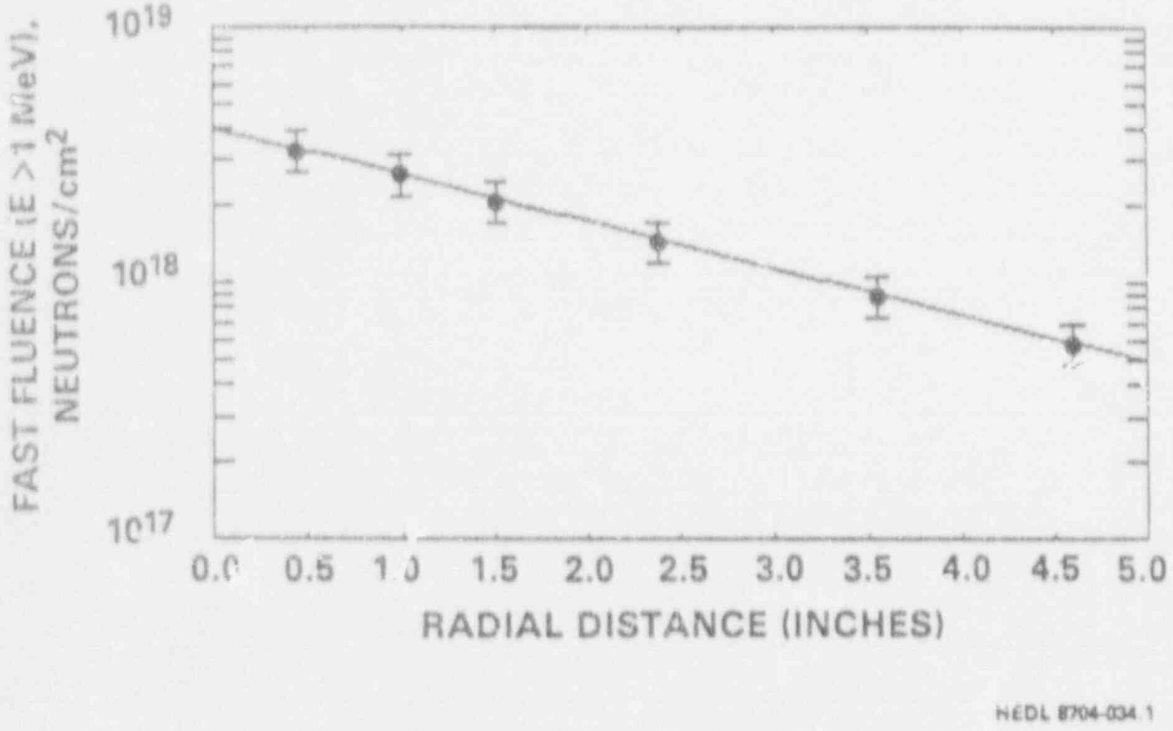

Figure 5.1.1 Radial dependence of the fast fluence deduced from ^{54}Mn observations in a trepan cut through the Gundremmingen PV. The smooth curve is a least squares fit of the data to an exponential function. Error bars represent the 1-σ uncertainty in the fluence deduced using the fission spectrum average cross section for the $^{54}Fe(n,p)^{54}Mn$ reaction.

5.2 Consistency of Experimental Data-UK Measurements

A F Thomas (Rolls-Royce & Associates)

The consistency analysis of the measured reaction rates in the UK dosimetry in both the ORR/PSF (4/12) 18 Day Start-up irradiation and the ORR/PSF (4/12) SSC1 and SSC2 capsules was conducted using both deterministic and statistical methods.

5.2.1 Deterministic Analysis

The deterministic approach to the consistency analysis of the measured reaction rates involved converting them into appropriate neutron exposure parameters i.e. fast neutron flux (E>1Mev) for the threshold reactions, epithermal flux for the gadolimum covered $^{59}Co(n,\gamma)$ and $^{58}Fe(n,\gamma)$ reactions and thermal flux for the bare $^{59}Co(n,\gamma)$ and $^{58}Fe(n,\gamma)$ reactions. These exposure parameter values were then compared for different reactions at the same location.

However in order to facilitate such conversions reliable values of the appropriate effective cross sections are required. This was achieved by means of calculated neutron spectra and reaction rates from an ANISN calculation of the ORR/PSF (4/12) configuration(see Section3.2,Ref.Mc87c).The calculational methodology and nuclear data, including dosimetry cross sections (taken from the IRDF 82 file which is based on ENDF/B-V) had been successfully benchmarked against the PCA Blind Test results (Mc81) and found to give excellent results. The calculated effective cross sections are therefore shown in Table 5.2.1 and the resulting estimates of exposure parameters (i.e. fast, epithermal, and thermal neutron flux) are shown in Table 5.2.2 (a and b).

It can be seen that the consistency between the $^{63}Cu(n,\alpha)$, $^{46}Ti(n,p)$, $^{54}Fe(n,p)$ and $^{58}Ni(n,p)$ reaction rate measurements is remarkably good in the case of the 18 Day Start-Up irradiation but less so in the case of the SSC1 and SSC2 irradiations. However, in all cases the $^{93}Nb(n,n')$ reaction rate measurements generally fall about 25% lower than the other threshold reactions in the prediction of flux (E>1Mev). The source of this discrepancy cannot be resolved by a deterministic analysis, since it may be due to a wide variety of causes such as cross section errors, measurement errors, spectral errors etc.

Where measurements were available the consistency of the resonance reaction rates (i.e. $^{58}Fe(n,\gamma)$ and $^{59}Co(n,\gamma)$ in gadolimum boxes) and the thermal reaction rates (i.e. the bare $^{58}Fe(n,\gamma)$ and $^{59}Co(n,\gamma)$) was also good and the values of fluxes consistent also with calculation.

Table 5.2.1 Effective Neutron Cross Sections for Activation Detectors Used in ORR/PSF (4/12) Configurations

Reaction	Effective Cross Section (millibarns)				
	SSC	0T	¼T	½T	¾T
FAST NEUTRON FLUX*					
$^{63}Cu(n,\alpha)^{60}Co$	0.44	0.61	0.48	0.38	0.31
$^{46}Ti(n,p)^{46}Sc$	8.11	10.1	7.77	5.95	4.63
$^{54}Fe(n,p)^{54}Mn$	63.3	70.6	55.5	43.4	34.3
$^{58}Ni(n,p)^{58}Co$	85.5	94.7	75.9	60.6	49.2
$^{93}Nb(n,n')^{93m}Nb$	222.5	225.6	228.4	238.9	255.0
EPITHERMAL NEUTRON FLUX*					
$^{58}Fe(n,\gamma)^{59}Fe(Gd)$	570	170	990	7,060	6,810
$^{59}Co(n,\gamma)^{60}Co(Gd)$	38,400	12,000	67,800	470,800	443,100
THERMAL NEUTRON FLUX*					
$^{58}Fe(n,\gamma)^{59}Fe(Bare)$	1,400	1,060	1,870	7,990	7,740
$^{59}Co(n,\gamma)^{60}Co(Bare)$	64,600	38,800	94,100	501,200	473,000

*N.B. Fast neutron flux = $n/cm^2/sec$ ($E>1Mev$)
Epithermal neutron flux = $n/cm^2/sec$ ($0.4ev<E<0.1Mev$)
Thermal neutron flux = $n/cm^2/sec$ ($E<0.4ev$)

Table 5.2.2a Comparison of Exposure Parameters Estimated from Detectors Irradiated In OBR/PSF (4/12) Start Up Irradiation

REACTION	Exposure Parameter Value				
	SSC	$\frac{1}{4}T$	$\frac{1}{4}T$(offset)	$\frac{1}{2}T$	$\frac{3}{4}T$
FAST NEUTRON FLUX*					
$^{63}Cu(n,\alpha)^{60}Co$	6.98E12	4.88E11	4.29E11	2.78E11	1.17E11
$^{46}Ti(n,p)^{46}Sc$	8.15E12	5.03E11	4.39E11	2.69E11	1.16E11
$^{54}Fe(n,p)^{54}Mn$	7.71E12	5.28E11	4.36E11	2.58E11	1.14E11
$^{58}Ni(n,p)^{58}Co$	7.72E12	5.15E11	4.24E11	2.48E11	1.13E11
$^{93}Nb(n,n')^{93m}Nb$	6.79E12	4.25E11	3.45E11	1.87E11	8.71E10
EPITHERMAL NEUTRON FLUX*					
$^{58}Fe(n,\gamma)^{59}Fe(Cd)$	-	-	-	-	-
$^{59}Co(n,\gamma)^{60}Co(Cd)$	-	-	-	-	-
THERMAL NEUTRON FLUX*					
$^{58}Fe(n,\gamma)^{59}Fe(Bare)$	3.34E12	2.37E11	1.20E11	1.10E10	5.10E9
$^{59}Co(n,\gamma)^{60}Co(Bare)$	3.05E12	2.09E11	-	1.02E10	5.20E9

* N.B. Fast neutron flux = $n/cm^2/sec$ ($E>1Mev$)
Epithermal neutron flux = $n/cm^2/sec/0.4ev<E<0.1Mev$)
Thermal neutron flux = $n/cm^2/sec$ ($E<0.4ev$)

Table 5.2.2b Comparison of Exposure Parameters Estimated from Detectors Irradiated In ORR/PSF(4/12) SSC1 and SSC2 Capsules

REACTION	Exposure Parameter Value(30MW) SSC1 (34-A)	SSC2 (34-A)
FAST NEUTRON FLUX*		
$^{63}Cu(n,\alpha)^{60}Co$	7.12E12	6.66E12
$^{46}Ti(n,p)^{46}Sc$	8.24E12	8.07E12
$^{54}Fe(n,p)^{54}Mn$	7.51E12	7.52E12
$^{58}Ni(n,p)^{58}Co$	7.82E12	7.64E12
$^{93}Nb(n,n')^{93m}Nb$	5.88E12	6.38E12
EPITHERMAL NEUTRON FLUX*		
$^{58}Fe(n,\gamma)^{59}Fe(Cd)$	-	2.65E12
$^{59}Co(n,\gamma)^{60}Co(Cd)$	2.64E12	2.52E12
THERMAL NEUTRON FLUX		
$^{58}Fe(n,\gamma)^{59}Fe(Bare)$	-	2.65E12**
$^{59}Co(n,\gamma)^{60}Co(Bare)$	-	2.38E12**

*N.B. Fast neutron flux = $n/cm^2/sec$ ($E>1Mev$)
Epithermal Neutron flux = $n/cm^2/sec$ ($0.4ev<E<0.1Mev$)
Thermal neutron flux = $n/cm^2/sec$ ($E<0.4ev$)

**34-B Locations

5.2.2 Statistical Analysis

For the purposes of a thorough statistically based consistency analysis a linear least squares adjustment method was adopted using the UK code SENSAK (Mc79a). This method employs full variance-covariance data to adjust prior estimates of neutron spectra and activation cross sections to achieve maximum likelihood estimates of exposure parameters and their uncertainties from given sets of activation measurements.

The prior estimates of the neutron spectra were again taken from the ANISN calculation described in section 3.2* and the cross section data from the IRDF82 dosimetry file. The variance-covariance data for the $^{63}Cu(n,\alpha)$, $^{46}Ti(n,p)$, $^{54}Fe(n,p)$, $^{58}Ni(n,p)$ and $^{93}Nb(n,n')$ reactions was taken from various literature sources (Pe82c, St80a, Sc79a) whilst for $^{58}Fe(n,\gamma)$ and $^{59}Co(n,\gamma)$, data from (Mc75c) was used and a narrow Gaussian correlation matrix assumed (i.e. FWHM of 2 groups).

The neutron spectra group flux errors were based on previous experience at Rolls-Royce and Associates (i.e. in the region of 30% to 50%) and a relatively wide Gaussian correlation matrix was assumed (FWHM of 5 groups). The measurement errors were based on those given in section 2.3.1.3. The correlation matrix of the measurements was based on the evaluated systematic errors due to nuclear data and calibration methods and is shown in general below:

	$^{59}Co(n,\gamma)$	$^{46}Ti(n,p)$	$^{54}Fe(n,p)$	$^{58}Fe(n,\gamma)$	$^{58}Ni(n,p)$	$^{63}Cu(n,\alpha)$	$^{93}Nb(n,n')$
$^{59}Co(n,\gamma)$	1.0	0.5	0.5	0.2	0.5	0.5	0.0
$^{46}Ti(n,p)$		1.0	0.5	0.2	0.5	0.5	0.0
$^{54}Fe(n,p)$			1.0	0.2	0.5	0.5	0.0
$^{58}Fe(n,\gamma)$				1.0	0.2	0.2	0.0
$^{58}Ni(n,p)$					1.0	0.5	0.0
$^{63}Cu(n,\alpha)$						1.0	0.0
$^{93}Nb(n,n')$							1.0

The required exposure parameters calculated by SENSAK from the adjusted flux spectra were:

(i) Neutron Flux (E>1Mev)
(ii) Neutron Flux (E>0.1Mev)
(iii) Atom Displacement Rate in Iron (for materials damage analysis) using ASTM E693-79 cross sections.
(iv) Atom Displacement Rate in Al_2O_3 (for Sapphire Damage Monitor analysis) using RECOIL calculations (Ga76) assuming Al displacements only.

* Ref. Mc87c

The results of the SENSAK analyses are summarised in Table 5.2.3. In addition to the estimates of exposure parameters and their errors, two other parameters are given: the source scale factor and the variance scale factor. The source scale factor reflects the average renormalisation of the ANISN calculated neutron spectra which was required to achieve broad prior agreement between calculated and measured reaction rates before adjustment. The variance scale factor (VSF) is the value of X^2 per degree of freedom and reflects the degree of consistency between the calculated and measured reaction rates.

The source scale factors were all within ±15% of unity indicating good prior estimates of the calculated neutron flux intensities. The values of VSF were all less than 1.0 indicating that the consistency between measured and calculated reaction rates was rather better than the errors on the input data suggested. It may be reasonably inferred that the errors on the input neutron group fluxes were somewhat exaggerated, since all the other data errors were from evaluated sources. Certainly none of the SENSAK calculations indicated that any of the measurements was suspect, since none of the calculated (adjusted) to measured reaction rate ratios deviated by more than 1% from unity.

It was noted from the results of the SENSAK data adjustments that, in all cases, the required reconciliation between the $^{93}Nb(n,n')$ reaction rates and the other threshold detector reaction rates (demanded by the deterministic analysis discussed earlier) was achieved by adjustments to the $^{93}Nb(n,n')$ cross section. This was manifest in all locations by a gradual reduction of the cross section in the threshold region (0.i - 2.0 Mev) by upto 25%. It may be therefore that the cross section of the $^{93}Nb(n,n')$ reaction in this energy range needs to be measured with greater accuracy before measurements of this reaction can significantly improve estimates of fast neutron exposure parameters, such as dpa.

The uncertainties on the exposure parameters estimated by the SENSAK analysis are all within ±7% to ±15% (1σ). Most of the variation is due to differences in consistency in the measurements at a given location which is reflected in the value of variance scaling factor. If the variance scaling factors are set to 1.0 for all locations the range of the errors reduce to ±13% to ±22%.

Table 5.2.3 Summary of Results of SENSAK Consistency Analysis of ORR/PSF (4/12) 18 Day Start-Up and SSC1 and SSC2 Capsules

LOCATION	SOURCE SCALE FACTOR	VARIANCE SCALE FACTOR	FLUX* (E >1Mev)	FLUX* (E >0.1Mev)	DPA RATE* (IRON)	DPA RATE* (SAPPHIRE)
SSC	0.96	0.39	6.77E12 ±8.3%	2.00E13 ±10.2%	1.07E-8 ±7.6%	6.50E-9 ±10.6%
PVS($\frac{1}{4}$T)	0.95	0.68	4.18E11 ±12.1%	1.61E12 ±15.0%	7.66E-10 ±11.5%	5.08E-10 ±15.6%
PVS($\frac{1}{4}$T off)	0.87	0.37	3.76E11 ±8.7%	1.46E12 ±11.1%	6.91E-10 ±8.3%	4.59E-10 ±11.6%
PVS($\frac{1}{2}$T)	1.16	0.23	2.19E11 ±7.8%	1.20E12 ±9.7%	4.94E-10 ±7.5%	3.67E-10 ±10.0%
PVS($\frac{3}{4}$T)	1.17	0.18	9.94E10 ±7.1%	7.05E11 ±8.9%	2.66E-10 ±7.4%	2.12E-10 ±9.4%
SSC1	0.95	0.23	7.05E12 ±8.1%	2.13E13 ±9.1%	1.13E-8 ±7.1%	6.84E-9 ±8.3%
SSC2	0.91	0.22	6.89E12 ±7.7%	2.07E13 ±8.3%	1.10E-8 ±6.5%	6.64E-9 ±7.6%

* FLUX = neutrons/cm^2/second (30MW)
DPA RATE = dpa/second (30MW)

All errors quoted are to one standard deviation (1σ)

6.0 EXPOSURE PARAMETER ESTIMATES - SUMMARY

W. N. McElroy (HEDL)

RR&A recommended exposure parameter values integrated over the appropriate exposure times for the ORR/PSF (4/12) 18-day Startup and SSC-1 and SSC-2 irradiations are presented in Section 6.1. It is noted that the RR&A exposure values are given for the locations of the UK dosimetry capsules. Exposure parameter values for fluence (E > 0.1 and 1.0 MeV), dpa in iron, and dpa in sapphire are presented. The irradiation times are also given, which permits the derivation of fluence and dpa rates.

HEDL's discussion and/or references to the results of physics-dosimetry studies of other LWR-PV-SDIP participants for the ORR/PSF (4/12) 18-day Startup, SPVC and SVBC experiments are presented in Section 6.2.

CEN/SCK derived average values of fluence rate [flux (E > 1 MeV)] at a nominal power of 30 MW from the different detector types irradiated in the 18-day startup test are presented in Ref. To82a. As stated by Tourwé et al. :

> *"Appreciable differences are observed in the flux (E > 1 MeV) data according to the interpretation based on the DOT spectra or on the ANISN spectra: The differences become more important when penetrating into the pressure vessel wall. The neutron flux > 1 MeV in the SSC position and the 1/4 T position could be determined with an accuracy better than 10%."*

For the 18-day startup test, HEDL analyzed the radiometric data supplied by six participants (Ke82) but did not derive any exposure parameter values.

The HEDL-ORNL recommended-consensus physics-dosimetry data and data bases for the metallurgical specimens for the SSC and SPVC experiments have been established and are discussed in Refs. Gu84d, St84, Mc86b, Mc87c, and Mc87d.

The KFA recommended physics-dosimetry data base for the metallurgical specimens for the SSC and SPVC experiments are presented in Ref. Sc86a.

In addition to these HEDL, ORNL and KFA results, other LWR-PV-SDIP participants have established their own evaluated data bases related to their use of data and/or analyses for Part I, II and III of the PSF Blind Test; see Ref. Mc86b.

Appendix B of Ref. Mc87c provides information on the HEDL analysis and derivation of exposure parameter values for the SVBC experiment; these results deserve more extensive study by LWR-PV-SDIP participants because they might provide more information on possible causes of some observed systematic biases between calculated and measured quantities (see Section 6.2 and Ref. Mc87c).

Using DM (Graphite and Tungsten) results, Saclay (C.E.A) damage exposure parameter values for four positions (SSC, 0T, 1/4T, 1/2T) are presented in Section 2.2. These experimentally derived graphite and tungsten damage/activation ratios are dimensionless quantities that are to be used with measured nickel fluences to derive damage fluences (E > 0.1 and 1.0 MeV) and dpa in iron.

6.1 RR&A Recommended Exposure Parameter Estimates

A F Thomas (Rolls-Royce and Associates Ltd UK)

The RR&A recommended exposure parameter estimates integrated over the appropriate exposure times for the ORR/PSF (4/12) 18 Day Start-Up and SSC1 and SSC2 irradiations are shown in Table 6.1.1. The uncertainty values associated with these estimates are based on the unscaled variances. Whilst it is probable that the input errors on the neutron flux spectra have been over estimated, until such time that these have been evaluated explicitly, it is more justifiable and more conservative to recommend the unscaled exposure parameter errors.

It should be emphasised that the exposure values quoted in Table 6.1.1 . are the exposure values at the locations of the UK dosimetry capsules which have been defined in sections 1.1 and 2.3 . In the case of the 18 Day Start-Up irradiation the only other measurements of interest were the irradiation induced changes in optical density of the Sapphire Damage Monitors. Since these were included in the activation dosimetry packs the exposure parameters in Table 6.1.1 . may be read across directly.

In the case of SSC1 and SSC2, extrapolations to both the metallurgical specimens and the UK Sapphires must be made. Since there were no UK measurements of gradients made on the capsules the chosen method was to adopt the analytical formulation of Stallman (see Refs. Mc87c and St84):

$$P(x,y,z) = P_o \cos B_x (x-x_o) . \cos B_z (z-z_o) . \exp(-\lambda(y-y_o))$$

where $P(x,y,z)$ is the damage parameter value at coordinate (x,y,x) and P_o is the damage parameter value at the geometric centre of the relevant capsule (NB x = lateral plane z = vertical plane and y = thickness plane of capsule).

For the purpose of estimating the relative exposure parameter on UK metallurgical specimens and sapphire dosimeters the following assumptions were made:

(i) For dosimetry capsules at locations 34A and 35A

$(x-x_o)$ = -4.1 cms (34A); + 5.1 cms (35A)
$(y-y_o)$ = -0.5 cms
$(z-z_o)$ = 5.6 cms

Table 6.1.1 RR&A Recommended Exposure Parameter Estimates in ORR/PSF (4/12) 18 Day Start-Up and SSC1 and SSC2 Capsules

LOCATION (DOSIMETER HOLE)	IRRADIATION TIME(S)	FLUENCE* (E>1Mev)	FLUENCE* (E>0.1Mev)	DPA (IRON)	DPA (SAPPHIRE)
SSC	1.512E6	1.02E19 ±13%	3.02E19 ±16%	1.62E-2 ±12%	9.83E-3 ±17%
PVS($\frac{1}{4}$T)	1.512E6	6.32E17 ±15%	2.43E18 ±18%	1.16E-3 ±14%	7.68E-4 ±19%
PVS($\frac{1}{4}$T offset)	1.338E6	5.03E17 ±14%	1.95E18 ±18%	9.25E-4 ±14%	6.14E-4 ±19%
PVS($\frac{1}{2}$T)	1.491E6	3.27E17 ±16%	1.79E18 ±20%	7.37E-4 ±16%	5.47E-4 ±21%
PVS($\frac{3}{4}$T)	1.489E6	1.48E17 ±17%	1.05E18 ±21%	3.96E-4 ±17%	3.16E-4 ±22%
SSC1 (34-A)	3.866E6	2.73E19 ±17%	8.23E19 ±19%	4.37E-2 ±15%	2.64E-2 ±17%
SSC2 (34-A)	7.746E6	5.34E19 ±16%	1.60E20 ±17%	8.52E-2 ±14%	5.14E-2 ±16%

*FLUENCE = neutrons/cm^2

All errors quoted are to one standard deviation (1σ)

(ii) For metallurgical specimens

$(x-x_o)$ = -9.9 cms (Left); +10.9 cms (Right)
$(y-y_o)$ = 1.07 cms
$(z-z_o)$ = 4.1 cms to 11.1 cms in 1 cm steps

(iii) For sapphire dosimeters at locations 17/18

$(x-x_o)$ = -2.0 cms (17); +3.0 cms (18)
$(y-y_o)$ = 0.0 cms (nominally)
$(z-z_o)$ = 5.6 cms

The values of the other parameters used were those given by Stallman.

The value of $P(x,y,z)/P_o$ for the UK dosimetry at locations 34A and 35A using this data is 1.02, 0.99 and 1.01 for fluence ($E > 1$ MEV), fluence ($E > 0.1$ MEV) and dpa (iron) respectively.

A summary of the relative extrapolated parameters for UK metallurgical specimens and Sapphire monitors is shown in Table 6.1.2. Values for other locations can be similarly evaluated.

For the metallurgical specimens the relative exposure values given in Table 6.1.2a have a precision in the region of a few percent. However, the location and design of the Sapphire Damage Monitor capsules were such that a significant flux gradient existed along their length. In addition the Sapphire itself did not sit symmetrically within the capsule. This uncertainty is reflected therefore in the relative exposure values quoted in Table 6.1.2b .

Table 6.1.2a Relative Values of Exposure Parameters for Rolls-Royce and Associates Metallurgy Specimens in SSC1 and SSC2 with Respect to UK Dosimetry

SPECIMEN NUMBER		EXPOSURE RELATIVE TO UK DOSIMETRY		
SSC1	SSC2	FLUENCE (E > 1 MEV)	FLUENCE (E > 0.1 MEV)	DPA (IRON)
R88T	R64T	0.88	0.82	0.85
R1	R31	0.89	0.83	0.86
R2	R32	0.91	0.84	0.88
R3	R33	0.93	0.86	0.90
R4	R34	0.95	0.88	0.92
R6	R36	0.97	0.90	0.94
R7	R37	0.99	0.92	0.96
R89T	R65T	0.88	0.82	0.85
R8	R38	0.89	0.83	0.86
R9	R39	0.91	0.84	0.88
R11	R41	0.93	0.86	0.90
R12	R42	0.95	0.88	0.92
R13	R43	0.97	0.90	0.92
R14	R44	0.99	0.92	0.96

Table 6.1.2b Relative Values of Exposure Parameters for UK Sapphire Damage Monitors in SSC1 and SSC2 with Respect to UK Dosimetry

SAPPHIRE NUMBER (HOLE)		EXPOSURE RELATIVE TO UK DOSIMETRY		
SSC1	SSC2	FLUENCE (E > 1 MEV)	FLUENCE (E > 0.1 MEV)	DPA (IRON)
1(2V17)	3(4V17)	0.9(±0.1)	0.9(±0.1)	0.9(±0.1)
2(2V18)	4(4V18)	0.9(±0.1)	0.9(±0.1)	0.9(±0.1)

6.2 OTHER EXPOSURE PARAMETER ESTIMATES

W. N. McElroy (HEDL)

HEDL's discussion and/or references to the results of physics-dosimetry studies of other LWR-PV-SDIP participants for the ORR/PSF (4/12) 18-day Startup, SPVC and SVBC experiments are presented in Sections 6.2.1 through 6.2.3.

6.2.1 CEN/SCK RESULTS AND ANALYSIS

CEN/SCK derived average values of fluence rate [flux (E > 1 MeV)] at a nominal power of 30 MW from the different detector types irradiated in the 18-day startup test are presented in Table 7, Ref. To82a. As stated by Tourwé et al., in Ref. To82a:

> *"Appreciable differences are observed in the flux (E > 1 MeV) data according to the interpretation based on the DOT spectra or on the ANISN spectra: The differences become more important when penetrating into the pressure vessel wall. The neutron flux > 1 MeV in the SSC position and the 1/4 T position could be determined with an accuracy better than 10%."*

6.2.2 SACLAY (C.E.A) RESULTS AND ANALYSIS

Using DM (Graphite and Tungsten) results, Saclay (C.E.A) damage exposure parameter values for four positions (SSC, OT, 1/4T, 1/2T) are presented in Section 2.2. These experimentally derived graphite and tungsten damage/activation ratios are dimensionless quantities that are to be used with measured nickel fluences to derive damage fluences (E > 0.1 and 1.0 MeV) and dpa in iron.

6.2.3 HEDL, ORNL, KFA, AND OTHER PARTICIPANT'S RESULTS AND ANALYSIS

For the 18-day startup test, HEDL analyzed the radiometric data supplied by six participants (Ke82) but did not derive any exposure parameter values.

The HEDL, ORNL, KFA and other LWR-PV-SDIP participants derived exposure parameter values for the SSC-1, SSC-2, and SPVC are presented in Refs. Gu84d, St84, Mc86b, Mc87c, Mc87d and Sc86a.

The HEDL-ORNL recommended-consensus physics-dosimetry data and data bases for the metallurgical specimens for the SSC and SPVC experiments have been established and are discussed in Sections 4.1 and 4.2 and in Appendices A through D of Ref. Mc87c.

The KFA recommended physics-dosimetry data base for the metallurgical specimens for the SSC and SPVC experiments are presented in Tables 4 and 5 of Ref. Sc86a.

In addition to the HEDL, ORNL, and KFA results, other LWR-PV-SDIP participants have established their own evaluated data bases related to their use of data and/or analyses for Part I, II and III of the PSF Blind Test. The reader is referred to Section S.0 and Appendix A of NUREG/CR-3320, Volume 1 (Mc87c) for more detailed information.

Appendix B of Ref. Mc87c provides information on the HEDL analysis and derivation of exposure parameter values for the SVBC experiment. Some relevant information (taken from Appendix B) on possible effects of the flooding of the void box on contributing to observed systematic biases between calculated and measured neutron exposure parameter and detector reaction rate values follows:

"Because of the water flooding of the void box during the early part of the irradiation, the SVBC target neutron exposure of ~5 x 10^{17} n/cm^2 (E > 1 MeV) was never achieved. It was estimated by ORNL that the actual fluence (E > 1 MeV) was a factor of 20 to 40 times lower than the target fluence based on an early assessment of preliminary results of the HEDL dosimetry measurements. The SVBC irradiation temperature was estimated to be ~37°C by ORNL.

The HEDL FERRET-SAND II results reported herein indicate that the actual neutron exposure values for the center location of the SVBC were 6.1 x 10^{-5} dpa and 4.8 x 10^{16} n/cm^2 (E > 1 MeV), with (1σ) uncertainties in the range of 14 to 22%.

These SVBC physics-dosimetry results are of additional interest because of the need to verify the ORNL estimates of the effect of the water flooding and voidage on the perturbation of the neutron exposure and exposure rates in the SPVC. Such perturbations could be contributing to some of the observed systematic biases between calculated and measured neutron exposure and dosimeter sensor reaction rates, particularly at the 1/2T position of the SPVC (see Figures A3-A6). The information of interest here is that associated with the HEDL determinations of individual sensor reaction rates gradients as reported in Appendix A by Kellogg et al. It is important to observe that the integrated effects of the SPVC perturbations resulting from the void box flooding are included in the HEDL and ORNL reported exposure values for the SSC-1, SSC-2, and SPVC (0T, 1/4T, 1/2T). What may not have been properly assessed by ORNL, however, would be small, but perhaps, non-negligible changes associated with the exposure rates.

Another reason for placing emphasis on the effects of the flooding of the void box, is to better define what the actual exposure rates were for the eight steel materials irradiated in the SVBC. Here, knowing the effect of flux level could be important for the future interpretation and use of the 42°F Charpy shift data point for the bulk weld material and the setting of upper bound limits for the observed shifts (≤15°F) for the other seven materials (Mc86).* The high shift of 42°F for the low-temperature (~67°F) irradiation of the bulk weld material for a neutron fluence in the low 10^{16} n/cm^2 (E > 1 MeV) exposure range was unexpected. This is partly why Perrin (Pe86) qualified this measured change as an "apparent increase in the transition temperature region and a possible drop in the upper-shelf energy level." Another important reason for the more careful quantification of the environmental exposure conditions for the eight SVBC steel materials is to provide documented-reference data that can be used in the event any of these irradiated materials were to be reused in future metallurgical testing programs related to end-of-life and plant life extension studies associated with shield tanks and support structure steel components (Go86,Mc86,Mc87f).

* Also see (Mc87f).

(Au85) M. Austin, A. Dolan and A. F. Thomas, "A Comparative Analysis of the Oak Ridge PCA and NESDIP PCA Replica Experiments Using the LONDON Adjustment Technique," Proc. of the 5th ASTM-EURATOM Symposium on Reactor Dosimetry, Geesthacht, Federal Republic of Germany, September 24-28, 1984, EUR 9869, Commission of the European Communities, 1985.

(Ba84a) C. A. Baldwin and F. B. K. Kam, "ORR-Surveillance Dosimetry Measurement Facility (ORR-SDMF) Simulated Surveillance Capsule Perturbation Experiment," LWR-PV-SDIP: Quarterly Progress Report, April 1983 - June 1983, NUREG/CR-3391, Vol. 2, HEDL-TME 83-22, pp. ORNL-9 - ORNL-25, April 1984.

(Bu84) J. Butler, M. D. Carter, I. J. Curl, M. R. March, A. K. McCracken, M. F. Murphy and A. Packwood, The PCA Replica Experiment Part I: Winfrith Measurements and Calibrations, NUREG/CR-3324, AEEW-R 1736, Part I, NRC, Washington, DC, January 1984.

(De82) S. De Lee w and R. Menil, "Silicon P.I.N. Diode Neutron Damage Monitors " Proc. of the 4th ASTM-EURATOM Symposium on Reactor Dosimet.y, Gaithersburg, MD, March 22-26, 1982, NUREG/CP-0029, Vol. 1, NRC, Washington, DC, pp. 387-412, July 1982.

(En67) W. W. Engle Jr, A User's Manual for ANISN, A One-Dimensional Discrete Ordinates Transport Code with Anisotropic Scattering, K-1693, Union Carbide Corp., Oak Ridge, TN, 1967.

(Fa76) A. Fabry et al., "Review of Microscopic Integral Cross Section Data in Fundamental Dosimetry Benchmark Neutron Fields," Neutron Cross Sections for Reactor Dosimetry, IAEA-208, Vol. 1, International Atomic Energy Agency, Vienna, Austria, p. 233, November 1976.

(Fa77) A. Fabry, H. Ceulemans, P. Vandeplas, W. N. McElroy and E. P. Lippincott, "Reactor Dosimetry Integral Reaction Rate Data in LMFBR Benchmark and Standard Neutron Fields: Status, Accuracy and Implications," Proc. of the 1st ASTM-EURATOM Symposium on Reactor Dosimetry, Petten, The Netherlands, September 22-26, 1975, EUR 5667, Vol. II, Commission of the European Communities, pp. 112-130, 1977.

(Fa79) A. Fabry and F. B. K. Kam, "Towards Adequate Evaluation of LWR Pressure Vessel Steel Irradiation Exposures," Proc. of an IAEA Specialist's Meeting on Accuracies in Correlation Between Property Change and Exposure Data from Reactor Pressure Vessel Steel Irradiations, Jülich, Federal Republic of Germany, September 24-27, 1979, Unnumbered IAEA Report, International Atomic Energy Agency, Vienna, Austria, 1979.

(Fa80a) A. Fabry et al., "Results and Implications of the Initial Neutronic Characterization of Two HSST Irradiation Capsules and the PSF Simulated LWR Pressure Vessel Irradiation Facility," Proc. of the 8th WRSR Information Meeting, Gaithersburg, MD, October 27-31, 1980, NUREG/CP-0023, NRC, Washington, DC, March 1982.

7.0 BIBLIOGRAPHY

(A177) A. A. Alberman, G. Allegraud, J. P. Genthon and L. Salon, "Damage Correction for the Mechanical Properties of Steels," Nucl. Technol. 36, p. 337, 1977.

(A179) A. A. Alberman et al., "The Miniaturized Tungsten Damage Detector," Proc. of the 3rd ASTM-EURATOM Symposium on Reactor Dosimetry, Ispra, Italy, October 1-5, 1979, EUR 6813, Vol. II, Commission of the European Communities, pp. 1104, 1980.

(A182) A. A. Alberman et al., "Nouveaux Developpements de la Dosimetrie des Dommages par Technique Tungstene," Proc. of the 4th ASTM-EURATOM Symposium on Reactor Dosimetry, Gaithersburg, MD, March 22-26, 1982, NUREG/CP-0029, Vol. 1, NRC, Washington, DC, pp. 321-329, July 1982.

(A182b) A. A. Alberman et al., "Mesure et Interpretation des Flux de Dommages dans le Simulateur de Cuve P.W.R. d'Oak Ridge (ORR-PSF)," Proc. of the 4th ASTM-EURATOM Symposium on Reactor Dosimetry, Gaithersburg, MD, March 22-26, 1982, NUREG/CR-0029, Vol. 2, NRC, Washington, DC, pp. 1051-1060, July 1982.

(A183) A. A. Alberman et al., DOMPI" Dosimetry Experiment Neutron Simulation of the Pressure Vessel of a Pressurized-Water Reactor, Characterization of Irradiation Damage, CEA-R-5217, Centre d'Etudes Nucleaires de Saclay, France, May 1983.

(As82) ASTM E706-81a, "Master Matrix for LWR Pressure Vessel Surveillance Standards," 1982 Annual Book of ASTM Standards, American Society for Testing and Materials, Philadelphia, PA, Part 45, 1982. (See most recent version of ASTM E706, Annual Book of ASTM Standards, Section 12, Volume 12.02, current edition.)

(As82b) ASTM E854-81, "Standard Method for Application and Analysis of Solid-State Track Recorder (SSTR) Monitors for Reactor Vessel Surveillance," 1982 Annual Book of ASTM Standards, American Society for Testing and Materials, Philadelphia, PA, Part 45, 1982.

(As83a) ASTM E910-82, "Standard Method for Application and Analysis of Helium Accumulation Fluence Monitors for Reactor Vessel Surveillance," 1983 Annual Book of ASTM Standards, American Society for Testing and Materials, Philadelphia, PA, Section 12, Volume 12.02, pp. 761-774, 1983.

(As87) ASTM E523, "Standard Method for Determing Fast-Neutron Flux Density by Radioactivation of Copper," Annual Book of ASTM Standards, American Society for Testing and Materials, Philadelphia, PA, current edition.

(Gr86a) J. A. Grundl and C. M. Eisenhauer, Compendium of Benchmark Neutron Fields for Reactor Dosimetry, NBSIR 85-3151, National Bureau of Standards, Gaithersburg, MD, January 1986.

(Gu72) R. Gunnink and J. B. Nidday, Computerized Quantitative Analysis by Gamma-Ray Spectrometry: The GAMANAL Program, UCRL-51667, Vol. 1, Lawrence Livermore National Laboratory, Livermore, CA, March 1972.

(Gu84d) G. L. Guthrie, E. P. Lippincott and E. P. McGarry, LWR-PV-SDIP: PSF Blind Test Workshop Minutes, HEDL-7467, Hanford Engineering Development Laboratory, Richland, WA, April 9-10, 1984.

(Ka82a) F. B. K. Kam, "Characterization of the Fourth HSST Series of Neutron Spectral Metallurgical Irradiation Capsules," Paper presented at the 4th ASTM-EURATOM Symposium on Reactor Dosimetry, Gaithersburg, MD, March 22-26, 1982, preprints available.

(Ka82b) F. B. K. Kam et al., "Neutron Exposure Parameters for the Fourth HSST Series of Metallurgical Irradiation Capsules," Proc. of the 4th ASTM-EURATOM Symposium on Reactor Dosimetry, Gaithersburg, MD, March 22-26, 1982, NUREG/CP-0029, Vol. 2, NRC, Washington, DC, pp. 1023-1033, July 1982.

(Ka83) F. B. K. Kam, F. W. Stallmann, R. E. Maerker and M. L. Williams, "LWR-PV Benchmark Facilities (PCA, ORR-PSF, ORR-SDMF) at ORNL," LWR-PV-SDIP: Quarterly Progress Report, April 1982 - June 1982, NUREG/CR-2805, Vol. 2, HEDL-TME 82-19, Hanford Engineering Development Laboratory, Richland, WA, pp. ORNL-1 - ORNL-19, January 1983.

(Ke80) D. J. Ketema, H. J. Nolthenius and W. L. Zijp, Neutron Metrology in the ORR: ECN Activity and Fluence Measurements for the LWR Pressure Vessel Surveillance Dosimetry Program, ECN-80-164, Petten, The Netherlands, 1980.

(Ke81) D. J. Ketema, H. J. Nolthenius and W. L. Zijp, Neutron Metrology in the ORR: Second Contribution of ECN Activity and Fluence Measurements for the LWR Pressure Vessel Surveillance Dosimetry Program, ECN-81-097, Petten, The Netherlands, 1981.

(Ke82) L. S. Kellogg and E. P. Lippincott, "PSF Interlaboratory Comparison," Proc. of the 4th ASTM-EURATOM Symposium on Reactor Dosimetry, Gaithersburg, MD, March 22-26, 1982, NUREG/CP-0029, Vol. 2, CONF-820321/V2, NRC, Washington, DC, pp. 929-945, July 1982.

(Ma80c) R. E. Maerker, "S_n Transport Calculations of the PCA Experiments with Some Estimated Uncertainties," Trans. Am. Nucl. Soc. 34, p. 628, 1980.

(Ma81) R. E. Maerker, J. J. Wagschal and B. L. Broadhead, Development and Demonstration of an Advanced Methodology for LWR Dosimetry Applications, EPRI NP-2188, (RP1399-01, Interim Report), Electric Power Research Institute, Palo Alto, CA, December 1981.

(Fa82) A. Fabry et al., "Improvement of LWR Pressure Vessel Steel Embrittlement Surveillance: Progress Report on Belgian Activities in Cooperation with the USNRC and other R&D Programs," Proc. of the 4th ASTM-EURATOM Symposium on Reactor Dosimetry, Gaithersburg, MD, March 22-26, 1982, NUREG/CP-0029, Vol. 1, NRC, Washington, DC, pp. 45-77, July 1982.

(Ga76) T. A. Gabriel, J. D. Gurney and N. M. Greene, Radiation-Damage Calculations: Primary Recoil Spectra, Displacement Rates, and Gas-Production Rates, ORNL/TM-5160, Oak Ridge National Laboratory, Oak Ridge, TN, March 1976.

(Ge74) J. P. Genthon, B. W. Hasenclever et al., Recommendations on the Measurement of Irradiation Received by the Structural Materials of Reactors, EUR 5274, Commission of the European Communities, 1974.

(Ge75) J. P. Genthon and L. Salon, "G.A.M.I.N. Technique and Applications," Nucl. Eng. and Design 33, p. 2, 1975.

(Gi78) D. M. Gilliam et al., "Reference and Standard Benchmark Field Consensus Fission Yields for U.S. Reactor Dosimetry Programs," Proc. of the 2nd ASTM-EURATOM Symposium on Reactor Dosimetry, Palo Alto, CA, October 3-7, 1977, NUREG/CP-0004, NRC, Washington, DC, p. 1507, 1978.

(Gi85) D. M. Gilliam, J. A. Grundl, G. P. Lamaze, E. D. McGarry and A. Fabry, "Cross-Section Measurements in the ^{235}U Fission Spectrum Neutron Field," Proc. of the 5th ASTM-EURATOM Symposium on Reactor Dosimetry, Geesthacht, Federal Republic of Germany, September 24-28, 1984, EUR 9869, Commission of the European Communities, 1985.

(Go87c) R. Gold and W. N. McElroy, "Light Water Reactor Pressure Vessel Surveillance Dosimetry Improvement Program (LWR-PV-SDIP): Past Accomplishments, Recent Developments, and Future Directions," Proc. of the 6th ASTM-EURATOM Symposium on Reactor Dosimetry, Jackson Hole, WY, May 31 - June 5, 1987.

(Go87i) R. Gold and W. N. McElroy, "Radiation-Induced Embrittlement in Light Water Reactor Pressure Vessels," Nuclear Engineering and Design, North-Holland, Amsterdam, 104, p. 155-174, 1987.

(Gr78) J. A. Grundl and C. M. Eisenhauer, "Benchmark Neutron Fields for Reactor Dosimetry," Neutron Cross Sections for Reactor Dosimetry, IAEA-208, Vol. I, International Atomic Energy Agency, Vienna, Austria, pp. 53-104, 1978.

(Gr78a) J. A. Grundl, C. M. Eisenhauer and E. D. McGarry, "Benchmark Neutron Fields for Pressure Vessel Surveillance Dosimetry," Compendium of Benchmark and Test Region Neutron Fields for Pressure Vessel Irradiation Surveillance, NUREG/CR-0551, NRC, Washington, DC, p. NBS-3, December 1978.

(Ma81f) R. E. Maerker and M. L. Williams, "Comparison of Calculations with Neutron Dosimetry Measurements Performed at the Oak Ridge Poolside Facility," Trans. Am. Nucl. Soc. 39, p. 812, 1981.

(Ma82) N. Maene, R. Menil, G. Minsart and L. Ghoos, "Gamma Dosimetry and Calculations," Proc. of the 4th ASTM-EURATOM Symposium on Reactor Dosimetry, Gaithersburg, MD, March 22-26, 1982, NUREG/CP-0029, Vol. 1, NRC, Washington, DC, pp. 355-363, July 1982.

(Ma82a) R. E. Maerker and M. Austin, "Workshop on Neutron and Gamma-Ray Transport Methods," Proc. of the 4th ASTM-EURATOM Symposium on Reactor Dosimetry, Gaithersburg, MD, March 22-26, 1982, NUREG/CP-0029, Vol. 2, NRC, Washington, DC, pp. 1235-1237, July 1982.

(Ma82e) R. E. Maerker and M. L. Williams, "Calculations of the Westinghouse Perturbation Experiment at the Poolside Facility," Proc. of the 4th ASTM-EURATOM Symposium on Reactor Dosimetry, Gaithersburg, MD, March 22-26, 1982, NUREG/CP-0029, Vol. 1, NRC, Washington, DC, pp. 131-141, July 1982.

(Ma82i) R. E. Maerker and M. L. Williams, Calculations of Two Series of Experiments Performed at the Poolside Facility Using the Oak Ridge Research Reactor, NUREG/CR-2696, ORNL/TM-8326, NRC, Washington, DC, May 1982.

(Ma84a) R. E. Maerker and B. A. Worley, Activity and Fluence Calculations for the Startup and Two Year Irradiation Experiments Performed at the Poolside Facility, NUREG/CR-3886, ORNL/TM-9435, NRC, Washington, DC, October 1984.

(Ma84b) R. E. Maerker and B. A. Worley, "Calculated Spectral Differences and Dosimeter Activities for the Metallurgical Blind Test Irradiations at the ORR-PSF," Proc. of the 5th ASTM-EURATOM Symposium on Reactor Dosimetry, Geesthacht, Federal Republic of Germany, September 24-28, 1984, EUR 9869, Commission of the European Communities, 1985.

(Ma85d) G. C. Martin, Jr. and C. O. Cogburn, "Special Considerations for LWR Neutron Dosimetry Experiments," 5th ASTM-EURATOM Symposium on Reactor Dosimetry, Geesthacht, Federal Republic of Germany, September 24-28, 1984, EUR 9869, Volume 1, p. 399, Commission of the European Communities, 1985.

(Ma87) R. E. Maerker, Analysis of the NESDIP2 and NESDIP3 Radial Shield and Cavity Experiments, NUREG/CR-4886, ORNL/TM-10384, NRC, Washington, DC, May 1987.

(Mc75c) W. N. McElroy and L. S. Kellogg, "Fuels and Materials Fast-Reactor Dosimetry Data Development and Testing," Nucl. Technol. 25 (2), pp. 180-223, 1975.

(Mc79a) A. K. McCracken, "Few Channel Unfolding in Shielding - The SENSAK Code," Proc. of the 3rd ASTM-EURATOM Symposium on Reactor Dosimetry, Ispra, Italy, October 1-5, 1979, EUR 6813, Vol. II, Commission of the European Communities, p. 732, 1980.

(Mc81) W. N. McElroy, Ed., LWR-PV-SDIP: PCA Experiments and Blind Test, NUREG/CR-1861, HEDL-TME 80-87, NRC, Washington, DC, July 1981.

(Mc81a) W. N. McElroy et al., LWR-PV-SDIP: 1980 Annual Report, NUREG/CR-1747, HEDL-TME 80-73, NRC, Washington, DC, April 1981.

(Mc81b) E. D. McGarry and A. Fabry, "Fission Ch mber Measurements," LWR PV-SDIP: PCA Experiments and Blind Test, W. N. McElroy, Ed., NUREG/CR-1861, HEDL-TME 80-87, NRC, Washington, DC, pp. 2.3-1 - 2.3-38, July 1981.

(Mc82) W. N. McElroy et al., "Surveillance Dosimetry of Operating Power Plants," Proc. of the 4th ASTM-EURATOM Symposium on Reactor Dosimetry, Gaithersburg, MD, March 22-26, 1982, NUREG/CP-0029, NRC, Washington, DC, pp. 3-43, July 1982. (LWR-PV-SDIP 1981 Annual Report.)

(Mc83d) W. N. McElroy and F. B. K. Kam, PSF Blind Test Instructions and Data Packages, HEDL-7448, Hanford Engineering Development Laboratory, Richland, WA, April 1983.

(Mc84b) W. N. McElroy and F. B. K. Kam, Eds., PSF Blind Test SSC, SPVC, and SVBC Physics-Dosimetry-Metallurgy Data Packages, HEDL-7449, Hanford Engineering Development Laboratory, Richland, WA, February 1984.

(Mc84f) A. K. McCracken, Ed., The PCA Replica Experiment, Part I: Winfrith Measurements and Calculations, NUREG/CR-3324, Vol. 1, AEEW-R 1736, UK Atomic Energy Establishment, Winfrith, UK, January 1984. (Use Bu84 instead.)

(Mc84i) W. N. McElroy, LWR-PV-SDIP: PCA Experiments, Blind Test, and Physics-Dosimetry Support for the PSF Experiments, NUREG/CR-3318, HEDL-TME 84-1, NRC, Washington, DC, September 1984.

(Mc85b) W. N. McElroy, Ed., LWR-PV-SDIP: PSF Experiments Summary and Blind Test Results, NUREG/CR-3320, Vol. 1, HEDL-TME 85-4, NRC, Washington, DC, 1985. (Use Mc86b instead).

(Mc86) W. N. McElroy et al., Trend Curve Data Development and Testing, MC2-TR-86-10, HEDL-7591, Metrology Control Corporation and Hanford Engineering Development Laboratory, Richland, WA, March 1986 and HEDL-SA-3400, Proc. of the 13th International Symposium on the Effects of Radiation on Materials, June 23-25, 1986, Seattle, WA, Metrology Control Corporation and Hanford Engineering Development Laboratory, Richland, WA, September 1986.

(Mc86b) W. N. McElroy, Ed., LWR-PV-SDIP: PSF Experiments Summary and Blind Test Results, NUREG/CR-3320, Vol. 1, HEDL-TME 86-8, NRC, Washington, DC, July 1986.

(Mc86c) E. D. McGarry, "PCA Experimental Results," Minutes of the 15th LWR-PV-SDIP Meeting in Gaithersburg, MD on October 21-24, 1985 and NESDIP/VENUS/PWR Workshop at Raleigh, NC on September 15-18, 1986, HEDL-7587, Section 4.2.1, Hanford Engineering Development Laboratory, Richland, WA, November 1986.

(Mc87) W. N. McElroy, LWR-PV-SDIP: 1986 Annual Progress Report, NUREG/CR-4307, Vol. 3, HEDL-TME 86-2, NRC, Washington, DC, February 1987.

(Mc87c) W. N. McElroy and R. Gold, Eds., LWR-PV SDIP: PSF Physics-Dosimetry Program, NUREG/CR-3320, Vol. 3, HEDL-TME 87-3, NRC, Washington, DC, August 1987.

(Mc87d) W. N. McElroy and R. Gold, Eds., LWR-PV-SDIP: PSF Metallurgical Program, NUREG/CR-3320, Vol. 4, HEDL-TME 87-4, NRC, Washington, DC, November 1987.

(Mc87f) W. N. McElroy et al., "Trend Curve Data Development and Testing," Proc. of the 13th International Symposium on Effects of Radiation on Materials, ASTM STP 956, Part II, p. 505-534, Seattle, WA, December 1987.

(Mc88) W. N. McElroy and L. S. Kellogg, "Dosimetry-Adjusted Reactor Physics-Parameters for Pressure Vessel Neutron Exposure Assessment," Trans. Am. Nucl. Soc., 57, p. 233, November 1988.

(Mc88a) W. N. McElroy and R. Gold, LWR-PV-SDIP: PSF Startup Experiments, NUREG/CR-3320 Vol. 2, WHC-EP-0204, NRC, Washington, DC, December 1988.

(Pe82) G. P. Pells, A. J. Fudge, M. J. Murphy and M. Wilkins, "An Investigation into the Use of Sapphire as a Fast Neutron Damage Monitor," Proc. of the 4th ASTM-EURATOM Symposium on Reactor Dosimetry, Gaithersburg, MD, March 22-26, 1982, NUREG/CP-0029, Vol. 1, NRC, Washington, DC, pp. 331-344, July 1982.

(Pe82c) M. Petilli, "TASHI Results for Multigroup Cross Sections and Their Uncertainties," Proc. of the IAEA Advisory Group Meeting on Nuclear Data for Radiation Damage Assessment and Related Safety Aspects, Vienna, Austria, October 12-16, 1981, IAEA-TECDOC-263, International Atomic Energy Agency, Vienna, Austria, p. 57, 1982.

(Pe86) J. S. Perrin et al., Simulated Void Box Capsule (SVBC) Charpy Impact Test Results, EPRI NP-4630, NUREG/CR-3320, Vol. 5, Electric Power Research Institute, Palo Alto, CA, August 1986.

(Ra77) F. J. Rahn, K. E. Stahlkopf, T. V. Marston, R. Gold and J. H. Roberts, "Standards for Dosimetry Beyond the Core," Proc. of the International Specialists Symposium on Neutron Standards and Applications, Gaithersburg, MD, March 28-31, 1977, NBS SP 493, Government Printing Office, Washington, DC, pp. 137-145, 1977.

(Ra78) F. J. Rahn, C. Z. Serpan, A. Fabry, W. N. McElroy, J. A. Grundl and J. Debrue, "Trends in Light Water Reactor Dosimetry Programs," Proc. of the 2nd ASTM-EURATOM Symposium on Reactor Dosimetry, Palo Alto, CA, October 3-7, 1977, NUREG/CP-0004, Vol. 3, NRC, Washington, DC, p. 1064, 1978.

(Rh79) W. A. Rhoades, D. B. Simpson, R. L. Childs and W. E. Engle, The DOT-IV Two-Dimensional Discrete Ordinates Transport Code with Space-Dependent Mesh and Quadrature, ORNL/TM-6529, Oak Ridge National Laboratory, Oak Ridge, TN, 1979.

(Sc79a) R. E. Schenter, F. Schmittroth and F. M. Mann, "Evaluation of the $^{54}Fe(n,\gamma)^{59}Fe$ and $^{54}Fe(n,p)^{54}Mn$ Reactions for the ENDF/B-V File," HEDL-SA-1908, Proc. of the International Conference on Nuclear Cross Sections for Technology, Knoxville, TN, October 1979.

(Sc86a) W. Schneider et al., Report on the Nuclear Radiation Measurements in KfA Jülich in the Frame of the Pressure Vessel Survillance Dosimetry Improvement Program (PVSDIP), KFA-ZBB-IB-14/36, Kernforschungsanlage Jülich GmbH, Federal Repulic of Germany, September 1986.

(Sh88) W. J. Shack, "Shippingport Ageing Studies - Results and Plans," Proceedings of the NRC 16th Water Reactor Safety Information Meeting, National Bureau of Standards, Gaithersburg, Maryland, October 24-27, 1988.

(St80a) L. E. Steele, "Review of IAEA Specialists' Meeting on Irradiation Embrittlement, Thermal Annealing and Surveillance of Reactor Vessels," Proc. of the 3rd ASTM-EURATOM Symposium on Reactor Dosimetry, Ispra, Italy, October 1-5, 1979, EUR 6813, Vol. 1, Commission of the European Communities, pp. 470-481, 1980.

(St81c) F. W. Stallmann, F. B. K. Kam, J. F. Eastham and C. A. Baldwin, Reactor Calculation "Benchmark" PCA Blind Test Results, ORNL/NUREG/TM-428, Oak Ridge National Laboratory, Oak Ridge, TN, 1981.

(St84) F. W. Stallmann, Determination of Damage Exposure Parameter Values in the PSF Metallurgical Irradiation Experiment, NUREG/CR-3814, ORNL/TM-9106, Oak Ridge National Laboratory, Oak Ridge, TN, 1984.

(To80) H. Tourwé and N. Maene, "Fast Neutron Fluence Measurement with the $^{93m}Nb(N,n')^{93m}Nb$ Reaction," Proc. of the 3rd ASTM-EURATOM Symposium on Reactor Dosimetry, Ispra, Italy, October 1-5, 1979, EUR 6813, Commission of the European Communities, 1980.

(To82) H. Tourwé and G. Minsart, "Surveillance Capsule Perturbation Studies in the PSF 4/12 Configuration," Proc. of the 4th ASTM-EURATOM Symposium on Reactor Dosimetry, Gaithersburg, MD, March 22-26, 1982, NUREG/CP-0029, Vol. 1, NRC, Washington, DC, pp. 471-480, July 1982.

(To82a) H. Tourwé et al., "Interlaboratory Comparison of Fluence Neutron Dosimeters in the Frame of the PSF Start-Up Measurement Programme," Proc. of the 4th ASTM-EURATOM Symposium on Reactor Dosimetry, Gaithersburg, MD, March 22-26, 1982, NUREG/CP-0029, Vol. 1, NRC, Washington, DC, pp. 159-168, July 1982.

(To83) H. Tourwé and J. LaCroix, PSF Blind Test Neutron Dosimetry, CEN/SCK 380/83-29, Reactor Physics Department, CEN/SCK (Study Center for Nuclear Energy), Mol, Belgium, October 1983.

(Vo81) D. R. Vondy, T. B. Fowler and G. W. Cunningham, The Bold VENTURE Computation System for Nuclear Reactor Core Analysis, Version III, ORNL-5711, Oak Ridge National Laboratory, Oak Ridge, TN, 1981.

(Wa80) J. J. Wagschal, R. E. Maerker and B. L. Broadhead, "LWR-PV Damage Estimate Methodology," Proc. of 1980 Advances in Reactor Physics and Shielding Conference, September 14-17, 1980, Sun Valley, ID, pp. 612-624, 1980.

(Wi82) M. L. Williams and R. E. Maerker, "Calculations of the Startup Experiments at the Poolside Facility," Proc. of the 4th ASTM-EURATOM Symposium on Reactor Dosimetry, Gaithersburg, MD, March 22-26, 1982, NUREG/CP-0029, Vol. 1, NRC, Washington, DC, pp. 149-158, July 1982.

(Zi79) W. L. Zijp and J. H. Baard, Nuclear Data Guide for Reactor Neutron Metrology, EUR 7167, Parts I and II, Energieonderzoek Centrum Nederland (Energy Research Center Netherlands), Petten, The Netherlands, August 1979.

DISTRIBUTION

DOE/HQ/Deputy Assistant Secretary
for Reactor Deployment (2)
GTN
Washington, DC 20545

D. J. McGoff NE-40
D. L. Harrison NE-42

DOE-HQ/Assistant Secretary
for Environment, Safety, and Health
EORS
Washington, DC 20585

R. W. Starostecki EH-30

DOE-RL/AMF
R&D Programs Branch (3)
P.O. Box 550
Richland, WA 99352

D. K. Jones FED/513
R. B. Goranson FED/511
R. F. Christensen FED/418

American Society
for Testing and Materials (2)
1916 Race Street
Philadelphia, PA 19103

K. C. Pearson
K. Schaaf

Ames Laboratory
Iowa State University
Ames, IA 50010

M. S. Wechsler

Argonne National Laboratory-East
9700 South Cass Avenue
Argonne, IL 60439

W. J. Schack

Arizona State University (2)
College of Engineering
and Applied Science
Tempe, AZ 85287

J. W. McKlveen
G. Stewart

Arkansas Power and Light
P.O. Box 551
Little Rock, AK 72203

O. Cypret

Babcock & Wilcox Co.
Lynchburg Research Center (5)
P. O. Box 11165
Lynchburg, VA 24506-1165

S. Q. King L. Petrusha
A. L. Lowe, Jr. F. Walters

Baltimore Gas & Electric Co.
Lexington and Liberty Streets
P.O. Box 1475
Baltimore, MD 21203

E. Titland

DISTRIBUTION (Cont'd)

Battelle
Pacific Northwest Laboratory (23)
P.O. Box 999
Richland, WA 99352

R. Allen
J. O. Barner
S. H. Bush
T. T. Claudson
D. G. Doran
M. D. Freshley
F. A. Garner
E. R. Gilbert
L. R. Greenwood
A. B. Johnson, Jr.
L. S. Kellogg (6)
A. G. King
W. C. Morgan
L. C. Schmid
W. B. Scott
B. D. Shipp
G. L. Tingey
Technical Files

Battelle Project Management Division
Office of Nuclear Waste Isolation
1301 W. First Street
Hereford, TX 79045

J. S. Perrin

Bechtel Power Corporation
15740 Shady Grove Road
Gaithersburg, MD 20760

W. C. Hopkins

Boeing Computer
Services Richland, Inc. (4)
P.O. Box 300
Richland, WA 99352

Central Files L8-04
Document Processing
and Distribution (2) L8-15
Information Release
Administration L8-07

Brookhaven National Laboratory
Upton, Long Island, NY 11973

J. Carew

Carolina Power & Light Co.
P.O. Box 1551
Raleigh, NC 27602

S. P. Grant

Central Electricity Generating
Board Research Division (4)
Berkeley Nuclear Laboratories
Berkeley, Gloucestershire, GL13 9PB UK

B. J. Darlaston
T. E. Lewis
P. J. Heffner
J. Young

Centre d'Etude de l'Energie Nucleaire
Studiecentrum voor Kernenergie (7)
Boeretang 200
B-2400 Mol, Belgium

J. Debrue
G. DeLeeuw
S. DeLeeuw
P. J. D'hondt
A. Fabry
G. Minsart
Ph. Van Asbroeck

CNEA
Dpto de Materiales, C.A.C.
Avda del Libertador 8250
1429 Buenos Aires, Argentina

M. Mondino

Combustion Engineering, Inc. (2)
1000 Prospect Hill Road
Windsor, CT 06095

S. Byrne
G. Cavanaugh

Comitato Nazional per l'Energia Nuclere
Centro di Studi Nucleari della Casaccia
Casella Postale 2400
I-00060 Santa Maria di Galeria
Rome, Italy

M. Petilli

DISTRIBUTION (Cont'd)

Commissariat a l'Energie Atomique
Centre d'Etudes Nucleaires de Saclay (2)
Boite Postale 21
F-91190 Gif-sur-Yvette, France

A. A. Alberman
P. Soulat

Commissariat a l'Energie Atomique
Centre d'Etudes Nucleaires de Cadarache
F-13115 St Paul Lez Durance, France

J. P. Genthon

Commissariat a l'Energie Atomique
Service des Transfers Thermiques
F-38041 Grenoble, France

P. Mas

Commonwealth Edison
P.O. Box 767
Chicago, IL 60690

E. Steeve

Consolidated Edison of NY
4 Irving Place
Room 1515S
New York, NY 10003

S. Rothstein

Consultants & Technology Services (6)
113 Thayer Drive
Richland, WA 99352

W. N. McElroy

Consumers Power
1945 W. Parnall Road
Jackson, MI 49201

H. Slagger

EG&G Idaho, Inc. (2)
P.O. Box 1625
Idaho Falls, ID 83415

C. W. Frank
J. W. Rogers

Electric Power Research Institute (5)
3412 Hillview Avenue
P.O. Box 10412
Palo Alto, CA 94304

J. Carey
T. Griesbach
T. U. Marston
O. Ozer
J. J. Taylor

Energieonderzoek Centrum Nederland (2)
Netherlands Energy Research Foundation
Westerdionweg 3
Postfach 1
NL-1755 ZG, Petten The Netherlands

H. Rottger
W. L. Zijp

Ente Nazionale per l'Energia Elettrica
Italian Atomic Power Authority
National Electric Energy Agency
Via le Regina Margherita 137
Rome, Italy

M. Galliani

EURATOM
European Atomic Energy Community
Materials Science Division
Joint Research Center Ispra
I-21020 Ispra, Varese, Italy

R. Dierckx

DISTRIBUTION (Cont'd)

Florida Power & Light (2)
9250 W. Flager Street
P.O. Box 52100
Miami, FL 33152

S. Collard
J. B. Sun

Forschungszentrum GKSS Geesthacht GmbH (3)
Max-Planck-Strasse
Postfach 1160
D-2054 Geesthacht,
Federal Republic of Germany

J. Ahlf
G. M. Richter
W. Spalthoff

General Electric Company
Vallecitos Nuclear Center-103
P.O. Box 460
Vallecitos Road
Pleasanton, CA 94566

G. C. Martin

General Public Utilities
100 Interpace Parkway
Parsippany, NJ 07054

A. P. Rochina

Grove Engineering
P.O. Box 720
Washington Grove, MD 20880

C. A. Negin

Helgeson Scientific Services
5587 Sunol Blvd
Pleasanton, CA 94566

W. H. Zimmer

Institut für Festkorperforschung der
Kernforschungsanlage Jülich GmbH (3)
Postfach 1913
D-5170 Jülich 1,
Federal Republic of Germany

G. Borchardt
D. Pachur

Institut für Kernenergetik
und Energiesysteme
Pfaffenwaldring 31
Postfach 801140
D-7000 Stuttgart 80 (Vaihingen),
Federal Republic of Germany

G. Hehn
G. Prillinger

International Atomic Energy Agency (3)
Wagramerstrasse 5, Postfach 100
A-1400 Vienna, Austria

A. Sinev
N. A. Titkov
J. J. Schmidt

IRT Corporation (2)
P.O. Box 80817
San Diego, CA 92183

N. L. Lurie
W. E. Selph

Japan Atomic Energy Research Institute
Tokai Research Establishment
Tokai-mura, Naka-gun,
Ibaraki-ken, 319-11 Japan

S. Mizazono

DISTRIBUTION (Cont'd)

Kraftwerk Union Aktiengesellschaft (3)
Postfach 3220
D-8520 Erlangen,
Federal Republic of Germany

A. Gerscha C. Leitz
J. Koban

La Societe FRAMATOME
Tour Fiat, Cedex 16
F-92084 Paris, La Defense, France

C. Buchalet

Lawrence Livermore National Laboratory (2)
P.O. Box 808
Livermore, CA 94550

M. Guinan
R. Van Konynenburg

Los Alamos National Laboratory (2)
P.O. Box 1663
Los Alamos, NM 87545

G. E. Hansen
L. Stewart

Maine Yankee Atomic Power Company
Edison Drive
Augusta, MA 04336

E. F. Jones

Materials Engineering Associates, Inc. (2)
111 Mel-Mara Drive
Oxen Hill, MD 20745

J. R. Hawthorne
F. J. Loss

Metrology Control Corporation (2)
1982 Greenbrook Blvd
Richland, WA 99352

R. Gold

National Institute of Standards
and Technology
Gaithersburg, MD 20899

J. A. Grundl E. D. McGarry
G. Lamaze

Naval Research Laboratory
Engineering Materials Division
Thermostructural Materials Branch
Code 6390
Washington, DC 20375

L. E. Steele

Northeast Utilities Service Co. (3)
P.O. Box 270
Hartford, CT 06101

M. F. Ahern M. Kupinski
J. F. Ely

Northern States Power
414 Nicollet Mall
Minneapolis, MN 55401

G. Neils

DISTRIBUTION (Cont'd)

Nuclear Regulatory Commission
Office of Nuclear Regulatory Research (8)
Division of Engineering Technology
Materials Engineering Branch
NL-5650
Washington, DC 20555

R. Alexander
W. Hazelton
L. Lois
P. N. Randall
C. Z. Serpan, Chief
A. Taboada
M. Vagin
J. P. Vora, Sr.

Nuclear Regulatory Commission
Office of Nuclear Reactor Regulation
Division of Safety Review and Oversight
Engineering Issues Branch
Washington, DC 20555

R. E. Johnson

Oak Ridge National Laboratory (4)
P.O. Box X
Oak Ridge, TN 37830

F. B. K. Kam
R. E. Maerker
L. E. Miller
F. M. Stallman

Oak Royal Naval College
Department of Nucl Science and Technology
Greenwich London, SE10 9NN, UK

J. R. A. Lakey

Omaha Public Power District
1623 Harney Street
Omaha, NE 68102

J. Gasper

Penn State University
231 Sackett Bldg.
University Park, PA 16802

M. P. Manahan (ONWI)

RACAH Institute of Physics
The Hebrew University
91904 Jerusalem, Israel

J. J. Wagschal

Radiation Research Associates
MS-644 [illegible]50 Hulen Street
Fort Worth TX 76107

K. M. Rubin

Rochester Gas & Electric Corp.
Supervisor of Material Engineering
89 East Avenue
Rochester, NY 14649

A. E. Curtiss, III

Rockwell International
Rocketdyne Division (2)
6633 Canoga Avenue
Canoga Park, CA 91304

H. Farrar
B. M. Oliver

Rolls-Royce & Associates Ltd (4)
P.O. Box 31
Derby, DE2 8BJ, UK

M. Austin
R. Squires
A. F. Thomas
T. J. Williams

SA Cockerill-Ougree
Recherches et Developments
Division de la Construction Mecanique
B-4100 Serraing, Belgium

J. Widart

DISTRIBUTION (Cont'd)

Sandia National Laboratory
P.O. Box 5800
Albuquerque, NM 87059

L. Bustard
W. B. Gauster

Science Applications, Inc.
1200 Prospect Street
La Jolla, CA 92037

G. L. Simmons

Ship Research Institute
Tokai Branch Office
Tokai-mura, Naka-gun,
Ibaraki-ken, 319-11 Japan

K. Takeuchi

Southwest Research Institute (2)
6220 Calebra Road
P.O. Box 28510
San Antonio, TX 78284

D. Cadena
P. K. Nair

Swiss Federal Institute
for Reactor Research
CH-5303 Wuerenlingen, Switzerland

F. Hegedus

TENERA Engineering Services
1995 University Ave.
Berkeley, CA 94704

P. D. Hedgecock

TVA, Office of Engineering
400 W. Summit Hill Drive
Knoxville, TN 37902

E. A. Merrick

United Kingdom Atomic Energy Authority
Atomic Energy Research
Establishment (2)
Harwell, Oxon, OX11 ORA, UK

L. M. Davies
A. J. Fudge

United Kingdom Atomic Energy Authority
Atomic Energy Establishment (5)
Winfrith, Dorchester,
Dorset, DT2 8DH, UK

J. Butler
M. D. Carter
I. Curl
P. Miller
A. Packwood

United Kingdom
Nuclear Installations Inspectorate
Health and Safety Executive
Thames House North
Millbank, London, SWIP 4QJ, UK

T. Currie

University of Arkansas (2)
Department of Mechanical Engineering
Fayetteville, AK 72701

C. O. Conburn
L. West

University of California
at Santa Barbara (2)
Department of Chem & Nucl Engineering
Santa Barbara, CA 93106

G. Lucas
G. R. Odette

DISTRIBUTION (Cont'd)

University of Illinois
Department of Engineering
214 Nuclear Engineering Laboratory
103 South Goodwin Ave.
Urbana, IL 61801

J. G. Williams

University of London Research Center
Silwood Park
Sunnyhill, Ascot,
Berkshire, SL5 7PY, UK

J. A. Mason

University of Tokyo
Department of Nuclear Engineering
7-3-1, Hongo, Bunkyo-ku,
Tokyo, 113 Japan

M. Nakazawa

University of Virginia
Department of Nuclear Engineering
Department of Material Science
Charlottesville, VA 22901

T. G. Williamson

Virginia Power and Light
P.O. Box 26666
Richmond, VA 23261

D. Hostetler

Westinghouse Hanford Co. (5)
P.O. Box 1970, W/C-123
Richland, WA 99352

J. J. Holmes	L5-55
R. L. Knecht	N1-47
W. F. Sheely	B4-03
R. L. Simons	H0-35
H. H. Yoshikawa	B1-31

Westinghouse
Nuclear Energy Systems (6)
P. O. Box 355
Pittsburgh, PA 15230

S. L. Anderson	E. P. Lippincott
A. H. Fero	T. R. Mager
F. Lau	S. E. Yanichko

Westinghouse
Research and Development Center
1310 Beulah Road
Pittsburgh, PA 15235

F. H. Ruddy

Yankee Atomic Electric Co. (2)
1671 Worchester Road
Framingham, MA 01701

J. Christie
E. Biemiller

NRC FORM 335 (2-89) NRCM 1102, 3201, 3202

U.S. NUCLEAR REGULATORY COMMISSION

BIBLIOGRAPHIC DATA SHEET

(See instructions on the reverse)

1. REPORT NUMBER (Assigned by NRC, Add Vol., Supp., Rev., and Addendum Numbers, if any.)

NUREG/CR-3320
WHC-EP-0204
Vol. 2

2. TITLE AND SUBTITLE

LWR Pressure Vessel Surveillance Dosimetry Improvement Program

PSF Startup Experiments

3. DATE REPORT PUBLISHED

MONTH: July
YEAR: 1992

4. FIN OR GRANT NUMBER

B9988

5. AUTHOR(S)

W. N. McElroy, R. Gold, E. D. McGarry

6. TYPE OF REPORT

Technical

7. PERIOD COVERED (Inclusive Dates)

8. PERFORMING ORGANIZATION - NAME AND ADDRESS (If NRC, provide Division, Office or Region, U.S. Nuclear Regulatory Commission, and mailing address; if contractor, provide name and mailing address.)

Pacific Northwest Laboratory
Richland, WA 99352

9. SPONSORING ORGANIZATION - NAME AND ADDRESS (If NRC, type "Same as above"; if contractor, provide NRC Division, Office or Region, U.S. Nuclear Regulatory Commission, and mailing address.)

Division of Engineering
Office of Nuclear Regulatory Research
U.S. Nuclear Regulatory Commission
Washington, DC 20555

10. SUPPLEMENTARY NOTES

11. ABSTRACT (200 words or less)

The metallurgical irradiation experiment at the Oak Ridge Research Reactor Poolside Facility (ORR-PSF) is one of the series of benchmark experiments in the framework of the Light Water Reactor Pressure Vessel Surveillance Dosimetry Improvement Program (LWR-PV-SDIP). The goal of this program is to test, against well-established benchmarks, the methodologies and data bases that are used to predict the irradiation embrittlement and fracture toughness of pressure vessel and support structure steels. The prediction methodology includes procedures for neutron physics calculations, dosimetry and spectrum adjustment methods, metallurgical tests, and damage correlations. The benchmark experiments serve to validate, improve, and standardize these procedures. The results of this program are implemented in a set of ASTM Standards on pressure vessel surveillance procedures. These, in turn, may be used as guides for the nuclear industry and for the Nuclear Regulatory Commission (NRC).

To serve as a benchmark, a very careful characterization of the ORR-PSF experiment is necessary, both in terms of neutron flux-fluence spectra and of metallurgical test results. Statistically determined uncertainties must be given in terms of variances and covariances to make comparisons between predictions and experimental results meaningful. Detailed descriptions of the PSF physics-dosimetry startup experiments and their results are reported.

12. KEY WORDS/DESCRIPTORS (List words or phrases that will assist researchers in locating the report.)

Light Water Reactor Pressure Vessel Surveillance
Physics-Dosimetry
Dosimetry Data Base

13. AVAILABILITY STATEMENT

Unlimited

14. SECURITY CLASSIFICATION

(This Page)
Unclassified

(This Report)
Unclassified

15. NUMBER OF PAGES

16. PRICE

UNITED STATES
NUCLEAR REGULATORY COMMISSION
WASHINGTON, D.C. 20555-0001

OFFICIAL BUSINESS
PENALTY FOR PRIVATE USE, $300

SPECIAL FOURTH-CLASS RATE
POSTAGE AND FEES PAID
USNRC
PERMIT NO. G-67